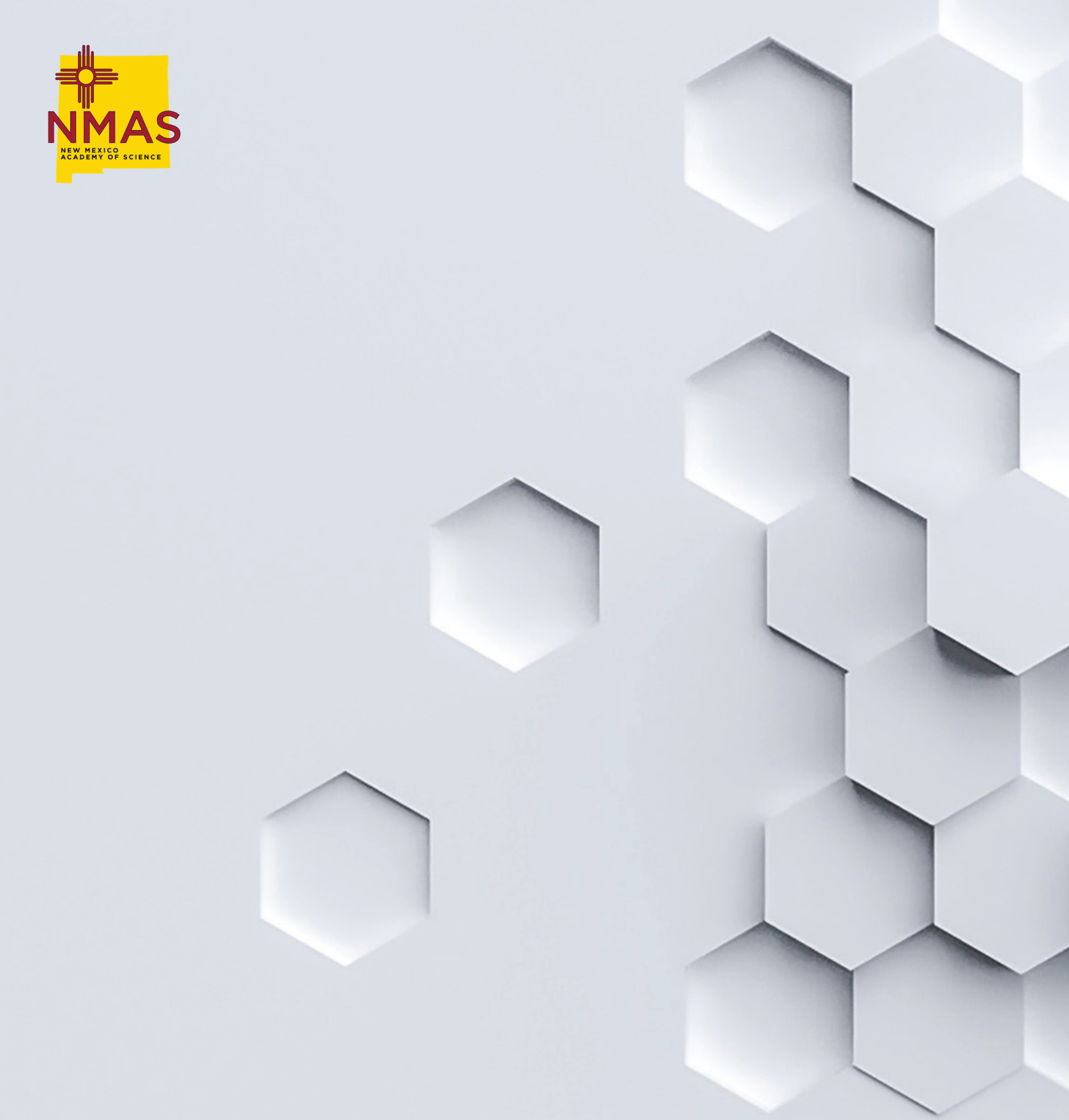

THE NEW MEXICO **JOURNAL OF SCIENCE**

Volume 54 No.1
December 2020

2020 NMJS Editorial Board

Editor-in-Chief

Anton Sumali
Sandia National Laboratories
Albuquerque, NM
E-mail: hsumali@sandia.gov

Associate Editor

Vladislav Sevostianov
Princeton University
Princeton, NJ

Associate Editor

Brittney Van Der Werff
New Mexico EPSCoR
Albuquerque, NM

Copy Editor

Selena Connealy
New Mexico EPSCoR
Albuquerque, NM

Copy Editor

Sara Pichette
New Mexico EPSCoR
Albuquerque, NM

Reviewers and Coaches

Matthew Barlow
Eastern New Mexico University

Maya Chung
Princeton University

Jess Diaz
University of California, San Diego

Budi Gunawan
Sandia National Laboratories

Stephen Karpowicz
Eastern New Mexico University

Duncan Lee
Massachusetts Institute of Technology

Yue Lin
Boston University

Conlan Olson
Harvard University

Sundar Sapkota
Eastern New Mexico University

Michael Shaugnessy
Eastern New Mexico University

Ronghua Wang
Intel Corporation

Garrett Brown
Harvard University

Tyler Coleman
University of Florida

Lena Eddings
Albuquerque Public Schools

Nick Joseph
OpenAI

Maddie Kelly
University of Chicago

Yang Li
Alert Innovation

Zhiming Liu
Eastern New Mexico University

Sanjib Sapkota
Eastern New Mexico University

Vladislav Sevostianov
Princeton University

Anton Sumali
Sandia National Laboratories

Zhihan Wang
Eastern New Mexico University

Table of Contents

© NMAS 2020. All rights reserved

Editor's Note

The *New Mexico Journal of Science* (*Journal*) is the annual publication of the New Mexico Academy of Science (NMAS). Each volume of the *Journal*, which began publication in 1960, contains research papers and review articles deemed of interest to the scientists, educators, and citizens of New Mexico. Some volumes have addressed topics of historical, social, or economic interest while others have emphasized scientific areas in which New Mexico is particularly active. Authors of papers in this volume are associated with Central South University of Forestry and Technology (China), Eastern New Mexico University, Harvard University, Princeton University, Simon Fraser University (Canada), Texas A&M University, University of New Mexico, University of Cambridge (UK), and University of the Southwest.

This volume of the *Journal* brings the number of papers back to the pre-2014[1] level of about 15 per year. This volume would not have been possible without the hard work of the authors and reviewers/coaches from prominent New Mexico institutions and other organizations including Alert Innovation (Billerica, MA); Boston University (MA); Harvard University (Cambridge, MA); Intel (Portland, OR); Massachusetts Institute of Technology (Cambridge, MA); Open AI (San Francisco, CA); Princeton University (NJ); the University of California, San Diego; The University of Chicago (IL); and the University of Florida. The publication of this volume was enabled by huge professional efforts from Associate Editors Mr. Vladislav Sevostianov (Princeton) and Ms. Brittney Van Der Werff (NM EPSCoR), and Copy Editors Dr. Selena Connealy (NM EPSCoR) and Ms. Sara Pichette (NM EPSCoR). A second volume of the 2020 *Journal*, is a special edition featuring winners of the 2020 New Mexico Junior Academy of Science paper competition for high school students, along with papers by the competition participants and contributors to recent volumes of the *Journal.*

NMAS and the New Mexico Established Program to Stimulate Competitive Research (NM EPSCoR) jointly hosted the New Mexico Research Symposium on November 9–13, 2020, all online due to the COVID-19 Pandemic. Oral and poster presentations at the Symposium described scientific research conducted by undergraduate students, graduate students, and faculty at New Mexico's colleges and universities. The abstracts of those presentations are included in this volume. The Keynote speech by Los Alamos Laboratory Fellow, Dr. Bette Korber, was entitled "Our Immune System, Vaccines, and Vaccine Strategies for AIDS and COVID-19". NMAS presented the Award for Outstanding Contributions to Science in NM to Dr. Angela Wandinger-Ness. Her acceptance address was titled "GTPases to Cures: My Path to Discovery and Innovation". NMAS presented NMAS Outstanding Science Teacher Awards to Ms. Eva Abeyta from Los Alamos Online Learning Academy and Ms. Lena Eddings from La Cueva High School in Albuquerque. NMAS and NM EPSCoR wish to acknowledge the co-sponsors of the 2020 Research Symposium: The American Chemical Society Central New Mexico Local Section, the New Mexico Alliance for Minority Participation, and the University of New Mexico Center for Water and the Environment.

The *New Mexico Journal of Science* is available for free download from the NMAS website at www.nmas.org. This enables the NMAS to reach a wide readership. Prior to 2008, the Academy mailed paper volumes of the *Journal* only to its members. Those hard copies are available to the public upon request.

Anton Sumali, Ph.D.
Editor-in-Chief
New Mexico Journal of Science

[1]Anderson, K. Water, Energy, and the Environment. *New Mexico Journal of Science*, 48, 2014, p 2; https://www.nmas.org/uploads/2/4/3/3/24330698/nmjs_2014_v-48_no-1_full.pdf#page=2

Mechanisms of VOC Pollution-Induced Respiratory Dysfunction: A Review

Basil M. Baccouche [a), b)]*

Vladislav I. Sevostianov [a)]†

[a)] Harvard University, Cambridge, MA

[b)] University of Cambridge, Cambridge, United Kingdom

ABSTRACT

Air pollutants are the largest documented environmental cause of death. A global increase in wildfire prominence has further exacerbated this problem. The specific mechanisms by which certain pollutants directly create adverse respiratory outcomes are incompletely understood. Improving this understanding of respiratory dysfunction becomes an especially important endeavor amid the ongoing COVID-19 pandemic and its associated respiratory complications. Volatile organic compounds (VOCs) play a major role in the production of harmful pollutants such as particulate matter and ozone. In this study, a systematic review was conducted to synthesize the current published medical literature on how volatile organic compounds (VOCs) directly affect respiratory function. We found a strong association of VOC pollution to respiratory dysfunction, but insufficient conclusions on causal mechanisms relating VOC-induced pollution to adverse health. To clinical and environmental ends, the development of new sensors to measure VOCs is also discussed.

KEYWORDS: COVID-19, Respiratory Dysfunction, Air Pollution, Respiratory Failure, Systematic Review, Sensors, VOCs

INTRODUCTION

Amid the ongoing COVID-19 pandemic, much of the academic discourse surrounding the prevention and treatment of respiratory dysfunction has been brought to center stage. Higher concentrations of particulate matter increase viral transmission, as well as exacerbate the susceptibility and severity of disease symptoms (Comunian et al., 2020). Additionally, in the wake of an endemic rise in wildfires, including areas such as Siberia, Australia, the western United States, among others, concerns regarding air quality and corresponding public health are of paramount interest.

Volatile organic compounds (VOCs) play a role in the formation of ozone and NO_x pollutants and are also related to atmospheric aerosol (particulate matter) concentrations. VOC is an umbrella term for a large class of compounds with thousands of unique species (Atkinson and Arey, 2003). Nearly every single activity involving biological organisms releases trace amounts of various organic species to the atmosphere, and VOCs are primarily removed through chemical oxidation by either OH, O_3, NO_3, or halogen radicals, and to a lesser extent through photolysis and deposition (Koppmann, 2007). While primary organic aerosols (POA)

may be directly released through fuel combustion and forest fires (for example, soot), VOCs are responsible for production of secondary organic aerosols (SOA), nucleations resulting from the oxidation of various gas-phase organic compounds (Griffin, Cocker and Seinfeld, 1999). Upon release or emission, VOCs are oxidized in the atmosphere and form low volatility products (Henze and Seinfeld, 2006). These are formed from successive oxidation of organic chemicals until their vapor pressure reduces sufficiently to partition partly or solely to the particle phase. Upon condensing, these products then form particulate matter. Globally, between 20% and 90% of fine aerosol (under 1 μm) is organic carbon based (Jimenez et al., 2009). Generally, the larger VOCs (i.e., sesquiterpenes vs terpenes or isoprenoids) yield more SOA per carbon atom (up to 67% more for sesquiterpenes) (Kanakidou et al., 2005).

Autooxidation of VOCs forms nearly half of secondary organic aerosols indoors, and VOCs are a major source of particulate matter pollution outdoors (Fenger, Hertel and Palmgren, 1998; Pagonis et al., 2019). Within urban areas, emitted VOCs are typically from transportation, industry, and increasingly, consumer products (Fenger, Hertel and Palmgren, 1998; McDonald et al., 2018). Consumer products, such as different cosmetics, paints, cooking products, and building materials have increasingly become the dominant source of VOCs, and thus may represent a new sector that may need further regulations to achieve further reductions in air pollution (Leung, 2015; McDonald et al., 2018). Furthermore, VOCs emitted by consumer products are typically more reactive than those emitted industrially or by automobiles, leading to a larger contribution of secondary organic aerosols formed from the total aerosol budget (McDonald et al., 2018). A larger component of the public health burden of disease due to air pollution is consequently becoming decentralized, which will complicate effective regulatory measures.

The greatest environmental risk to human health is air pollution, which adds the largest burden of disease (Schraufnagel et al., 2019). Globally, particulate matter air pollution reduces life expectancy by approximately one year on average, with reductions of nearly two life years in polluted countries in Asia and Africa (Apte et al., 2018). In the United States, a decrease of 10 micrograms per cubic meter in the concentration of fine particulate matter ($PM_{2.5}$) is associated with an average life expectancy increase of 0.61 years (over 7 months) (Arden Pope III, Ezzati and Dockery, 2009). Consequently, reductions in air pollution can account for up to a 15% overall increase in life expectancy (Arden Pope III, Ezzati and Dockery, 2009). This direct link between life expectancy and particulate matter pollution, which is directly measured, provides clear justification and motivation for regulations to limit and decrease emissions of particulate matter, both primary and secondary sources. Besides particulate matter, other air pollutants, such as ozone, further contribute to the total mortality burden and life years lost due to air pollution (Lippmann, 1989; Anenberg et al., 2010). Globally, estimates range from 2.9 to 4.2 million premature deaths occurring annually directly due to outdoor air pollution alone (Lelieveld et al., 2015; Schraufnagel et al., 2019). Around 3.8 million more deaths occur annually due to indoor air pollution, and the resulting pulmonary diseases are the 4th leading cause of death globally (Ferkol and Schraufnagel, 2014; Schraufnagel et al., 2019). Most of the burden of mortality is due to ozone and fine particulate matter pollution, among other compounds such as NO_2, SO_2, and CO (Folinsbee, 1992; Silva et al., 2016). Additionally, VOCs are a direct health hazard, besides their role in forming hazardous ozone and particulate matter pollutants (Ten Brinke et al., 1998; Kim, 2011).

Air pollution plays a significant role in many ailments, notably being a major contributor to various heart and nervous system diseases, such as heart failure, stroke, hypertension, dementia, and other cognitive impairments (Brook, 2007; Allen et al., 2014; Bos et al., 2014). Several specific examples of common air-pollution induced diseases targeting the respiratory and cardiovascular systems include chronic obstructive pulmonary disease (due to elevated ozone concentrations and particulate matter), acute lower respiratory illness (due to particulate matter), cerebrovascular disease (due to particulate matter), ischemic heart disease (due to particulate matter), lung cancer (due to particulate matter), and sick-building syndrome (due to VOCs) (Ten Brinke et al., 1998; Perez-Padilla, Schilmann and Riojas-Rodriguez, 2010; Ferkol and Schraufnagel, 2014; Lelieveld et al., 2015). Better sensing and measurement systems, technical modifications to limit pollutant emission or exposure, and new and increasingly targeted treatment tools all represent necessary components for improving public health concerns regarding air and other environmental pollutants. In fact, reducing these environmental pollutants represents the primary and possibly the most effective way to reduce the burden of all cancers (Danaei et al., 2005). Thus, reducing air pollution is a major opportunity for improving global health and represents a significant and effective disease prevention measure (Ferkol and Schraufnagel, 2014).

Particularly in energy efficient buildings (largely built after the 1970s) in highly developed countries, where the buildings are well insulated ("air-tight") and consequently air circulation is kept to a minimum, VOCs tend to accumulate to unsafe levels (Ten Brinke et al., 1998; Zhang and Smith, 2003). Consequently, certain diseases, such as sick-building syndrome, can be directly tied to VOCs (Ten Brinke et al., 1998). Health issues arising from exposure to indoor contaminants is one of the most common health concerns people face, with sick-building syndrome becoming an increasingly common concern (Ledford and Lockey, 1994). Sick-building syndrome health ailments are typically non-fatal but can be extremely debilitating (Redlich, Sparer and Cullen, 1997). Consequently, chronic, low-level indoor exposure to VOCs leads to numerous symptoms, the most common including mucous-membrane irritations (eye and throat irritations, cough), neurotoxic effects (headaches, fatigue, lack of concentration), respiratory symptoms (shortness of breath, cough, wheeze), skin symptoms (rash, pruritus, dryness), chemosensory changes (enhanced or abnormal odor perception), and visual disturbances (Redlich, Sparer and Cullen, 1997).

The correlation between VOC pollution and respiratory distress (among other major somatic dysfunctions) has been thoroughly documented (Bentayeb et al., 2013). In this paper, the authors undertake a review of the published medical literature on the nature of the direct causal relationship between VOC pollution and respiratory dysfunction. A synthesized understanding of the direct pathways by which VOC pollutants damage the respiratory system may illuminate treatment of respiratory dysfunction from pollution and other sources, including but not limited to coronavirus-associated respiratory complications. Investigation into causal mechanisms of non-VOC-related pulmonary dysfunction was beyond the scope of this study.

MATERIALS AND METHODS

2.1 Systematic Review

The question of interest in the present review is as follows: "What is currently known about

how VOC pollution proximately affects the respiratory system?" To answer this specific research question, sixteen appropriate search terms, specified to Title/Abstract, were developed. The Sciome Workbench for Interactive computer-Facilitated Text-mining (SWIFT)-Review was used to conduct a systematic review of our search results within the United States National Library of Medicine's PubMed database (Howard et al., 2016). The principal function of the SWIFT-Review technology was to assimilate and sort search results for centralized manual review. This review adhered to rigorous standards of reproducibility and was conducted using a PRISMA-guided approach (Liberati et al., 2009). The visual workflow representing this systematic effort, as well as the search terms used, are shown in Figure 1.

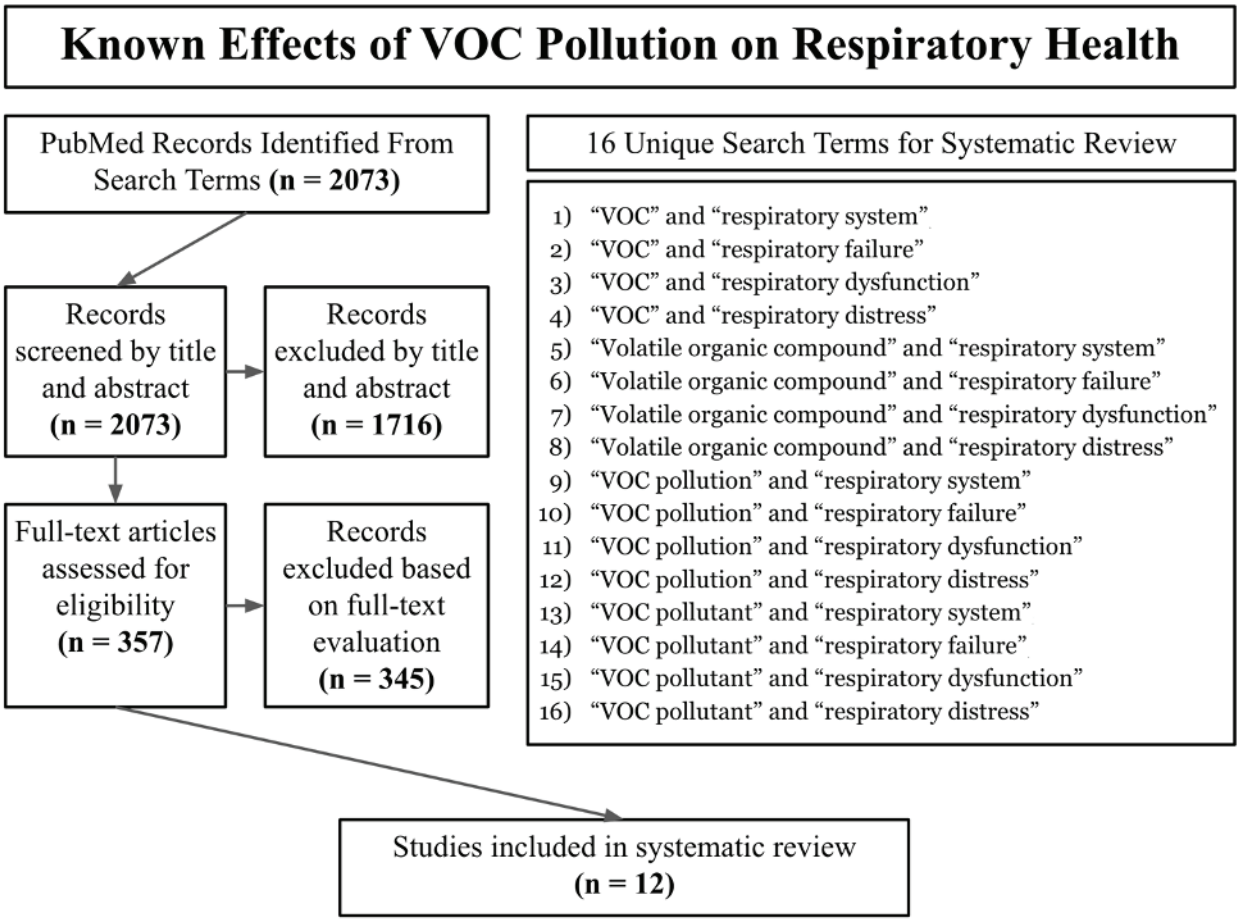

Figure 1. Systematic review workflow (including search terms) investigating the proximate mechanism(s) by which volatile organic compound (VOC) pollution causes respiratory dysfunction.

Duplicates and articles identified as irrelevant to the research question were excluded automatically and manually, respectively. Upon full-text review, only studies in which direct association to a respiratory dysfunction was established or a specific causal mechanism of action was proposed were included. We identified twelve studies whose data fulfilled our investigative criteria.

RESULTS

The review identified twelve papers whose content matched our study criteria by directly addressing the association between VOC pollution and adverse respiratory health outcomes. The robust association between VOC pollution and adverse respiratory outcomes (including but not limited to breathlessness, pulmonary dysfunction, dyspnea, wheezing, upper respiratory symptoms, and asthma) is confirmed by our review (D'Amato, G., Liccardi, G., D'Amato, M., Cazzola, 2002; Delfino et al., 2003; Yoon et al., 2010; Tanyanont, W., Vichit-Vadakan, 2012; Bentayeb et al., 2013; Kim et al., 2015; Gostner et al., 2016; Norbäck et al., 2017; Paciência et al., 2019; Zhao et al., 2019). The results of the review are shown in Table 1.

Study	**Association?**	**Mechanism Proposed?**
Bönisch et al., 2012	Yes	"Our results demonstrate that exposure to VOCs may increase the allergic immune response by interfering with DC function and by inducing oxidative stress and has therefore to be considerate (sic) as risk factor for the development of allergic diseases."
Bayzar et al., 2019	Yes	N/A
Gostner et al., 2016	Yes	Suggests the investigation of molecular effects of VOCs *in vitro*.
Kim et al., 2015	Yes	N/A - "In addition, risk assessment recognizes the association between air fresheners and adverse health effects, but the distinct causal relationship remains unclear."
Paciência et al., 2019	Yes	N/A
Tanyanont & Vichit-Vadakan, 2012	Yes	N/A
Yoon et al., 2010	Yes	"We hypothesised that VOCs impair pulmonary function through enhancing oxidative stress, especially in the elderly population."
Bentayeb et al., 2013	Yes	"The underlying mechanisms could consist of oxidative stress and irritation damaging the airways mucosa."
Zhao et al., 2019	Yes	"These findings indicate that VOCs exposure may induce potential pulmonary health risk due to the alteration of gas-liquid interfacial properties of PS."
D'Amato et al., 2002	Yes	N/A
Delfino et al., 2003	Yes	N/A
Norbäck et al., 2017	Yes	N/A

Table 1. Overview of review results.

The most common causative mechanism linking VOC exposure with the development of pulmonary dysfunction was mentioned by Yoon et al. (2010), Bentayeb et al. (2013), and Bönisch et. al.(2012), suggesting that VOC exposure induces oxidative stress, leading to impaired pulmonary function. Also proposed is the suggestion that microinteractions at the gas-liquid interface may be responsible for adverse pulmonary outcomes (Zhao et al., 2019). Beyond these, robust alternative mechanisms were not identified by the authors.

DISCUSSION

Our systematic review demonstrates that the current medical literature provides an incomplete understanding of the respiratory health risks posed by VOC exposure. Both principal proposed mechanisms from the review, as well as hitherto-unproposed hypotheses for the causal association between VOC pollution and respiratory dysfunction, require elevated particle sensing technology to validate or reject and replace. The COVID-19 pandemic has dramatically elevated the importance of understanding respiratory dysfunction risk factors and causative mechanisms as healthcare professionals race to treat respiratory complications in affected patients. Beyond the ongoing pandemic, the rise of pollution-associated pulmonary dysfunction, particularly in industrialized areas, presents a global public health crisis that requires the urgent attention of medical researchers. In particular, we strongly recommend further study into causal mechanisms of VOC-induced respiratory illness. Furthermore, present-day VOC detection capabilities, which may increase our ability to assess their proximate effects on respiratory function, are insufficient. Several opportunities exist for new data collection and VOC measurement.

Novel sensing techniques such as those based on advancing optical particle counters, metal-oxide semiconductors, and photoionization detectors provide exciting perspectives for rapid detection of different aerosols and their precursors. Traditional techniques most commonly used today (such as gas chromatography or mass spectroscopy) require large expensive detectors with slow response times. Thus, new techniques for rapid and widespread testing provide possibilities such as breath diagnostics, highly localized air quality and composition monitoring, and improved forecasting.

Besides new testing technologies, new testing techniques unlock exciting possibilities for air quality measurements. Unmanned aerial vehicles (UAVs) provide an opportunity for dynamic measurements at unprecedented resolutions. Mounting sensor systems to UAVs allows for real time data collection at varying horizontal and vertical scales, potentially autonomously. The same sensor systems, which must be sufficiently portable and lightweight for use on UAVs, may be used by clinicians and other healthcare professionals for disease diagnostics. Measuring environmental factors influencing health through air quality and directly making diagnoses by measuring breath exhalation composition provide rapid and affordable advances in healthcare.

Newly developed photoionization detectors, utilizing tubular electrodes, allow for sub-parts per billion detection of gases such as isoprene (the most common VOC globally). Measuring VOCs permits improved diagnostics not only of the aforementioned VOC-linked health conditions but also of particulate matter. New detection methods help quantify VOCs and

other air pollutants and will help identify their sources.

Portable VOC detectors not only permit high spatio-temporal measurements of primary VOC emissions but also can be directly used to identify health care conditions linked to particular VOCs. Many different diseases, from malaria to tuberculosis to cancers, can be directly tied to specific biomarkers. These biomarkers are released via VOCs either through breath or skin emissions (Poling et al., 2011; Kelly et al., 2015; Sun, Shao and Wang, 2016; Schraufnagel et al., 2019). Measuring these VOCs permits non-invasive and rapid disease diagnostics. Additionally, breath-based diagnostics may complement existing procedures, decreasing risk of misdiagnosis and clinical error.

AUTHOR INFORMATION

Corresponding Author

*Basil M. Baccouche
Department of Public Health and Primary Care
University of Cambridge
Strangeways Research Laboratory
Wort's Causeway
Cambridge, CB1 8RN, United Kingdom
E-mail: bmb38@medschl.cam.ac.uk

Present Addresses

†Presently at the Department of Civil and Environmental Engineering, Princeton University, Princeton, New Jersey, USA

REFERENCES

Allen, J. L.; Liu, X.; Pelkowski, S.; Palmer, B.; Conrad, K.; Oberdörster, G.; Weston, D.; Mayer-Pröschel, M.; Cory-Slechta D. A. Early Postnatal Exposure to Ultrafine Particulate Matter Air Pollution: Persistent Ventriculomegaly, Neurochemical Disruption, and Glial Activation Preferentially in Male Mice. *Environmental Health Perspectives*. **2014**, 122(9), pp. 939–945. DOI: 10.1289/ehp.1307984.

Anenberg, S. C.; Horowitz, L. W.; Tong, D. Q.; West, J. J. An Estimate of the Global Burden of Anthropogenic Ozone and Fine Particulate Matter on Premature Human Mortality Using Atmospheric Modeling. *Environmental Health Perspectives*. **2010**, 118(9), pp. 1189–1195. DOI: 10.1289/ehp.0901220.

Apte, J. S.; Brauer, M.; Cohen, A. J.; Ezzati, M.; Arden Pope III, C. Ambient PM 2.5 Reduces Global and Regional Life Expectancy. *Environmental Science & Technology Letters*. **2018**, 5(9), pp. 546–551. DOI: 10.1021/acs.estlett.8b00360.

Arden Pope III, C.; Ezzati, M.; Dockery, D. W. Fine-Particulate Air Pollution and Life Expectancy in the United States. *The New England Journal of Medicine*. **2009**, 360(4), pp. 376–386. DOI: 10.1056/NEJMsa0805646.

Atkinson, R.; Arey, J. Atmospheric Degradation of Volatile Organic Compounds. *Chemical Reviews*. **2003**, 103(12), pp. 4505–4638. DOI: 10.1021/cr0206420.

Bentayeb, M.; Billionnet, C.; Baiz, N.; Derbez, M.; Kirchner, S.; Annesi-Maesano, I. Higher prevalence of breathlessness in elderly exposed to indoor aldehydes and VOCs in a representative sample of French dwellings. *Respiratory Medicine*. **2013**, 107(10), pp. 1598–1607. DOI: 10.1016/j.rmed.2013.07.015.

Bönisch, U.; Böhme, A.; Kohajda, T.; Mögel, I.; Schütze, N.; von Bergen, M.; Simon, J. C.; Lehmann, I.; Polte, T. Volatile organic compounds enhance allergic airway inflammation in an experimental mouse model. *PLoS ONE*. **2012**, 7(7), pp. 1–14. DOI: 10.1371/journal.pone.0039817.

Bos, I.; De Boever, P.; Panis, L. I.; Meeusen, R. Physical Activity, Air Pollution and the Brain. *Sports Medicine*. **2014**, 44(11), pp. 1505–1518. DOI: 10.1007/s40279-014-0222-6.

Ten Brinke, J.; Selvin, S.; Hodgson, A. T.; Frsk, W. J.; Mendell, M. J.; Koshland, C. P.; Daisey, J. M. Development of New Volatile Organic Compound (VOC) Exposure Metrics and their Relationship to "Sick Building Syndrome" Symptoms. *Indoor Air. **1998***, 8(510), pp. 140–152. DOI: 10.1111/j.1600-0668.1998.t01-1-00002.x.

Brook, R. D. Is Air Pollution a Cause of Cardiovascular Disease? Updated Review and Controversies. *Reviews on Environmental Health*. **2007**, 22(2), pp. 115–138. DOI: 10.1515/reveh.2007.22.2.115.

Comunian, S.; Dongo, D.; Milani, C.; Palestini, P. Air pollution and covid-19: The role of particulate matter in the spread and increase of covid-19's morbidity and mortality. *International Journal of Environmental Research and Public Health*. **2020**, 17(12), pp. 1–22. DOI: 10.3390/ijerph17124487.

D'Amato, G.; Liccardi, G.; D'Amato, M.; Cazzola, M. Respiratory allergic diseases induced by outdoor air pollution in urban areas. *Monaldi Archives for Chest Disease.* **2002**, 57(3–4), pp. 161–163. PMID: 12619373.

Danaei, G.; Vander Hoorn, S.; Lopez, A., D.; Murray, C. J. L.; Ezzati, M., Comparative Risk Assessment collaborating group (Cancers). Causes of cancer in the world: comparative risk assessment of nine behavioural and environmental risk factors. *The Lancet.* **2005**, 366(9499), pp. 1784–1793. DOI: 10.1016/S0140-6736(05)67725-2.

Delfino, R. J.; Gong, H.; Linn, W. S.; Hu Y.; Pellizzari E. D. Respiratory symptoms and peak expiratory flow in children with asthma in relation to volatile organic compounds in exhaled breath and ambient air. *Journal of Exposure Analysis and Environmental Epidemiology*. **2003**, 13(5), pp. 348–363. DOI: 10.1038/sj.jea.7500287.

Fenger, J.; Hertel, O.; Palmgren, F. *Urban Air Pollution - European Aspects*. Springer Science + Business Media: Dordrecht, 1998.

Ferkol, T.; Schraufnagel, D. The Global Burden of Respiratory Disease. *Annals of the American Thoracic Society*. **2014**, 11(3), pp. 404–406. DOI: 10.1513/AnnalsATS.201311-405PS.

Folinsbee, L. J. Human Health Effects of Air Pollution. *Environmental Health Perspectives*. **1992**, 100(12), pp. 45–56. DOI: 10.1289/ehp.9310045.

Freedman, A. N. Photoionization Detector Response, *Journal of Chromatography*, **1982**, 236, pp. 11–15. DOI: 10.1016/S0021-9673(00)82494-2.

Gostner, J. M.; Zeisler, J.; Alam, M. T.; Gruber, P.; Fuchs, D.; Becker, K.; Neubert, K.; Kleinhappl, M.; Martini S.; Überall F. Cellular reactions to long-term volatile organic compound (VOC) exposures. *Scientific Reports*. **2016**, 6(37842), pp. 1–14. DOI: 10.1038/srep37842.

Griffin, J.; Cocker, D. R.; Seinfeld, H. Estimate of global atmospheric organic aerosol from oxidation of biogenic hydrocarbons. *Geophysical Research Letters*. **1999**, 26(17), pp. 2721–2724. DOI: 10.1029/1999GL900476.

Henze, D. K.; Seinfeld, J. H. Global secondary organic aerosol from isoprene oxidation. *Geophysical Research Letters*. **2006**, 33(May), pp. 6–9. DOI:10.1029/2006GL025976.

Howard, B. E.; Phillips, J.; Miller, K.; Tandon, A.; Mav, D.; Shah, M. R.; Holmgren, S.; Pelch, K. E.; Walker, V.; Rooney, A. A.; Macleod, M.; Shah, R. R.; Thayer K. SWIFT Review: A text-mining workbench for systematic review. *Systematic Reviews*. **2016**, 5(1), pp. 1–16. DOI: 10.1186/s13643016-0263-z.

Jimenez, J. L.; Canagaratna, M. R.; Donahue, N. M.; Prevot, A. S. H.; Zhang, Q.; Kroll, J. H.; DeCarlo, P. F.; Allan, J. D.; Coe, H.; Ng, N. L.; Aiken, A. C.; Docherty, K.S.; Ulbrich, I. M.; Grieshop, A. P.; Robinson, A. L.; Duplissy, J.; Smith, J. D.; Wilson, K. R.; Lanz, V. A.; Hueglin, C.; Sun, Y. L.; Tian, J.; Laaksonen, A.; Raatikainen, T.;Rautiainen, J.; Vaattovaara, P.; Ehn, M.; Kulmala, M.; Tomlinson, J. M.; Collins, D. R.; Cubison, M. J.; Dunlea, E. J.; Huffman, J. A.; Onasch, T. B.; Alfarra, M.R.; Williams, P. I.; Bower, K.; Kondo, Y.; Schneider, J.; Drewnick, F.; Borrmann, S.; Weimer, S.; Demerjian, K.; Salcedo, D.; Cottrell, L.; Griffin, R.; Takami, A.; Miyoshi, T.; Hatakeyama, S.; Shimono, A.; Sun, J. Y.; Zhang, Y. M.; Dzepina, K.; Kimmel, J. R.; Sueper, D.; Jayne, J. T.; Herndon, S. C.; Trimborn, A. M.; Williams, L. R.; Wood, E. C.; Middlebrook, A. M.; Kolb, C. E.; Baltensperger, U.; Worsnop, D. R. Evolution of Organic Aerosols in the Atmosphere. *Science*. **2009**, 326(5959), pp. 1525–1530. DOI: 10.1126/science.1180353.

Kanakidou, M.; Seinfeld, J. H.; Pandis, S. N.; Barnes, I.; Dentener, F. J.; Facchini, M. C.; Van Dingenen, R.; Ervens, B.; Nenes, A.; Nielsen, C. J.; Swietlicki, E.; Putaud, J. P.; Balkanski, Y.; Fuzzi, S.; Horth, J.; Moortgat, G. K.; Winterhalter, R.; Myhre, C. E. L.; Tsigaridis, K.; Vignati, E.; Stephanou, E. G.; Wilson, J. Organic aerosol and global climate modelling : a review. *Atmospheric Chemistry and Physics.* **2005**, 5, pp. 1053 1123. DOI: 10.5194/acp-5-1053-2005.

Kelly, M.; Su, C.; Schaber, C.; Crowley, J. R.; Hsu, F.; Carlson, J. R.; Odom A. R.. Malaria parasites produce volatile mosquito attractants. *mBio.* **2015**, 6(2), pp. 1–6. DOI: 10.1128/mBio.00235-15.

Kim, B. R. VOC Emissions from Automotive Painting and Their Control: A Review. *Environmental Engineering Research*. **2011**, 16(1), pp. 1–9. DOI: 10.4491/eer.2011.16.1.001.

Kim, S.; Hong, S.; Bong, C.; Cho M. Characterization of air freshener emission: The potential health effects. *Journal of Toxicological Sciences*. **2015**, 40(5), pp. 535–550. DOI: 10.2131/jts.40.535.

Koppmann, R. *Volatile Organic Compounds in the Atmosphere*. Blackwell Publishing: Oxford, 2007.

Ledford, D. K.; Lockey, R. F. Building- and home-related complaints and illnesses: "Sick building syndrome". *The journal of Allergy and clinical immunology*. **1994**, 94(2.2), pp. 275–276. DOI: 10.1053/ai.1994.v94.a56005.

Lelieveld, J.; Evans, J. S.; Fnais, M.; Giannadaki D.; Pozzer A. The contribution of outdoor air pollution sources to premature mortality on a global scale. *Nature.* **2015**, 525, pp. 367–371. DOI: 10.1038/nature15371.

Leung, D. Y. C. Outdoor-indoor air pollution in urban environment: challenges and opportunity. *Frontiers in Environmental Science*. **2015**, 2(January), pp. 1–7. DOI: 10.3389/fenvs.2014.00069.

Liberati, A.; Altman, D. G.; Tetzlaff, J.; Mulrow C.; Gøtzsche P. C.; Ioannidis, J. P. A.; Clarke, M.; Devereaux, P. J.; Kleijnen, J.; Moher, D. The PRISMA statement for reporting systematic reviews and meta-analyses of studies that evaluate healthcare interventions: explanation and elaboration. *BMJ (Clinical research ed.)*. **2009**, 339. DOI: 10.1136/bmj.b2700.

Lippmann, M. Health effects of ozone. *JAPCA*. **1989**, 39(5), pp. 672–695. DOI: 10.1080/08940630.1989.10466554.

McDonald, B. C.; de Gouw, J. A.; Gilman, J. B.; Jathar, S. H.; Akherati, A.; Cappa,C. D.; Jimenez, J. L.; Lee-Taylor, J.; Hayes, P. L.; McKeen, S. A.; Cui, Y. Y; Kim, S.; Gentner, D. R.; Isaacman-VanWertz, G.; Goldstein, A. H.; Harley, R. A.; Frost, G. J.; Roberts, J. M.; Ryerson, T. B.; Traine M.*al.* Volatile chemical products emerging as largest petrochemical source of urban organic emissions. *Science*. **2018**, 764(February), pp. 760 764. DOI: 10.1126/science.aaq0524.

Mckinney, K. A.; Wang, D.; Ye, J.; de Fouchier, J.; Guimarães, P. C.; Batista, C. E.; Souza, R. A. F.; Alves E. G.; Gu, D.; Guenther, A. B.; Martin, S. T. A sampler for atmospheric volatile organic compounds by copter unmanned aerial vehicles. *Atmospheric Measurement Techniques*. **2018**, 12(September), pp. 3123–3135. DOI: 10.5194/amt-12-3123-2019.

Norbäck, D.; Hashim J. H.; Hashim Z.; Ali, F. Volatile organic compounds (VOC), formaldehyde and nitrogen dioxide (NO2) in schools in Johor Bahru, Malaysia: Associations with rhinitis, ocular, throat and dermal symptoms, headache and fatigue. *Science of the Total Environment*. **2017**, 592, pp. 153–160. DOI: 10.1016/j.scitotenv.2017.02.215.

Paciência, I.; Rufo J. C.; Silva D.; Martins C.; Mendes F. C.; Farraia M.; Delgado L.; Fernandes E. D. O.; Padrão P.; Moreira P.; Severo, M; Barros, H; Moreira, A. Exposure to indoor endocrine-disrupting chemicals and childhood asthma and obesity. *Allergy: European Journal of Allergy and Clinical Immunology*. **2019**, 74(7), pp. 1277–1291. DOI: 10.1111/all.13740.

Pagonis, D.; Algrim, L. B.; Price, D. J.; Day, D. A.; Handschy A. V.; Stark, H.; Miller, S. L.; de Gouw, J. A.; Jimenez, J. L.; Ziemann, P. J. Autoxidation of Limonene Emitted in a University Art Museum. *Environmental Science & Technology Letters*. **2019**, 6, pp. 520 524. DOI: 10.1021/acs.estlett.9b00425.

Perez-Padilla, R.; Schilmann, A.; Riojas-Rodriguez, H. Respiratory health effects of indoor air pollution. *The International Journal of Tuberculosis and Lung Disease*. **2010**, 14(9), pp. 1079–1086. PMID: 20819250.

Poling, A.; Weetjens, B.; Cox, C.; Beyene, N.; Durgin A.; Mahoney A. Tuberculosis detection by giant African pouched rats. *Behavior Analyst*. **2011**, 34(1), pp. 47–54. DOI: 10.1007/BF03392234.

Redlich, C. A.; Sparer, J.; Cullen, M. R. Sick-building syndrome. *The Lancet*. **1997**, 349(9057), pp. 1013–1016. DOI: 10.1016/S0140-6736(96)07220-0.

Schraufnagel, D. E.; Balmes, J. R.; Cowl C. T.; De Matteis, S.; Jung, S. H.; Mortimer, K.; Perez-Padilla, R.; Rice, M. B.; Riojas-Rodriguez, H.; Sood, A.; Thurston G. D.; To, T.; Vanker, A.; Wuebbles, D. J. Air Pollution and Noncommunicable Diseases: A Review by the Forum of International Respiratory Societies' Environmental Committee, Part 1 : The Damaging Effects of Air Pollution. *CHEST*. **2019**, 155(2), pp. 409–416. DOI: 10.1016/j.chest.2018.10.042.

Silva, R. A.; Adelman, Z.; Fry, M. M.; West J. J. The Impact of Individual Anthropogenic Emissions Sectors on the Global Burden of Human Mortality due to Ambient Air Pollution. *Environmental Health Perspectives.* **2016**, 124(11), pp. 1776 1784. DOI: 10.1289/EHP177.

Sun, X.; Shao, K.; Wang, T. Detection of volatile organic compounds (VOCs) from exhaled breath as noninvasive methods for cancer diagnosis Young Investigators in Analytical and Bioanalytical Science. *Analytical and Bioanalytical Chemistry.* **2016**, 408(11), pp. 2759–2780. DOI: 10.1007/s00216-015-9200-6.

Tanyanont, W.; Vichit-Vadakan, N. Exposure to volatile organic compounds and health risks among residents in an area affected by a petrochemical complex in Rayong, Thailand. *Southeast Asian Journal of Tropical Medicine and Public Health*. **2012**, 43(1), pp. 201–211. PMID: 24851576.

Villa, T. F.; Gonzalez, F.; Miljievic, B.; Ristovski, Z. D.; Morawska, L. An Overview of Small Unmanned Aerial Vehicles for Air Quality Measurements: Present Applications and Future Prospectives. *Sensors*. **2016**, 16(1072), pp. 12–20. DOI: 10.3390/s16071072.

Yoon, H. I.; Hong, Y.; Cho, S.; Kim, H.; Kim, Y. H.; Sohn, J. R.; Kwon, M.; Park, S.; Cho, M.; Cheong, H. Exposure to volatile organic compounds and loss of pulmonary function in the elderly. *European Respiratory Journal*. **2010**, 36(6), pp. 1270–1276. DOI: 10.1183/09031936.00153509.

Zhang, J. J.; Smith, K. R. Indoor air pollution: a global health concern. *British Medical Bulletin*. **2003**, 68(1), pp. 209–225. DOI: 10.1093/bmb/ldg029.

Zhao, Q.; Li, Y.; Chai, X.; Xu, L.; Zhang, L.; Ning, P.; Huang, J.; Tian, S. Interaction of inhalable volatile organic compounds and pulmonary surfactant: Potential hazards of VOCs exposure to lung. *Journal of Hazardous Materials*. **2019**, 369(January), pp. 512 520. DOI: 10.1016/j.jhazmat.2019.01.104.

Using SWIFT-Review as a New and Robust Tool for Comprehensive Systematic Review

Basil M. Baccouche [a), b)]*

Tejas E. Shivkumar [c)]

[a)] Harvard University, Cambridge, MA

[b)] University of Cambridge, Cambridge, United Kingdom

[c)] Brentwood School, Los Angeles, CA

ABSTRACT

The systematic review process, while critical to a typical research effort, is highly laborious and time-consuming. The increasing rate at which academic literature is being published only exacerbates this problem. In this paper, we independently and without conflict of interest demonstrate the use of new text-mining software developed by Sciome LLC for conducting swift, efficient, and reproducible systematic reviews.

KEYWORDS: Systematic Review, SWIFT-Review, Comprehensive, Literature Review

INTRODUCTION

Systematic literature reviews are an inextricable part of robust academic research. A systematic review (rather than a non-systematic review) defines a clear question of interest, identifies relevant studies, evaluates their quality, and summarizes their evidence with an explicit and reproducible methodology (Khan et al., 2003). Systematic reviews are particularly relevant to medical and epidemiological disciplines, where the increasing rate at which studies are published can present a daunting challenge to researchers interested in evaluating the current published knowledge on a topic.

This challenge is made even more difficult when the topic of investigation is not highly specialized or niche. For example, a researcher interested in what has been published on breast cancer in the past ten years would have to sift through nearly a quarter of a million studies on PubMed alone. Nevertheless, a systematic review holds tremendous value as the research itself and as a necessary complement to bench or fieldwork. Systematic reviews are essential to the practice of evidence-based medicine by clinicians and researchers who require comprehensive, up-to-date synthesis of current medical findings (Gopalakrishnan & Ganeshkumar, 2013). Systematic reviews and their associated meta-analyses have identified potential risk factors for fatal diseases, allowed public health experts to make significant policy decisions with population-wide effects, and evaluated the efficacy of experimental diagnostic techniques (Dobbins et al., 2001; Eichler et al., 2006; Belbasis et al., 2015).

The aim of this paper is to act as an independent third party in demonstrating the utility of the Sciome Workbench for Interactive computer-Facilitated Text-mining (SWIFT)-Review, a

new text-mining software developed by SCIOME, in conducting PRISMA-compatible systematic reviews within the United States National Library of Medicine's PubMed Central archive (Howard et al., 2016).

MATERIALS AND METHODS

To demonstrate the use of SWIFT-Review for conducting a systematic review, we will refer to the step-by-step procedure of a review conducted by Baccouche & Sevostianov investigating the link between VOC pollution and respiratory health (Baccouche & Sevostianov, 2021). The research question of interest is as follows: "What is currently known about how VOC pollution proximately affects the respiratory system?" Sixteen search terms were developed for use within the United States National Library of Medicine's PubMed database, shown in Figure 1.

Known Effects of VOC Pollution on Respiratory Health

16 Unique Search Terms for Systematic Review

1) "VOC" and "respiratory system"
2) "VOC" and "respiratory failure"
3) "VOC" and "respiratory dysfunction"
4) "VOC" and "respiratory distress"
5) "Volatile organic compound" and "respiratory system"
6) "Volatile organic compound" and "respiratory failure"
7) "Volatile organic compound" and "respiratory dysfunction"
8) "Volatile organic compound" and "respiratory distress"
9) "VOC pollution" and "respiratory system"
10) "VOC pollution" and "respiratory failure"
11) "VOC pollution" and "respiratory dysfunction"
12) "VOC pollution" and "respiratory distress"
13) "VOC pollutant" and "respiratory system"
14) "VOC pollutant" and "respiratory failure"
15) "VOC pollutant" and "respiratory dysfunction"
16) "VOC pollutant" and "respiratory distress"

Figure 1. Sixteen search terms developed for systematic review.

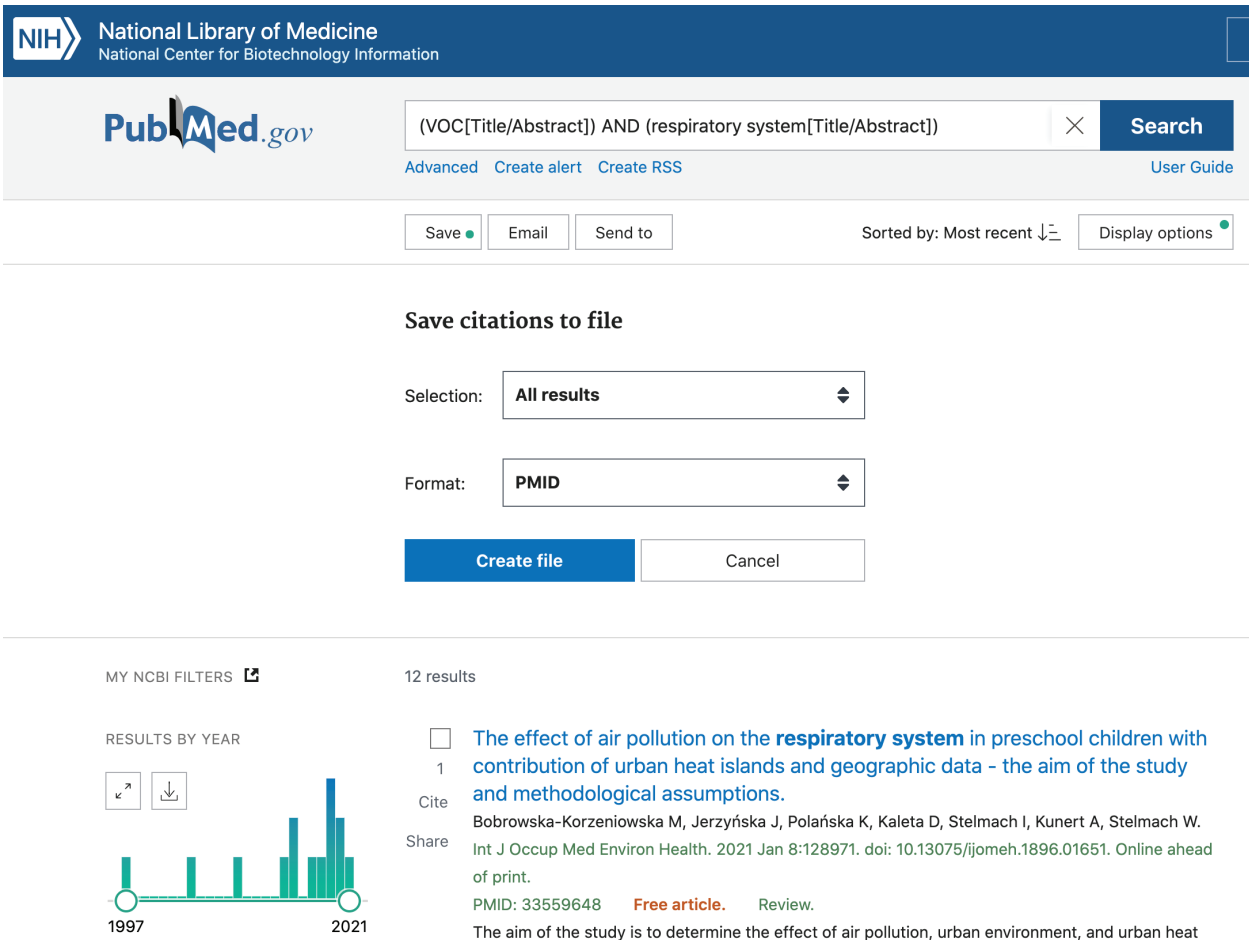

Figure 2: Saving the results of one search to a PMID list. This is done sixteen times, and the results of each search are combined into one master txt file.

The search terms were entered into the PubMed search engine and the results saved to a txt master list containing the PMIDs resulting from all sixteen search terms (Figure 2).

The master list is then imported into SWIFT-Review via the "Load Reference File" command. SWIFT-Review automatically excludes duplicates when importing PMIDs. The resulting SWIFT-Review screen, from which the systematic review can begin, is shown in Figure 3.

SWIFT-Review allows automated sorting of review results, including but not limited to the ability to browse by MeSH term and search for specific terms within your results. Pure manual screening remains possible as SWIFT-Review aggregates article titles and abstracts for chronological review if automated screening is unsuitable to the review at hand. After the conclusion of the SWIFT-Review, articles identified for full-text review can be analyzed and the results documented in a PRISMA-compatible figure, such as the one shown in Figure 4.

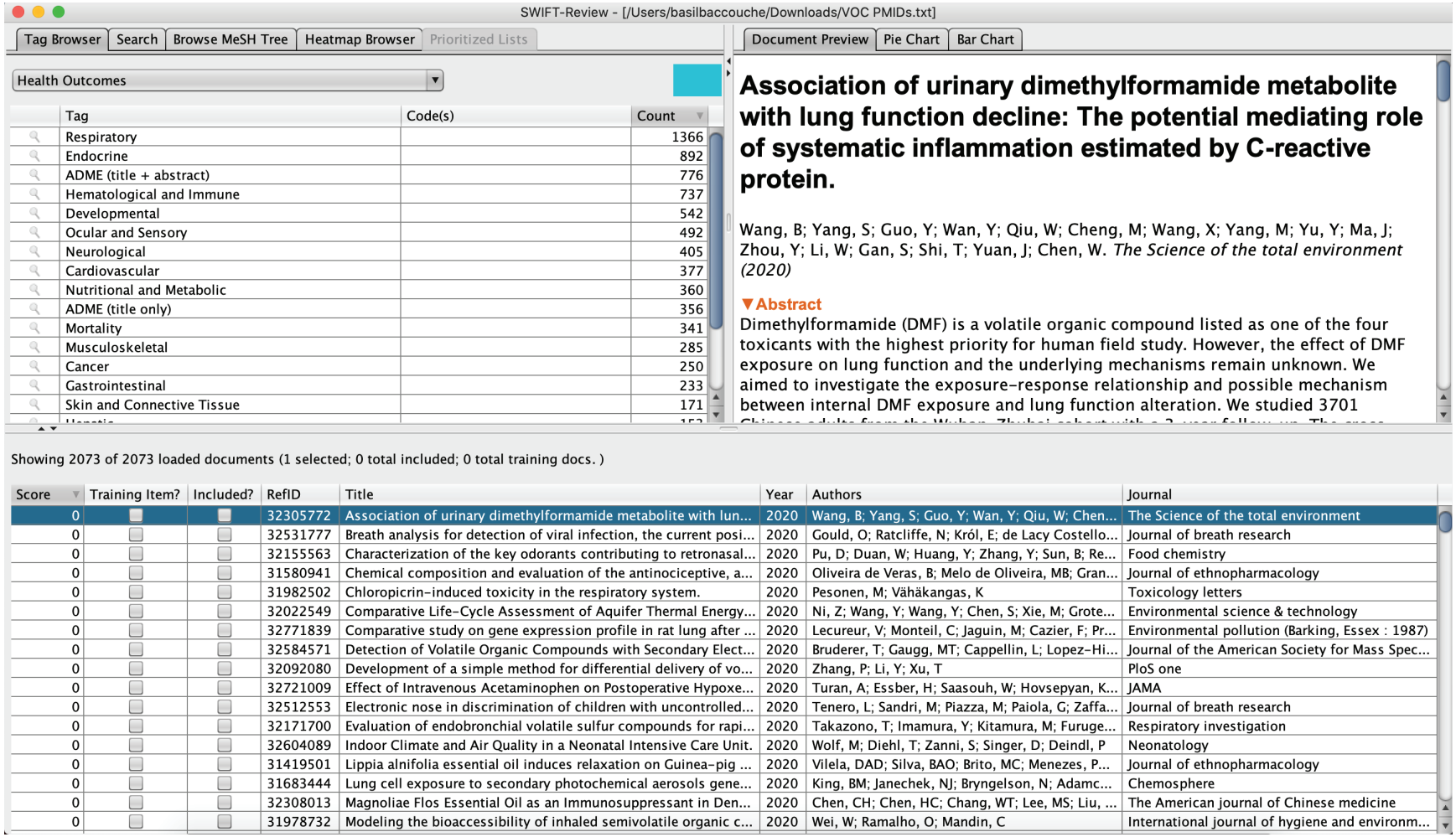

Figure 3. SWIFT-Review articles imported and ready for review.

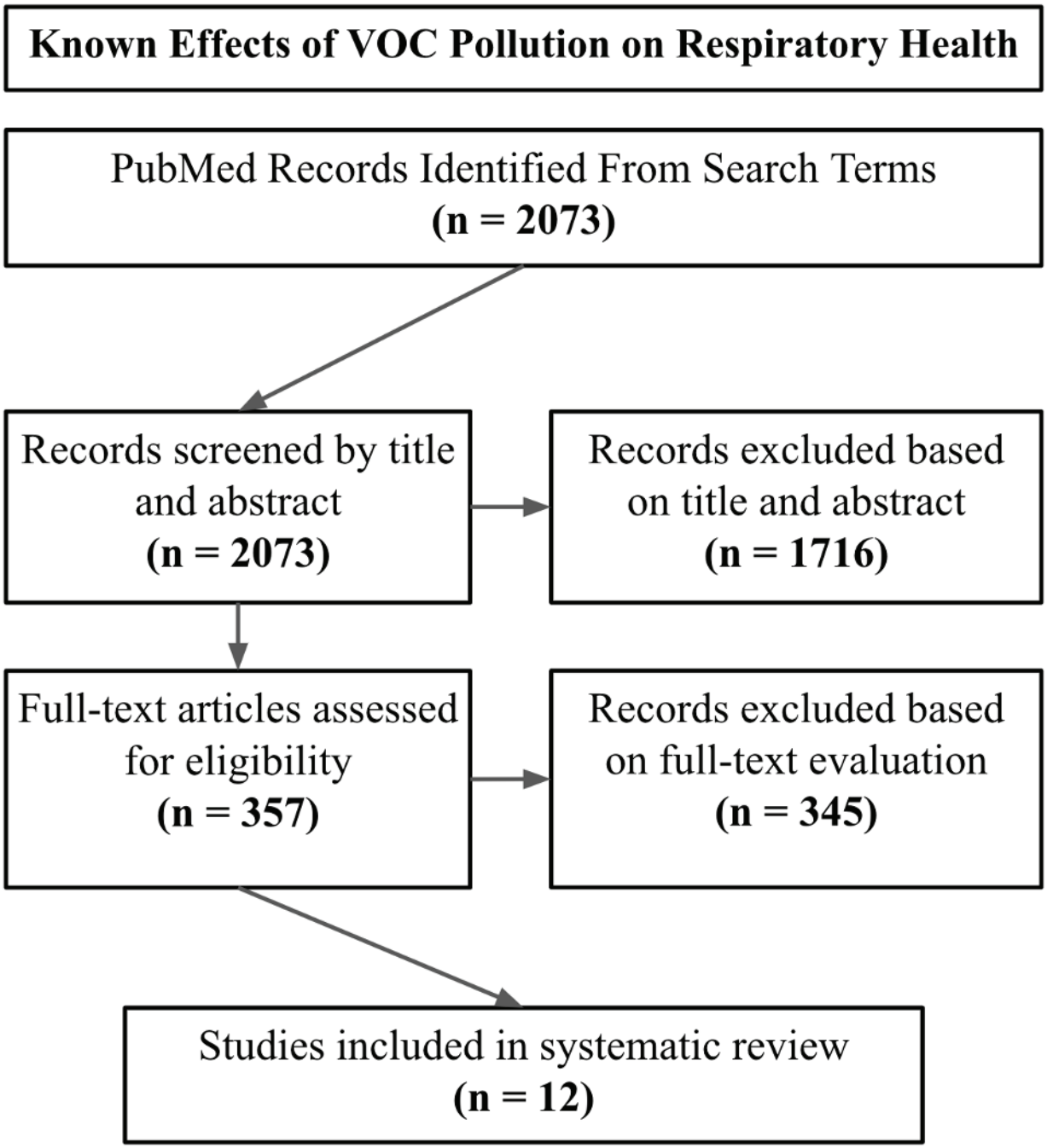

Figure 4. A sample PRISMA-compatible diagram representing the results of the VOC pollution review by Baccouche & Sevostianov (2021).

DISCUSSION

The ability of a modern researcher to centralize and expedite the systematic review process evolves from a convenience to a necessity as the rate at which scientific papers are published continues to rise. The SWIFT-Review technique, created by Howard et al. in 2016 and demonstrated within this paper, has enormous potential to scale up the scope of systematic reviews whilst simultaneously scaling down the amount of time and manual effort involved. The ease

with which additional search terms can be added to the review, combined with SWIFT-Review's ability to process tens of thousands of search results, allows the modern researcher to conduct a review of hundreds or even thousands of searches. This becomes particularly useful when a granular search is warranted, such as in the case where a researcher is interested in identifying every vertebrate species in which a particular pathological condition naturally arises and must specify hundreds of genus and species names in order to cast as comprehensive a net as possible. Additionally, the assembly of all search results into one navigable list (rather than manually clicking through search results or employing librarians and research assistants to meticulously centralize the search results) itself is long-due automation of a highly time-intensive and inefficient process. The authors conclude that SWIFT-Review can and should be used to great effect by the modern researcher to conduct efficient, systematic, and fully reproducible reviews of the literature critical to robust academic research.

AUTHOR INFORMATION

Corresponding Author

*Basil M. Baccouche
Department of Public Health and Primary Care
University of Cambridge
Strangeways Research Laboratory
Wort's Causeway
Cambridge, CB1 8RN, United Kingdom
E-mail: bmb38@medschl.cam.ac.uk

REFERENCES

Baccouche, B. M., & Sevostianov, V. I. Mechanisms of VOC Pollution-Induced Respiratory Dysfunction: A Review. *New Mexico Journal of Science*. **2020.**

Belbasis, L., Bellou, V., Evangelou, E., Ioannidis, J. P. A., & Tzoulaki, I. Environmental risk factors and multiple sclerosis: An umbrella review of systematic reviews and meta-analyses. *The Lancet. Neurology*. **2015**, 14(3), 263–273. https://doi.org/10.1016/S1474-4422(14)70267-4

Dobbins, M., Cockerill, R., Barnsley, J., & Ciliska, D. Factors of the innovation, organization, environment, and individual that predict the influence five systematic reviews had on public health decisions. *International Journal of Technology Assessment in Health Care.* **2001**, 17(4), 467–478.

Eichler, K., Hempel, S., Wilby, J., Myers, L., Bachmann, L. M., & Kleijnen, J. Diagnostic value of systematic biopsy methods in the investigation of prostate cancer: A systematic review. *The Journal of Urology*. **2006,** 175(5), 1605–1612. https://doi.org/10.1016/S0022-5347(05)00957-2

Gopalakrishnan, S., & Ganeshkumar, P. Systematic Reviews and Meta-analysis: Understanding the Best Evidence in Primary Healthcare. *Journal of Family Medicine and Primary Care.* **2013**, 2(1), 9–14. https://doi.org/10.4103/2249-4863.109934

Howard, B. E., Phillips, J., Miller, K., Tandon, A., Mav, D., Shah, M. R., Holmgren, S., Pelch, K. E., Walker, V., Rooney, A. A., Macleod, M., Shah, R. R., & Thayer, K. SWIFT-Review: A text-mining workbench for systematic review. *Systematic Reviews.* **2016**, 5. https://doi.org/10.1186/s13643-016-0263-z

Khan, K. S., Kunz, R., Kleijnen, J., & Antes, G. Five steps to conducting a systematic review. *Journal of the Royal Society of Medicine*. **2003,** 96(3), 118–121.

Prospects and Significance of Chinese Jujube (*Ziziphus jujuba*) in New Mexico: A Review

Sundar Sapkota [a)]

Sanjib Sapkota [b)]

Sen Wang [c)]

Zhiming Liu [a)*]

[a)] Eastern New Mexico University, Portales, NM

[b)] Simon Fraser University, Burnaby, Canada

[c)] Central South University of Forestry and Technology, Hunan, China

ABSTRACT

This is a review paper on the jujube plant. The jujube (*Ziziphus jujuba* Mill.) is a medium-sized tree indigenous to northern China. It is cultivated mainly for its nutritious fruits. The tree adapts well to subtropical and temperate climates and can be easily cultivated where peaches and apples grow. Prospects of jujube as a future crop are increasing in the United States, including New Mexico. However, there are only a few studies relating to jujubes reported from New Mexico. The lack of planting materials and research information are a few factors limiting its cultivation. Researchers should focus on improving propagation techniques to ensure proper supply and availability of jujube planting materials. Although New Mexico has a suitable climate for jujube, many farmers are unfamiliar with the crop due to the lack of proper extension and promotion approaches. Therefore, participatory research projects with farmers' involvement are necessary to identify and address several challenges relating to crop establishment, growth, production, post-harvest, and marketing phases. These findings could help establish jujube orchards and industries in New Mexico. Here, we review the characteristics, significance, and potential of jujube in New Mexico, USA.

KEYWORDS: Jujube, Ziziphus, Plant, Cultivation, New Mexico

INTRODUCTION

This is a review paper on the jujube plant, especially its relevance to horticulture in New Mexico. Jujube (*Ziziphus jujuba* Mill., Rhamnaceae) is a versatile deciduous tree primarily planted for edible fruit.[1] It originally grew along the Yellow River of northern China. These trees were moved to almost all parts of China and subsequently to neighboring Asian countries. Today, jujube is dispersed in approximately 50 countries all around the world, mainly in Asia, Europe, Russia, Africa, Australia, and North America.[2] Jujube easily adapts to arid and semi-arid climate at an elevation of 0–2000 m with diverse temperature ranges of 5.5–28 °C.[3,4] Its cultivation ranges from poor marginal land to fertile soil, but it does much better in

sandy loam soil with slightly acidic to alkaline soil (pH 4.5–8.4).[4,5] Jujube could survive annual precipitation of 87–2000 mm.[4] Young jujube trees in Portales, New Mexico (NM) are as shown in Figure 1.

Figure 1. Jujubes as drought-tolerant crops in Portales, NM.

Morphological and Phenomenological Behavior

Jujube is a perennial tree that reaches a height of 5–10 m. Young plants have thorns in branches (straight or curvy) but are usually absent in mature trees.[4] Green leaves are usually alternate, simple, and ovate to lanceolate. The inflorescence type is a cyme having 2–13 number of flowers. Flowers are formed in leaf axils, are short-stalked, 3.5–10 mm in diameter, and greenish-white to yellow.[4,6] Fruit type is a drupe, ellipsoid to elongate to round and bright reddish-brown. Fruit diameter ranges from 14–40 mm and differs among varieties.[4]

The management of the jujube orchard depends on the occurrence of particular growth stages. The growth stages of plants, however, vary with location, climate, and environment.[7] In Portales, NM, Sapkota et al. studied the growth stages of jujube and reported eight principal growth stages (Table 1, Figure 2).[8]

Major growth stages	Months
Bud growth	mid-March to first week of April
Leaf formation and growth	mid-April to mid-May
Shoot formation and growth	May to June
Inflorescence formation	mid-May to late June
Flowering	late-May to July
Fruiting	mid-June to mid-August
Fruit maturation	mid-August to late September
Winter dormancy	mid-October to mid-March

Table 1. Phenological stages of jujubes in Portales, NM.

The phenological knowledge might help farmers to plan and perform management practices such as irrigation scheduling, fertilizer application, timely harvesting, etc. at optimum growth stage.[9] For example, water requirement of the jujube tree is relatively higher at fruit

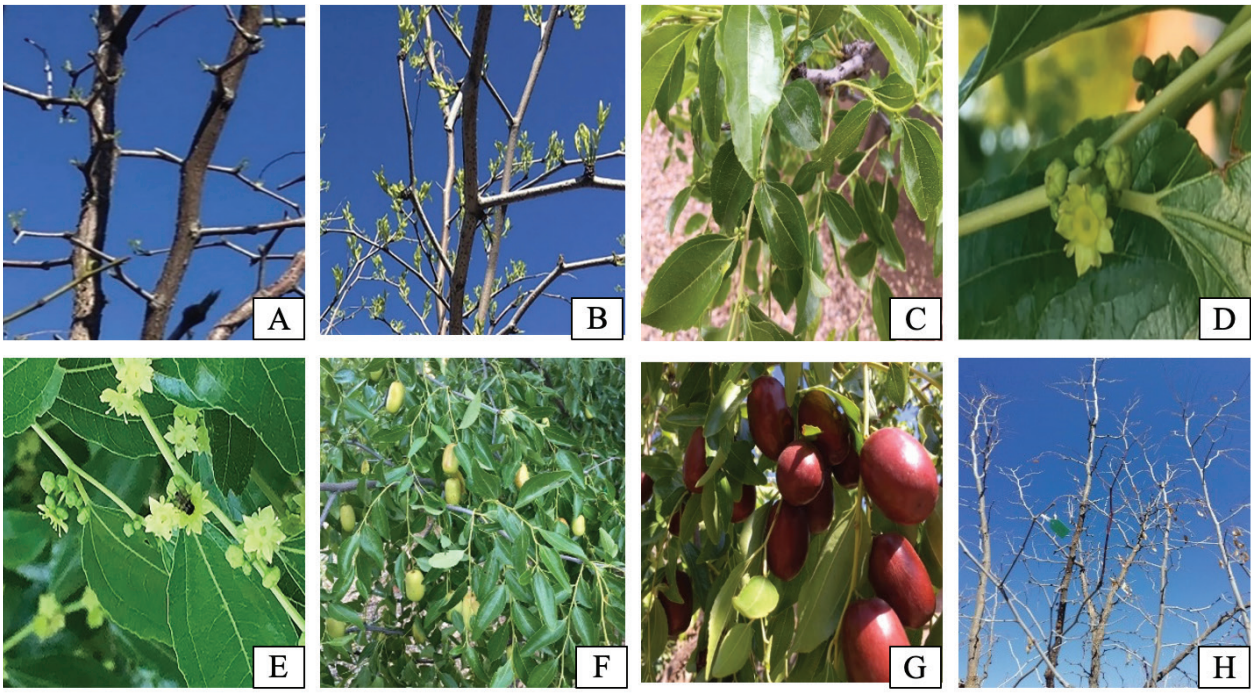

Figure 2. Major growth stages of jujube in Portales, NM: A-H refers to bud growth, leaf formation and growth, shoot growth, inflorescence formation, flowering, fruiting, fruit maturation, and winter dormancy, respectively.

setting and growth,[4] and the stage occurs from mid-June to early August in Portales, NM. Farmers may consider watering the trees during this period to get more production. Jujube phenology differs from other similar crops in NM. For example, peach and apple produce leaves in mid-February to early-March, and flowers in early to mid-April in Alcalde, NM.[10] In case of apricot, the leaf formation, flowering, fruiting, fruit growth and maturation, and harvesting stages occur in mid-Feb to early March, early to mid-March, late June to late July, depending on the cultivars.[10] Thus, the winter frost in this region is more likely to damage similar crops (peach, apple, and apricot), but jujube could skip the damage since the leaf formation and flowering stage occurs late.

Jujube Benefits and Industrial Applications

The jujube tree has several advantages: i) broad environmental adaptability, ii) provision of edible fruits, nectars, and fodder, and iii) landscape benefits.[1,11] Vegetatively propagated tree generally begins to produce fruits two years after transplantation and continues for 50 years.[12] The fruit yield of jujube ranges from 50–250 kg/tree depending on the cultivars and management practices.[12] The yield is higher compared to similar crops grown in semi-arid regions: peach (45–70 kg/tree) in Spain[13] and apricot (20–100 kg/tree) in Turkey.[14] In Alcalde, NM peach yield ranged from 12.1–67.2 kg/tree depending on cultivars.[15]

Jujube fruits are sweet and texturally similar to apple. The fruits can be consumed in fresh, dried, and processed form.[3,16] Besides, the fruits can be diversified into various products such as paste, syrup, puree, jam, candy, beverages (juice, wine, tea), powder, and confections for value addition and industrial applications.[1,3,16] Jujube also provides ecological benefits as they cover the land and reduce soil erosion.[17] The commercial uses of jujube are as shown

in Table 2. Jujube fruits are rich sources of vitamin C, minerals, and antioxidants.[22] The 100 g dried fruits contain 192-359 mg vitamin C.[23] Table 3 displays the nutritional composition of jujube fruit.[24]

Plant organ	Use/s	Reference(s)
fruits	food	1,16
wood	furniture, musical materials, cup, plate, handicrafts, agricultural equipment, fuel	1,18
leaves	tea, wine, fodder	1,19
flowers	nectar, honey	20
spiny branches	live fences	21

Table 2. Commercial uses of jujube trees.

Nutrients	Raw fruits	Dried fruits
Water (g/100 g)	77.86	20.19
Energy (kcal/100 g)	79	281
Protein (g/100 g)	1.2	4.72
Total Lipid (g/100 g)	0.2	0.5
Carbohydrates (g/100 g)	20.23	72.52
Sucrose (g/100 g)	-	8.63
Glucose (g/100 g)	-	18.28
Fructose (g/100 g)	-	20.62
Fiber (g/100 g)	-	6
Ash (g/100 g)	0.51	2.08
Calcium (mg/100 g)	21	63
Iron (mg/100 g)	0.48	5.09
Magnesium (mg/100 g)	10	-
Phosphorous (mg/100 g)	23	68
Potassium (mg/100 g)	250	217
Sodium (mg/100 g)	3	5
Zinc (mg/100 g)	0.05	0.39
Copper (mg/100 g)	0.073	-
Manganese (mg/100 g)	0.084	-
Vitamin C (mg/100 g)	69	217.6
Thiamin (mg/100 g)	0.02	0.047
Riboflavin (mg/100 g)	0.04	0.053
Vitamin B-6 (mg/100 g)	0.081	-
Vitamin A (IU/100 g)	40	-
Niacin (mg/100 g)	0.9	-

Table 3. Nutritional composition of Chinese jujube fruit based on information from USDA food and nutrient database.[24]

Jujube has great medicinal values. Almost all plant parts (root, bark, leaf, flower, fruit, and seeds) have been utilized to make drug ingredients in ancient Chinese medicine.[23,25] The fruit extract contains several bioactive compounds such as triterpenic acids (ceanothic, oleanolic,

zizybernalic, ursolic, and betulinic acids), α-tocopherol, and polysaccharides and is useful in the treatment of different types of cancers such as breast, cervical, hepatoma, lung, and ovarian.[26,27] The pharmaceutical components found in jujube and their importance in the medical field are as shown in Table 4.

Plant parts	Compound(s)	Biological activities	Reference(s)
fruits	aqueous extracts	anti-tumor, prevents breast and cervical cancer cells, reduced the growth of C643's cells (human thyroid carcinoma cells), antioxidant activity	28,29,30
	alphitolic acid	act against human cancer cells (PC-3 cells and MAD-MB-231 cells)	31
leaves	flavonoids	antidiabetic, antiaging, cardioprotective, neuroprotective, sedative,	19
	triterpenic acids	anti-inflammatory, antimicrobial, antioxidant	32,33
	polyphenols	antimicrobial, antitumor, antioxidant	34,35
seeds	flavonoids, saponins, oil, and unsaturated fatty acids	sedative and hypnotic	36,37
roots	ceanothane- and lupane-type triterpenoids	anti-cancer, anti-inflammatory, antiviral activity for human immunodeficiency virus	38

Table 4. Pharmaceutical components found in jujube.

Propagation Techniques

The seedlings produced from jujube seeds require a longer period to reach the fruit-bearing stage. Thus, seed germinated seedlings are generally not used to grow fruit trees for commercial orchards directly, but one-year-old seed germinated seedlings are used as a rootstock for grafting propagation.[39,40] Previous study has reported that jujube seeds have a germination rate of 5% at room temperature and 37% at 30 °C.[41] Propagation success has also been achieved with jujube softwood cuttings. Xiang-dong reported wild jujube softwood cuttings had 32% (no hormone treated), 74% (3000 mg/L NAA) and 64% (3000 mg/L IAA) rooting success.[42] Several propagation techniques have been reported for the jujube plant (Table 5).

Propagation	Location	Methods	Key research finding(s)	Ref
grafting	Korea	Compared 7 techniques (chip budding, whip and tongue graft, bark graft, splice graft, standard ono graft, modified rootstock ono graft, and modified scion ono graft) without hormonal treatments	Bark graft resulted 100% propagation success (~5 weeks) followed by modified scion ono (58.33%). Similarly, bark, modified, splice, and modified scion ono graft had produced comparatively higher emergence of vegetative shoots (100, 47.6, and 33.3%), respectively	43
Branch cuttings	China	Stem cuttings (15 cm long, taken from secondary shoots) were treated with water (control) and IBA (500, 1000, 1500 mg/L) for 5 seconds, and inserted in sand	Cuttings dipped in 1500 mg/L IBA yielded best rooting after 20 days of treatment (rooting = 93.3%, average number of roots = 4.35, average root length = 17.64 mm)	44
Micro propagation	Turkey	Used two types of jujube genotypes (20-C-52 and 20-c-51) and different combinations of plant growth hormones	All the jujube shoots explants (100%) cultured in Murashige and Skoog medium containing 0.1 mg /L thidiazuron (TDZ) + 0.5 mg /L BAP + 0.1 mg /L indole butyric acid (IBA) + 0.3 mg /L gibberellic acid nutrients produced shoots (M = 5.5)	45
Seed propagation	Turkey	Jujube seeds were subjected to seven treatments (control, hot water (45 °C for 30 min), water (for 24 hour), scarification, sulfuric acid (30 min) plus water treatments (24 hour), dehulled damaged membrane, and dehulled seeds)	Dehulled seeds had the greatest germination rate (63.3%) followed by scarification treatment (50%) whereas control (no treatment) had lowest germination (3.3%)	46

Table 5. Propagation techniques for jujube.

Jujubes in New Mexico

The published statistics on detailed crop information such as cultivated area, production, import/export, and market in NM are not yet available. Interestingly, the demand for jujube fruits has been growing, probably due to an increasing number of Asian people, changing consumer preferences, and growing education on the taste, nutritional, and medicinal values of the fruit; however, the supply is short. Many regions of the US, including NM, have great potential to produce jujubes at a volume high enough to meet domestic demand,[6,8,47] but the lack of research facilities and extension services has restricted its commercial cultivation.

To our knowledge, at present, New Mexico has jujube orchards in four different locations: Alcalde, Los Lunas, Leyendecker, and Portales (establishing phase); and all of them are oriented for research activities. Additionally, scattered jujube trees are found in Las Cruces and Tucumcari. Information on farmer-owned jujube orchards is unavailable. Limited plant cultivars, difficulties in plant propagation likely due to the hard seed coat,[46,48] and poor marketing/extension are few factors for the infrequent cultivation of jujube in the United States.[8,47] Grafting (bark and whip)[6] and root suckers[47] are currently being used in the United States for jujube propagation. To our understanding, tissue culture technique has a great potentiality to address the shortage of jujube saplings, but it requires sophisticated technology, skilled manpower and is relatively expensive.

THE MOST RECENT RESEARCH ACTIVITIES ON JUJUBE IN NEW MEXICO

Considering the multiple benefits of jujube, two universities, New Mexico State University (NMSU) and Eastern New Mexico University, have initiated jujube research projects. The past and current research in NM have focused on cultivar trials, fruit nutrient dynamics, and plant propagation. For example, Yao et al. conducted trials taking nineteen drying and multipurpose jujube cultivars (including 'Kongfucui', 'Sihong', 'Jinkuiwang', 'Lang', and 'Xiangzao') at three different locations in NM (Alcalde, Leyendecker, and Los Lunas),[49] found jujube performance varied with location, and reported the most suited cultivar to particular locations in terms of higher fruit yield: 'Kongfucui' (13.3 kg/tree) for Alcalde, Jinkuiwang (12.31 kg/tree) for Leyendecker, and Jinsi-2 (8.37 kg/tree) for Los Lunas.[49] The authors further mentioned that all experimented cultivars did better in terms of fruit yield and nutrients contents (total soluble solids) at Leyendecker than Alcalde and Los Lunas. Based on their studies, the researchers suggested not to cultivate drying cultivars at Alcalde that are best suited to Los Lunas and Leyendecker.

A similar experiment with 4 ornamental jujube cultivars (3 years old) at Alcalde and Los Lunas reported relatively higher fruit yield for 'Teapot' (4.536 kg/tree) followed by 'Mushroom' (3.629 kg/tree), 'So' (1.724 kg/tree), and 'Dragon' (0.091 kg/tree).[50] Despite lower yield, 'Dragon' produced comparatively larger flowers than others.[50] Among tested cultivars, 'Teapot' had higher soluble sugar content (31.7% at Alcalde and 32.2% at Los Lunas) and vitamin C (313 mg/100 g fresh weight in Alcalde). According to Yao and Heyduck, 'So' and 'Dragon' cultivars can serve as year-round ornamentation whereas 'Mushroom' and 'Teapot' provide ornamentation for three seasons.[50] We think more multilocation cultivar research trials should be carried out in NM to recommend region-specific cultivars for farmers.

Huang et al. evaluated the nutrient dynamics (46 jujube cultivars) and vitamin C content (10 cultivars) of jujube fruits at Alcalde and Los Lunas and found a relatively higher vitamin C content for 'Youzao' cultivar with a value of 820 mg/100 g fresh jujube.[51] According to the authors, the soluble solid contents and titratable acidity of evaluated fruits were in the range of 27.2–33.7% and 0.27–0.46%, respectively. Furthermore, Sapkota et al. performed jujube propagation experiments in 2019 at Portales, NM using four different categories of jujube root suckers (height and diameter: <50 cm and 0.15–0.35 cm, 50–100 cm and 0.36–0.75 cm, 100–150 cm and 0.76–1.25 cm, and >150 cm and 1.26–2.45 cm, respectively).[47] The authors found that the sucker (height of 50-100 cm and diameter of 0.36–0.75 cm) had the greatest field survivability (84%) followed by the sucker category (height of 100–150 and diameter of 0.76–1.25 cm) (67%). Their work emphasized that the size of the planting material is one of the major factors determining crop establishment in field conditions.

To date, no economic pest damage was reported for jujube in NM with the exception of Yao observation of peach moth incidence to sour jujube fruits (but not significant loss) at Las Cruces.[6] However, a few insect and disease damaging jujube were reported from other countries: peach moth in China[52] and Korea[53] and witches' broom in China[54] and Korea.[55]

Because the jujube crop is relatively new to most New Mexican farmers, we think research related to propagation, crop physiology, cultivation, and orchard establishment, simulated with extension services, might encourage them to start planting jujubes. Furthermore, such studies might provide growers with information useful for planting and to deal with the challenges that may be encountered in the process of crop cultivation. Additionally, research studies on jujube genetics, breeding, and pests should be considered to develop better cultivars and minimize the potential cultivation problems in the future.

SIGNIFICANCE AND POTENTIAL OF JUJUBE IN NEW MEXICO

New Mexico generally experiences semi-arid climate (hot summer, mild winter) and most of the land in this region is dry. The past 10 years (2010-2019) climate data (https://www.ncdc.noaa.gov/cdo-web)[56] show that Portales, NM experiences an annual average temperature of 15.85 °C, an average minimum temperature of 4.25 °C (January), an average maximum temperature of 26.86 °C (July), and the total average annual precipitation of 520.65 mm. Interestingly, New Mexico has a very similar climate to the Shaanxi area of China (average annual temperature: 12.5 °C, precipitation: 632 mm)[57] where jujube has been widely cultivated. As such, it is possible to cultivate jujube in NM's environment with good production. Even though New Mexico's elevation permits the growth of many other temperate crops (such as apple, peach, and pear), late winter frost/snow is the major threat to these crops. Late spring cold fronts in NM often damage flowers, block pollination, and cause heavy losses to fruit growers.[58] Yao and Welser reported that the winter frost in 2011 heavily damaged the flower buds of peaches in Alcalde, NM; leaving a varying percentage of live flower buds ranged from 11% ('Blazingstar' cultivar) to 85% ('Encore' cultivar).[15] Moreover, Yao et al. shared their experience of not harvesting any apricot fruits for years (2001-2014) due to frost damage in Alcalde, NM.[58] Notably, jujube remains physiologically dormant during winter, produces leaves 1–2 months later than similar fruit trees (e.g., peach), and could easily skip the frost damage and injury.

Reports indicated that the water table of New Mexico is very low,[59,60] and well-designed irrigation facilities have yet to be constructed in different regions. Jujube, after field establishment, can tolerate very high temperatures and requires much less water supply as it has deeper vertical roots (as deep as 13 m).[4] Water requirements for jujube is variable depending on location. Liu mentioned that jujube can survive and produce a satisfactory yield in arid to semi-arid regions of northeast China with under 200 mm annual rainfall.[4] Similarly, in Shanxi, China, an application of an annual volume of 33.33 mm water resulted in the desirable root traits of jujube trees (12-years).[61] For rainfed areas in western Australia, jujube has been growing well with a yearly rainfall of 200-1000 mm.[5] We were unable to find the information relating to water requirements of similar crops in NM, but researchers from other regions have reported such information. According to Zambrano et al., the daily water demand of young (3-years) peach trees from August to October in 2018 was 23.7 L per tree and total cumulative water consumption was 731 mm (January to October) in Florida.[62] In drier regions of California, peach requires annual irrigation of 1034 mm.[63]

Jujube does not demand intensive care.[4] Timely irrigation, fertilization, pruning, mulching, and weeding are suggested to get maximum potential yield from trees. The nature of the jujube plant to perform satisfactorily even in dry and alkaline soil makes it most suited for cultivation in the southwestern US.[3] Additionally, expanding desertification and decreasing water sources in the future may increase jujube's importance as a fruit product.

There have been raising concerns about plant species becoming invasive to the new area. Azam-Ali et al. mentioned that uncontrolled propagation may convert jujube to weedy species for a particular region.[39] Jujube can spread through seeds (via birds and animals)[64] and root suckers.[65] To date, no reports are available for Chinese jujube acting as invasive species and harming other plant/animal species in NM. But, literature indicated that Indian jujube is becoming weedy species in Florida, USA[66] and Queensland, Australia.[64]

Short-term and long-term strategies should be made to assess the potential risk status of jujube (for example, no risk at all, low risk, moderate risk, high risk, etc.) for becoming invasive to a particular ecological range, and proper preventative as well as control measures may be required to tackle the potential problems. Additionally, the growers, researchers, and other authorized bodies should be made aware of the above-mentioned potential challenges. We think with proper planning, the cultivation of jujube would help cover hectares of fallow lands in NM along with economic and ecological benefits (for example, soil cover, erosion control, etc.). In short, jujube could be a great prospective future crop in NM.

CONCLUSION

Jujube is a versatile fruit tree rich in nutritional and medicinal properties. The crop's physiology and agronomic requirements suggest that it could be a well-adapted fruit tree in semi-arid regions throughout the United States, including NM. Aside from its use as a raw fruit, jujube has high industrial value for processing and diversification. With respect to commercial cultivation, participatory research trials should be carried out to encourage farmers and small enterprises. On the other hand, crop breeders could help extend jujube cultivation by creating jujube varieties with better yield, quality, stress-resistance, and broad environmental

adaptation. At present, in the United States, improved propagation strategies are needed to ensure the adequate supply of planting materials.

We think jujubes could contribute to farmers' income and food security as the trees grow and produce good yields even with drought and poor marginal lands that, in most cases, are unsuitable for other crops. To achieve such benefits, jujube research programs that involve farmers from the initial phase are needed to identify and tackle different challenges during crop establishment, growth, and production. Better extension and promotional techniques could encourage both farmers and other professionals to plant at least a few jujube trees (maybe one or two or many) in their yard and get multiple benefits (fruits, shade, landscape, etc.). With adequate research and marketing facilities, the NM environment guarantees sustainable jujube production in the near future.

AUTHOR INFORMATION

Corresponding Author

*Zhiming Liu, zhiming.liu@enmu.edu

REFERENCES

(1) Outlaw, W. H.; Zhang, S.; Riddle, K. A.; Womble, A. K.; Anderson, L. C.; Outlaw, W. M.; Outlaw, N. N.; Outlaw, E. C.; Thistle, A. B. The Jujube (*Ziziphus jujuba* Mill.), A Multipurpose Plant. *Econ. Bot.* **2002,** *56* (2), 198–200.

(2) Xiao, J.; Zhao, J.; Liu, M.; Liu, P.; Dai, L.; Zhao, Z. Genome-Wide Characterization of Simple Sequence Repeat (SSR) Loci in Chinese Jujube and Jujube SSR Primer Transferability. *PLoS One* **2015**, *10* (5), 1–13.

(3) Thomas, C. C. The Chinese Jujube.*US Department of Agriculture Bulletin No. 1215*, Washington, D.C, **1924**, 1–30.

(4) Liu, M. Chinese Jujube: Botany and Horticulture. *Hortic. Rev.* **2006**, *32*, 229–298.

(5) Crawford, R.; Shan, F. C.; McCarthy, A. Chinese Jujube: A Developing Industry in Australia. *Acta Hortic.*, **2013**, *993*, 29–36.

(6) Yao, S. Past, Present, and Future of Jujubes—Chinese dates in the United States. *HortScience* **2013**, *48* (6), 672–680.

(7) Fitchett, J. M.; Grab, S. W.; Thompson, D. I. Plant Phenology and Climate Change: Progress in Methodological Approaches and Application. *Prog. Phys. Geogr.* **2015**, *39* (4), 460–482.

(8) Sapkota, S.; Sapkota, S.; Wang, S.; Liu, Z. Phenological Study of Chinese Jujube Trees Using Biologische Bundesanstalt, Bundessortenamt and CHemische Industrie (BBCH) Scale. *J. Hortic. Sci. Res.* **2020**, *3* (1), 68–73.

(9) Kishore, K. Phenological growth Stages of Dragon Fruit (*Hylocereus Undatus*) According

to the Extended BBCH-Scale. *Sci. Hortic.* **2016**, *213*, 294–302.

(10) Yao, S. Jujube Phenology, Pollen Germination, and Two Unique Germplasm Resources in New Mexico. *HortScience* **2018**, *53 (*1), 23–27.

(11) Galindo, A.; Cruz, Z. N.; Rodríguez, P.; Collado-González, J.; Corell, M.; Memmi, H.; Moreno, F.; Moriana, A.; Torrecillas, A.; Perez-Lopez, D. Jujube Fruit Water Relations at Fruit Maturation in Response to Water Deficits. *Agric. Water Manag.* **2016**, *164,* 110–117.

(12) Meena, S.; Meena, H. P.; Meena, R. S. Diversified Uses of Ber (*Ziziphus* spp.). *Popular Kheti* **2014**, *2* (1), 154–159.

(13) Jiménez, C. M.; Díaz, J. B. R. A Statistical Model to Estimate Potential Yields in Peach Before Bloom. *J. Am. Soc. Hortic. Sci.* **2003**, *128* (3), 297–301.

(14) Asma, B. M.; Ozturk, K. Analysis of Morphological, Pomological and Yield Characteristics of Some Apricot Germplasm in Turkey. *Genet. Resour. Crop Evol.* **2005**, *52* (3), 305–313.

(15) Yao, S., Walser, R. "Peach Cultivar Evaluation in Northern New Mexico." *Saturn* **2012**, *109*, 16–6.

(16) Gao, Q. H.; Wu, C. S.; Wang, M. The Jujube (*Ziziphus jujuba* Mill.) Fruit: A Review of Current Knowledge of Fruit Composition and Health Benefits. *J. Agric. Food Chem.* **2013**, *61*(14), 3351–3363.

(17) Wu, C. S.; Gao, Q. H.; Kjelgren, R. K.; Guo, X. D.; Wang, M. Yields, Phenolic Profiles and Antioxidant Activities of *Ziziphus jujuba* Mill. in Response to Different Fertilization Treatments. *Molecules* **2013**, *18* (10), 12029–12040.

(18) Arndt, S. K.; Clifford, S. C.; Popp, M. *Ziziphus*—A Multipurpose Fruit Tree for Arid Regions. *Sustainable Land Use in Deserts*. Springer, Berlin, Heidelberg, **2001**, 388–399.

(19) Zhang, R.; Chen, J.; Shi, Q.; Li, Z.; Peng, Z.; Zheng, L.; Wang, X. Phytochemical Analysis of Chinese Commercial *Ziziphus jujuba* Leaf Tea Using High Performance Liquid Chromatography–Electrospray Ionization-Time of Flight Mass Spectrometry. *Food Res. Int.* **2014**, *56*, 47–54.

(20) Crane, E.; Walker, P.; Day, R. Directory of Important World Honey Sources. *International Bee Research Association*, London, UK. **1984**, 384.

(21) Jones, H. G. Selection of Drought-Tolerant Fruit Trees for Summer Rainfall Regions of Southern Africa and India. *European Commission STD-3, Brussels, Belgium: CTA*, **1999**, 118–120.

(22) Pareek, S. Nutritional Composition of Jujube Fruit. *Emir. J. Food Agric.* **2013**, 463–470.

(23) Li, J. W.; Fan, L. P.; Ding, S. D.; Ding, X. L. Nutritional Composition of Five Cultivars of Chinese Jujube. *Food Chem.* **2007**, *103* (2), 454–460.

(24) United States Department of Agriculture (USDA). USDA Food and Nutrient Database, **2018**, https://fdc.nal.usda.gov/fdc. Accessed May 12 2020.

(25) Shahrajabian, M. H.; Khoshkharam, M.; Zandi, P.; Sun, W.; Cheng, Q. Jujube, A Super-Fruit in Traditional Chinese Medicine, Heading for Modern Pharmacological Science. *J. Med. Plants Stud.* **2019**, *7* (4), 173–178.

(26) Choi, S. H.; Ahn, J. B.; Kim, H. J.; Im, N. K.; Kozukue, N.; Levin, C. E.; Friedman, M. Changes in Free Amino Acid, Protein, and Flavonoid Content in Jujube (*Ziziphus jujuba*) Fruit During Eight Stages of Growth and Antioxidative and Cancer Cell Inhibitory Effects by Extracts. *J Agric. Food Chem.* **2012**, *60* (41), 10245–10255.

(27) Tahergorabi, Z.; Abedini, M. R.; Mitra, M.; Fard, M. H.; Beydokhti, H. "*Ziziphus jujuba*": A Red Fruit with Promising Anticancer Activities. *Pharmacogn. Rev.* **2015**, *9* (18), 99–106.

(28) Zhao, H. X.; Zhang, H. S.; Yang, S. F. Phenolic Compounds and Its Antioxidant Activities in Ethanolic Extracts from Seven Cultivars of Chinese Jujube. *Food Sci. Hum. Wellness* **2014**, *3*, 183–190.

(29) Abedini, M. R.; Erfanian, N.; Nazem, H.; Jamali, S.; Hoshyar, R. Anti-proliferative and Apoptotic Effects of *Ziziphus jujuba* on Cervical and Breast Cancer Cells. *Avicenna J. Phytomed.* **2016**, *6* (2), 142–148.

(30) Dabaghian, F. H.; Hassani, A.; Nayeri, N. Shojaii, A.; Entezari, M. Anti-Proliferative and Apoptotic Effects of Aqueous Extract of *Ziziphus jujuba* in Human Thyroid Carcinoma Cell Lines (C643). *Int. J. Cancer Manag.* **2018**, *11* (7), 1–7.

(31) Shin, M.; Lee, B.M.; Kim, O.; Tran, H.N.K.; Lee, S.; Hwangbo, C.; Min, B.S.; Lee, J.H. Triterpenoids from *Ziziphus jujuba* Induce Apoptotic Cell Death in Human Cancer Cells Through Mitochondrial Reactive Oxygen Species Production. *Food Funct.* **2018**, *9* (7) 3895–3905.

(32) Guo, S.; Duan, J. A.; Tang, Y.; Qian, Y.; Zhao, J.; Qian, D.; Su, S.; Shang, E. Simultaneous Qualitative and Quantitative Analysis of Triterpenic Acids, Saponins and Flavonoids in the Leaves of Two *Ziziphus* Species by HPLC–PDA–MS/ELSD. *J. Pharm. Biomed. Anal.* **2011**, *56* (2), 264–270.

(33) Damiano, S.; Forino, M.; De, A.; Vitali, L.A.; Lupidi, G. Taglialatela-Scafati, O. Antioxidant and Antibiofilm Activities of Secondary Metabolites from *Ziziphus jujuba* Leaves Used for Infusion Preparation. *Food Chem.* **2017**, *230*, 24–29.

(34) Kim, Y. J.; Son, D.Y. Hot Water Leaves Extracts of *Zizyphus jujuba* Exert Antioxidative Effects *In Vitro* and Cytotoxicity in Human Cancer Cell Lines. *Hortic. Environ. Biotechnol.* **2011**, *52* (6) 635–640.

(35) Naz, S.; Sultana, B.; Shahid, M. Alteration in Antioxidant and Antimicrobial Attributes of Leaves of *Zizyphus* Species in Response to Maturation. *J. Med. Plants Res.* **2013**, *7* (2), 61–70.

(36) Choi, S. H.; Ahn, J. B.; Kozukue, N.; Levin, C. E.; Friedman, M. Distribution of Free Amino Acids, Flavonoids, Total Phenolics, And Antioxidative Activities of Jujube (*Ziziphus jujuba*) Fruits and Seeds Harvested from Plants Grown in Korea. *J. Agric. Food Chem.* **2011**, *59* (12), 6594–6604.

(37) Jiang, J. G.; Huang, X. J.; Chen, J.; Lin, Q. S. Comparison of the Sedative and Hypnotic Effects of Flavonoids, Saponins, and Polysaccharides Extracted from Semen *Ziziphus jujuba*. *Nat. Prod. Res.* **2007**, *21* (4), 310–320.

(38) Kang, K. B.; Kim, J. W.; Oh, W. K.; Kim, J.; Sung, S. H. Cytotoxic Ceanothane-and Lupane-Type Triterpenoids from the Roots of *Ziziphus jujuba*. *J. Nat. Prod.* **2016**, *79* (9), 2364–2375.

(39) Azam-Ali, S.; Bonkoungou, E.; Bowe, C.; deKock C.; Godara, A.; Williams, J. T. Ber and Other Jujubes. *International Centre for Underutilized Crops*, Southampton, UK **2006**, *2*, 1–289.

(40) Johnstone, R. Propagating Jujubes. *Department of Agriculture and Food,* Western Australia. **2016**, 1–10.

(41) Laamouri, A.; Ammari, Y.; Albouchi, A.; Dachraoui, A.; Yakoubi, M. T. Studies on Seed Germination of Tunisian Jujubes. *Acta Hortic.* **2009**, *840*, 315–320.

(42) Xiang-dong, C. U. I. Research on the Technique of Wild Jujube Softwood Cutting [J]. *J. Anhui Agric. Sci.* **2009**, *28*. [in Chinese with English abstract].

(43) Park, H. S.; Kim, Y. K.; Chung, K. H.; Ahn, Y. H. Effective Grafting Method for Korean Jujube Nursery Tree. *J. Environ. Sci. Int.* **2003**, *12* (2), 119–124.

(44) Shao, F.; Wang, S.; Huang, W.; Liu, Z. Effects of IBA on the rooting of branch cuttings of Chinese jujube (*Zizyphus jujuba* Mill.) and changes to nutrients and endogenous hormones. *J. For. Res.* **2018**, *29* (6), 1557–1567.

(45) Yıldırım, A. N.; Şan, B.; Yıldırım, F.; Ecevit, F. M.; Ercişli, S. Micropropagation of Promising Jujube (*Ziziphus jujuba* Mill.) Genotypes. *Erwerbs-Obstbau* **2015**, *57* (3), 135–140.

(46) Gozlekci, S.; Adak, N.; Tozlu, I. Influence of Seed Pre-Treatments on Seed Germination and Early Seedling Developments of Jujube (*Ziziphus jujuba* Mill.). *Acta Hortic.* **2019**, *1242*, 321–326.

(47) Sapkota, S.; Sapkota, S.; Wang, S.; Liu, Z. Height and Diameter Affect Survival Rate of Jujube Suckers Transplanted in a Semi-Arid Farmland of New Mexico. *J. Appl. Hortic.* **2019**, *21* (3), 249–251.

(48) Karimpour, S.; Davarynejad, G. H.; Rouhbakhsh, H.; Ardakani, E. Data on Scarification and Stratification Treatments on Germination and Seedling Growth of *Ziziphus jujuba* Seeds. *Adv. Environ. Biol.* **2013**, *7* (3), 501–505.

(49) Yao, S.; Heyduck, R.; Guldan, S.; Sapkota, G. Early Performance of Jujube Drying and Multipurpose Cultivars in the Southwestern United States. *HortScience* **2020**, *55* (11), 1804–1810.

(50) Yao, S.; Heyduck, R. Ornamental jujube cultivar evaluation in the Southwestern United States. *Horttechnology* **2018**, *28* (4), 557–561.

(51) Huang, J.; Heyduck, R.; Richins, R. D.; VanLeeuwen, D.; O'Connell, M. A.; Yao, S. Jujube Cultivar Vitamin C Profile and Nutrient Dynamics during Maturation. *HortScience* **2017**, *52* (6), 859–867.

(52) Zhang, Z.; Li, X.; Xue, Y.; Zhao, Z.; Li, J.; Ma, R. Increased Trapping Efficiency for the Peach Fruit Moth *Carposina sasakii* (Matsumura) with Synthetic Sex Pheromone. *Agric. For. Entomol.* **2017**, *19* (4), 424–432.

(53) Lee, S. K.; Lee, K. H.; Oh, H. K.; Lee, J. W.; Kim, C. W.; Kang, H. J.; Kim, S. H. Effects of Insect Screen Net on Insect Pest Control for Jujube. *Korean J. Org. Agric.* **2017**, *25 (*3), 619–630. [in Korean with English abstract]

(54) Wang, J.; Song, L.; Jiao, Q.; Yang, S.; Gao, R.; Lu, X.; Zhou, G. Comparative Genome Analysis of Jujube Witches'-Broom Phytoplasma, An Obligate Pathogen that Causes Jujube Witches' Broom Disease. *BMC Genomics* **2018**, *19 (*1), 1–12.

(55) Brown, W. M.; Moon, D. S. Control of Witches'-Broom Disease of Jujube with Oxytetracycline Injection. *Korean J. Appl. Entomol.* **1976**, *15* (3), 107–110. [in Korean with English abstract]

(56) National centers for environmental information. https://www.ncdc.noaa.gov/cdo-web. Accessed 12 November 2020.

(57) Feng, Y.; Cui, N.; Du, T.; Gong, D.; Hu, X.; Zhao, L. Response of Sap Flux and Evapotranspiration to Deficit Irrigation of Greenhouse Pear-Jujube Trees in Semi-Arid Northwest China. *Agric. Water Manag.* **2017**, *194*, 1–12.

(58) Yao, S.; Guldan, S.; Heyduck, R. High Tunnel Apricot Production in Frost-prone Northern New Mexico. *HortTechnology* **2019**, *29 (*4), 457–460.

(59) Wilson, C. R. Water Conservation and Use Report. City of Portales, **2019**, 1–142.

(60) Rawling, G. C. A Hydrogeologic Investigation of Curry and Roosevelt Counties, New Mexico. *Aquifer Mapping Program, New Mexico Bureau of Geology and Mineral Resources* **2016**, 1–54.

(61) Ma, L. H.; Liu, X. L.; Wang, Y. K. 2013. Effects of Drip Irrigation on Deep Root Distribution, Rooting Depth, and Soil Water Profile of Jujube in a Semiarid Region. *Plant Soil* **2013**, *373*, 995–1006.

(62) Zambrano-Vaca, C.; Zotarelli, L.; Beeson Jr, R. C.; Morgan, K. T.; Migliaccio, K. W.; Chaparro, J. X.; Olmstead, M. A. Determining Water Requirements for Young Peach Trees in a Humid Subtropical Climate. *Agric. Water Manag.* **2020**, *233*, 1–7.

(63) Ayars, J. E.; Johnson, R. S.; Phene, C. J.; Trout, T. J.; Clark, D. A.; Mead, R. M. Water Use by Drip-Irrigated Late-Season Peaches. *Irrig. Sci.* **2003**, *22,* 187–194.

(64) Grice, A. C. Ecology in The Management of Indian Jujube (*Ziziphus mauritiana*). *Weed Sci.* **1998**, *46* (4), 467-474.

(65) Krewer, G. W.; Crocker, T. F.; Bertrand, P. F.; Horton, D. L. Minor Fruits and Nuts in Georgia.*University of Georgia, Cooperative Extension Service Bulletin* **2009***, 992,* 1–16.

(66) Sellers, B. Biology and Control of Indian Jujube (*Ziziphus mauritiana*): A Weed to Watch in Florida Pastures and Natural Areas. *IFAS Extension Service, University of Florida* vol. **2008**, *2008* (6), 1–3.

Measuring Hydrodynamic Drag of Swimsuits Using Acoustic Doppler Velocimetry

Anita X. Sumali [a)*]

Smriti Chaulagain [b)]

Mario F. Sumali [c)]

Mark C. Stone [b)]

[a)] Texas A&M University, College Station, TX

[b)] University of New Mexico, Albuquerque, NM

[c)] La Cueva High School, Albuquerque, NM

ABSTRACT

Some scientific publications (e.g., Luo et al., 2015) mention that expensive Fastskin swimsuits have a special texture to lower hydrodynamic drag and give an advantage in swimming competitions. Our research attempted to investigate that claim. In particular, we measured the skin drag (part of the total passive drag) of different swimsuits using an experimental flume and an Acoustic Doppler Velocimeter (ADV). In the boundary layer, downstream velocity was measured at several distances from the swimsuit surface. The resulting plot of velocity versus distance was curve-fit with an exponential function that decays towards the free-flow velocity as distance increases. From the decay exponent, a metric of drag (proportional to the shear stress on the swimsuit surface) was derived to characterize the skin drag of the swimsuit. Finally, the metric was plotted against the prices of the swimsuits. The result indicates that a more expensive swimsuit does not necessarily give less skin drag than a less expensive swimsuit. We discovered that velocity readings from the ADV near the boundary is biased, and explain that the bias applies consistently to all the swimsuits we tested. Therefore, our conclusion is not affected by the bias.

KEYWORDS: Aquatic Sport, Swimwear, Friction, Flume, Signal Convolution

INTRODUCTION

Morrison (2012) reports that a racing swimsuit reduces drag by 16.6% and therefore increases swimming speed. The racing swimsuit is several times more expensive than average swimsuits. Moreover, that racing swimsuit is excessively tight, uncomfortable, and takes a lot of effort to put on or take off (an average of 30 - 45 minutes with the help of one or more assistants (Mountjoy et al., 2009)). Although many swimmers claim to feel faster racing in an expensive swimsuit than in a regular practice swimsuit (Mooney, 2012), to our knowledge there has not been any scientific proof that indicates a relationship between the cost of swimsuits and the suits' speed through the water. Our research was designed to test the belief that more expensive swimsuits have lower drag.

BACKGROUND LITERATURE

Prior to the 2004 Athens Olympic Games, Krieger (2004) investigated the performance of the then-new "Fastskin" swimsuit which were becoming extremely popular among competitive swimmers. Bixler (2007) modelled the fluid dynamics for the swimsuit manufacturer and reported that the design reduced the passive drag force, thereby enabling the wearer to swim faster. Krieger mentions a statistical model of Olympic swimming time average improvement over time. The model was able to tell if an unexpected improvement was drastic enough to be an outlier such as a new doping method. The model was used to analyze the swimming times of swimmers wearing a new Fastskin swimsuit in competitions and did not show that the new swimsuit actually resulted in a revolutionary performance improvement. Krieger's report might be evidence that the new competition swimsuits were not likely to cause a radical improvement in swimming time. In fact, preliminary data from the 2000 Sydney Olympics showed that a small group that wore the Fastskin showed slightly poorer time than another small group that wore conventional suits.

Luo et al. (2015) mentions that special swimsuit surface textures emulate shark skin and reduce drag. Zhang et al. (2011) shows that the shark skin surface effectively inhibits turbulence in the water, and as a result reduces the wall friction. Their article discusses experiments and computer simulations to understand the mechanism of drag reduction. It shows a method to simulate the turbulent flow on grooved-scale surfaces. The numerical simulation is based on the real biological shark skin, through an accurate scanning of the surface using a scanning electron microscope. The simulation result explains the drag reduction mechanism. To validate the model of the drag-reducing effect of the shark skin surface, Zhang et al. performed measurements of drag forces on their textured versus non-textured surfaces in a water tunnel. The experimental results are fairly consistent with the numerical simulation. Bixler and Bhushan (2013) measured drag forces on surfaces with various "riblets" designed to emulate the pattern of the scales on the skin of the shark. Bixler and Bhushan conclude that scalloped riblets with a staggered configuration are similar to the shark skin. Compared to smooth surfaces, riblets of certain geometry and spacing are able to reduce water drag forces by up to 5%. This result shows that it is possible that the texture of the shark skin results in lower drag forces compared to smooth surfaces.

Benjanuvatra et al. (2002) examined the drag forces of full-length Fastskin swimsuits and compared them with those of standard swimsuits using a cross-sectional comparison completed with nine Australian national-level (elite) swimmers. The data suggested that the full-length Fastskin swimsuits created less total hydrodynamic resistance than normal swimsuits. The study focuses on drag during surface towing, which is much more complex than drag on fully-immersed body. A moving body on the water surface introduces complex surface wave drags (Mollendorf et al., 2004). More importantly, the use of human swimmers would introduce unwanted variability in the results, which may well overwhelm the difference in drags between Fastskin and regular swimsuits. Toussaint et al. (2002) presented a thorough analysis of drag forces on swimmers including measurements on several swimmers under numerous motions and conditions. They developed sophisticated methods to measure drags, including the system to "measure active drag" (MAD-system) and velocity perturbation method (VPM), among other techniques that will advance drag measurement technology for swimmers. An important point learned from their article is that active drag (the drag

on moving swimmers) is far more complex than we will be able to measure and analyze. In our research, we measure the drag contribution from the swimsuit only, not the overall drag during swimming. Thus, we measure only passive drag caused by the swimsuit.

Vennell et al. (2006) performed measurements of passive drag using a pool with a flow generator, and a towed mannequin. The measurements spanned common human swimming speeds. This test setup focused on the measurement of passive drag, especially the drag caused by the swimsuit. The use of a mannequin eliminated the variability caused by human swimmers. Mollendorf et al. (2004) measured passive drag forces on towed swimmers at varying speeds. Using regression analysis, they decomposed the drag forces into: 1) Pressure drag assumed to be proportional to velocity squared; 2) Wave drag assumed to be proportional to velocity to the fourth power. Wave drag is the smallest component of drag; and 3) Skin friction drag which is the total drag minus the other two drags. Their data showed that skin friction drag is the largest component of total drag when the swimsuit covered the whole torso. Mollendorf et al. also showed that skin friction drag was the drag most affected by swimsuits. The difference in drag forces caused by different swimsuits is small. However, that difference is what the expensive swimsuit manufacturers claim to be the advantage of their expensive swimsuit. Our method is designed to measure this small difference among swimsuits.

Based on Mollendorf et al. (2004), our experiments will measure only the skin friction drag. Unlike the methods discussed above, our method of measuring skin friction drag does not require measurement of forces. Instead, we use the boundary layer theory (e.g., Kreith, 2000) to directly measure how the surface or the swimsuit slows down water flow.

EXPERIMENT

In our experiment, the swimsuit was held stationary, and water flowed over the swimsuit. We measured the velocity of the water at different distances from the swimsuit and used the different velocities to estimate a skin drag coefficient. To measure the flow velocity, we used an Acoustic Doppler Velocimeter (MicroADV®, three-probe, SonTek Technical Notes, 2016). This ADV generates 16 MHz ultrasonic vibration at the end of a rod. The vibration excites particulate matter in the flow. The resulting particle vibration frequency is Doppler-shifted by the velocity of the water flow. Frequency shifts in three directions are sensed by three probes beyond the end of the rod. These frequency shifts are transformed into flow velocity components (u, v, and w) in three cartesian directions (x, y and z). The ADV also measures the distance from the swimsuit surface by measuring the time of flight of ultrasonic pulses from and back to the generator. The sampling rate was 50 Hz.

Our tests were done in a laboratory hydraulic flume (Figure 1), which created laminar water flow (e.g., Neufeld, 2008). Figure 2 shows our experimental setup. The swimsuit was fixed on a flat board on the bottom of the flume. The temporary angle profile bar showing on the left was removed before the test. A test point was chosen at 200 mm from the leading edge of the swimsuit, on the mid-line between the side walls. Above the test point on the swimsuit, the ADV was fixed in the downstream and sideways positions. The stem appears offset in Figure 2 because of light refraction in the water. A slider enabled the ADV to be positioned arbitrarily in the vertical (y) direction. Water in the flume was made to flow over the swimsuit at

a constant, controlled flow rate. High above the swimsuit surface, the free-stream velocity u_0 was measured using the velocimeter. The depth of the flowing water in the flume was a few hundred millimeters. For each test, the free stream velocity u_0 was measured at three depths near the water surface. The u_0 that was chosen was the one that resulted in the highest coefficient of correlation in the regression analysis below. For "Swimsuit 1", the free stream velocity used was u_0 = 0.280 m/s. As the ADV was brought down closer to the swimsuit surface, the measured velocity $u(y)$ decreased. The velocities in the boundary layer are listed with the corresponding distances from the swimsuit surface in Table 1.

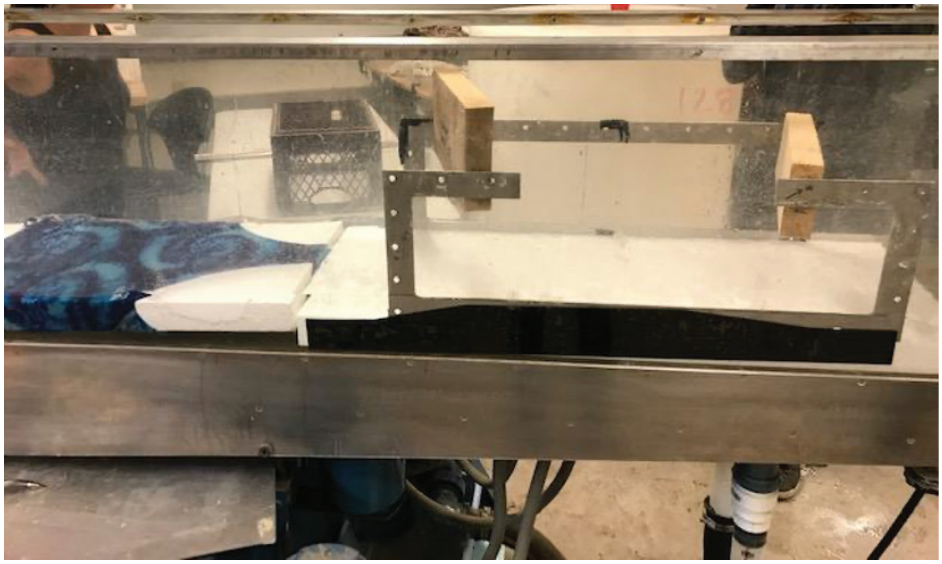

Figure 1. Flume used in the skin friction measurement.

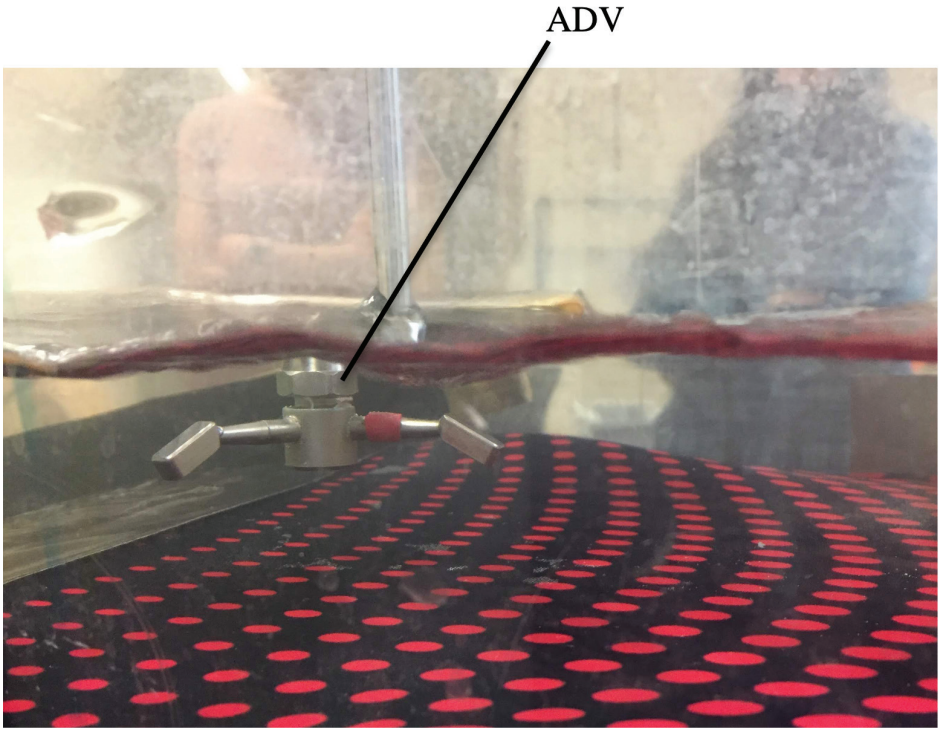

Figure 2. Acoustic Doppler Velocimeter (ADV) over a swimsuit.

y, mm	3.041	3.041	3.569	3.813	3.813	4.416	5.762
u, mm/s	236.7	239.9	241.0	247.0	248.7	243.7	256.4
y, mm	6.863	6.904	8.276	9.633	10.089	12.545	19.856
u, mm/s	257.9	262.5	262.4	263.4	266.2	274.3	276.2

Table 1. Velocity versus distance from Swimsuit 1.

For Swimsuit 2, the velocities in the boundary layer, along with the distances from the swimsuit surface, are listed in Table 2. The free flow velocity was also 280 mm/s.

y, mm	3.405	3.765	5.825	6.403	7.058
u, mm/s	234.02	242.29	252.95	257.05	260.09
y, mm	8.026	8.891	10.199	14.026	15.453
u, mm/s	262.53	265.52	270.15	275.74	276.61

Table 2. Velocity versus distance from Swimsuit 2.

HYDRODYNAMICS OF THE EXPERIMENTAL METHOD

Figure 3 illustrates how a solid surface like a swimsuit affects water flow. On the surface of the swimsuit, the water velocity is zero because of the no-slip boundary condition. Within a fraction of millimeter from the surface, the velocity increases with distance from the surface. In this layer, the increase is rapid but linear. This layer is called the laminar sublayer or viscous sublayer. The ADV is not capable of measuring velocity in this layer (for a reason that will be explained near the end of this paper). As the velocimeter is moved farther from the viscous sublayer (vertical distance y is increased), the downstream velocity u grows higher with distance y from the surface, approaching the free velocity u_o, which is the unimpeded velocity and the highest velocity for any distance y). However, the rate of the velocity growth decays with distance. Thus, we assume that $u(y) = u_0 - u_0 \exp(-ay)$, and define

$$u_{loss} = u_0 - u(y) \tag{1}$$

which can be assumed to decay exponentially with y, i.e.,

$$u_{loss} = u_0 \exp(-ay) \tag{2}$$

where a is a constant that is a property of the swimsuit surface. Water flows slower near the swimsuit surface because that surface 'drags' the water with a shear stress τ_0. In the flow, the shear stress is the gradient of the velocity times the density of water. Right on the swimsuit surface, this shear stress is τ_0 where

$$\tau_0/\varrho = du/dy|_{y=0} \tag{3}$$

(where ϱ = density of water). Equations (2) and (3) show that a higher shear stress on the surface of a swimsuit (i.e. higher drag) will result in a steeper gradient of velocity in the boundary layer.

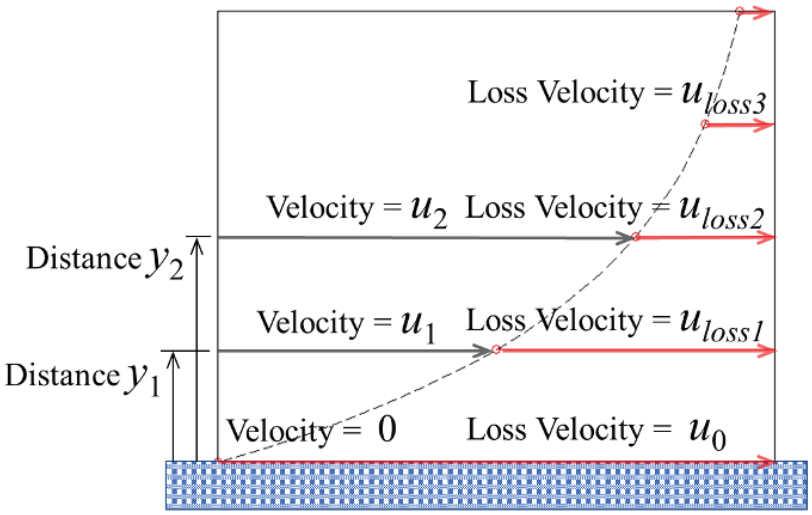

Figure 3. Speed loss decays exponentially with distance from swimsuit surface.

Now, because u_{loss} has the opposite sign of u (Eq. (1)), the shear stress on the swimsuit surface is

$$\tau_0 = - \varrho \, du_{loss}/dy|_{y=0} \tag{4}$$

Inserting Eq. (2) into Eq. (4), we obtain the skin drag, which is the shear stress on the surface of the swimsuit:

$$\tau_0 = a \, \varrho \, u_0 \tag{5}$$

Thus, a swimsuit with a greater value of a gives a higher skin drag. This skin drag coefficient a can be obtained by performing a linear regression analysis on $\ln(u_{loss})$ as a function of y.

We could take advantage of the knowledge that on the swimsuit surface,

$$u_{loss}|_{y=0} = u_0 \tag{6}$$

by fixing the intercept of the regression line to u_0. However, letting the linear regression analysis determine the intercept gives a higher goodness of fit (smaller error) in the curve-fitting. Also, results below will indicate that the ADV measurement had a bias that grew large as it was brought closer to the swimsuit surface. It is important to note that the best region for measuring skin drag is the very thin viscous sublayer right on the swimsuit surface, where du/dy is nearly constant. An ADV does not have the required accuracy to be used in that viscous layer. Therefore, the method in this paper is a stretch from the "gold-standard" method of measuring skin drag by measuring velocities only in the thin viscous layer. Near the end of this paper, we will discuss a bias caused by using an ADV in the boundary layer region that is two orders of magnitude thicker than the viscous sublayer. Fortunately, the biased measurements were still able to be curve-fit and be used for relative comparison among different swimsuits, as the results below will suggest.

RESULTS

The ADV recorded velocities in three directions at several heights above the swimsuit surface. We use only the velocity u in the downstream direction x. The much lower velocities in the two other directions (v and w, Fig. B1 in Appendix B) are not used.

The "loss velocity" as a function of distance y from the surface,

$$u_{loss}(y) = u_0 - u(y) \tag{7}$$

was used to calculate the drag coefficient in the analysis below.

Linear regression analysis was performed, with y as the independent variable, and $\ln(u_{loss})$ as the dependent variable. The linear regression gives the slope of the line $\ln(u_{loss})$ vs y. This slope has a negative value because the loss velocity u_{loss} decreases as the distance y from the surface increases. Equation (2) defined the coefficient that indicates drag as the negative of the slope. Each swimsuit gives a different slope a. A swimsuit with a larger value of a gives a higher skin friction, and therefore a higher drag. The captions in Figure 4 and Figure 5 for each swimsuit shows the negative of the slope (= a) and the price of Swimsuit 1 and Swimsuit 2. A steeper slope means a higher skin drag, which is manifested in the measurement by a more rapid loss of velocity as the probe gets closer to the swimsuit.

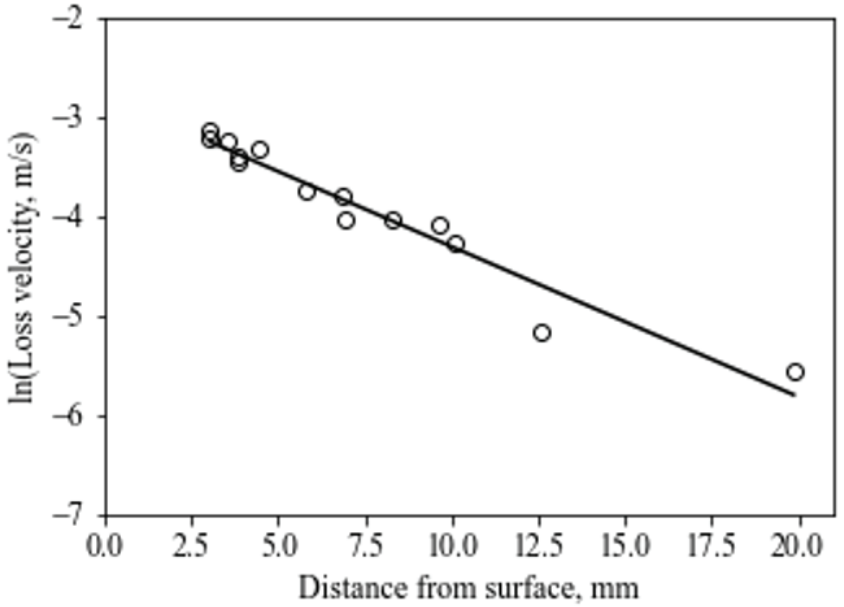

Figure 4. Regression analysis of Swimsuit 1. Price = $32, a = 149.

The measurement of velocity versus distance from the surface, and the calculation of drag a as above, were performed on three other swimsuits of various prices. Appendix A shows the linear regression graphs, the skin drags a, and the prices of Swimsuits 3, 4, and 5. Figure 6 plots skin drag versus price for all the swimsuits. The results suggest that the more expensive swimsuits do not necessarily have lower skin drag. In fact, linear regression analysis would show a positive correlation between skin drag and price. That is, a more expen-

sive swimsuit tends to have a higher skin drag. This result is contrary to the belief that more expensive swimsuits have lower skin drag. Swimsuit skin drag should not be correlated with price. (Unlike, for example, the square footage of a house in a neighborhood is correlated with price.) However, the motivation for this research from the beginning was to fact-check the publications that associate expensive swimsuits with lower drag. The natural scatter of the data points and the small number of swimsuits tested do not allow us to make a strong conclusion beyond that "Our experiment does not support the belief that more expensive swimsuits have lower skin drag".

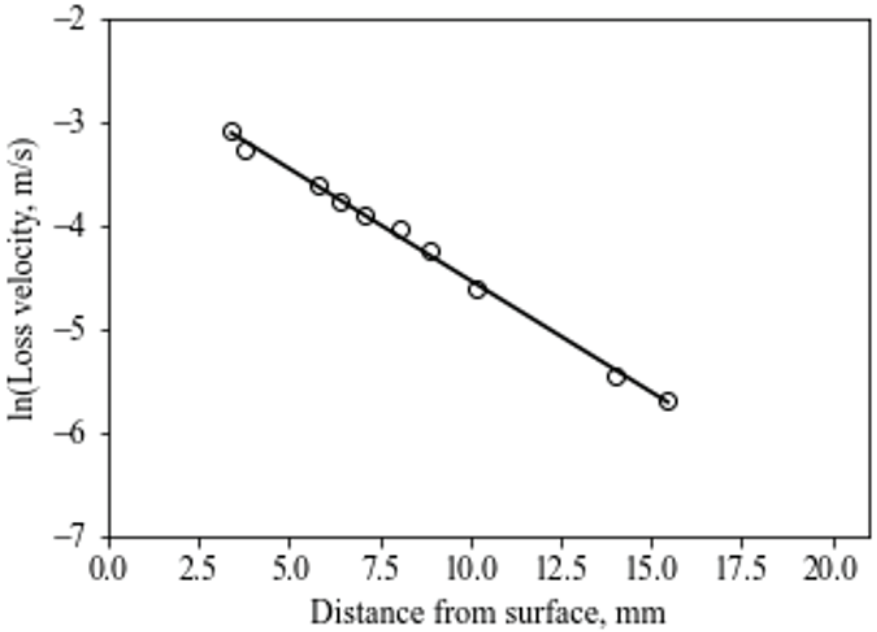

Figure 5. Regression analysis of Swimsuit 2. Price = $350, a = 215.

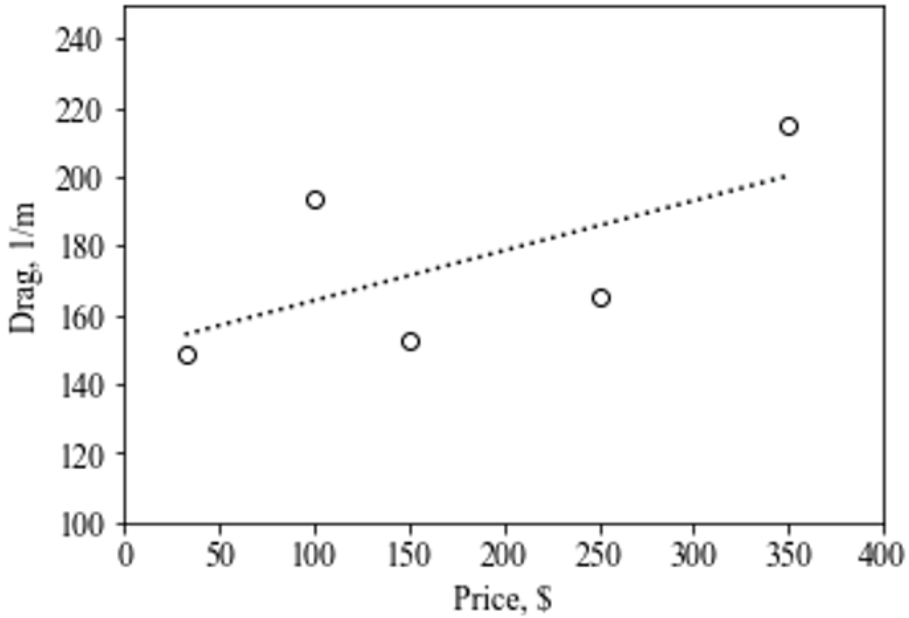

Figure 6. Skin Drag vs. Price of Five Swimsuits.

ACCURACY LIMITATION

The curve-fitting for the five swimsuits gives good correlation coefficients (R > 0.9). The goodness of fit indicates good precision of the velocity slopes which we use to differentiate the skin drags of different swim suites. However, the vertical-axis-intercept is far from predicting the loss velocity u_{loss} on the swim suit surface. From the regression analysis, the vertical-axis-intercept for Swimsuit 2 would correspond to u_{loss} = 92 mm/s. No-slip boundary condition requires that u_{loss} = 280 mm/s on the surface of Swimsuit 2. Measurements on all the swimsuits we tested gave low u_{loss} on their surfaces. In our experiment, u_{loss} was never measured, but inferred from Eq. (1) and the measurement of $u(y)$. The fact that u_{loss} is biased low means that the measurement of $u(y)$ is biased high. The high bias can be explained below.

The ADV that we utilized in this research is not the highest-accuracy instrument for a boundary layer in general. In free flow, the ADV has an accuracy better than 1% (Voulgaris and Trowbridge, 1998). However, as the probe gets close to the swimsuit surface ("the boundary"), the accuracy deteriorates, perhaps rapidly. The monotonous loss of accuracy with proximity to the boundary can be attributed to the fact that the ADV averages particle velocities over a relatively large volume. The type of ADV we used was a three-probe, 16MHz ADV. According to the manufacturer (Xylem Analytics, 1998), the velocity measurement is an average over a "cylindrical" volume with a radius under 2.25 mm and height of 4.5 mm. SonTek Technical Notes (2016) specifies a radius of 2.00 mm. (In reality, the "cylinder wall" is not straight, but a Gaussian curve revolved around the vertical axis.) Those dimensions of the sample volume are not much less than the range over which we varied the distance y from the swimsuit surface. In using the velocities to estimate drag, we rely on the assumption that the averaged velocity over the height of the sample volume adequately represents the velocity at the distance y from the swimsuit surface. This assumption introduces considerable bias in our measurements. Within the 4.5 mm from the boundary, the ADV averages the lower velocity closer to the boundary with the higher velocity farther from the boundary. This averaging causes the measurement to be significantly higher than the true velocity near the swimsuit surface. In fact, the true zero velocity on the boundary can never be read by the ADV, hence the apparent violation of the no-slip boundary condition. (Daroudian et al. (2010) mentions a method that could be used to provide some correction; but this is outside the scope of our research.) As the ADV gets closer to the boundary, the measurement of $u(y)$ is biased higher, and u_{loss} is biased lower (Eq. (1)). Then all our calculated velocity gradients and drag are biased low. Therefore, our estimate of the drag coefficient is biased low. Fortunately, the low-biasing of the gradient and drag applies consistently to all the swimsuits we tested. Thus, our relative ranking holds true: A swimsuit with higher skin drag still gives a greater velocity gradient measurement in the boundary layer.

For a mathematical explanation of why the velocity-averaging volume results in high bias near the boundary, see Appendix C. We have shown that the ADV is valuable in comparing skin drag of different surfaces under similar flow conditions. However, the ADV cannot be used for measuring the true skin drag of any particular swimsuit alone. For future researchers in this topic who have the resources, we suggest replacing the ADV with a Laser Doppler Velocimetry (LDV) or a modern Particle Image Velocimetry (PIV), which are today's "gold-standard" methods for measuring velocity in the sub-layers of the boundary layer. Due

to their high spatial resolution, LDV and PIV can accurately measure velocities in a very thin viscous sublayer region. The viscous sublayer is the ideal region where skin drag should be measured. The thickness of the viscous sublayer is about five times the kinematic viscosity divided by the free velocity (in our case, about 0.02 mm). In the viscous sublayer, du/dy is practically constant. See for example Mazumder et al. (1981), who performed skin drag measurement with an LDV whose averaging volume had a size of around 0.04 mm. Their measurement in a turbulent wind tunnel requires microscopes and very different instruments than what was available to our research here. The much higher resolution would also enable investigation into whether du/dy is constant in the region closest to the swimsuit surface, which would be revealed if u is plotted against y on a normal scale (not semi log like ours). Only the thin viscous sublayer (about 1% of the boundary layer thickness) would exhibit this constant gradient. With the ADV, the bias and coarse spatial resolution of our method does not allow us to probe that close to the swimsuit with any accuracy. Thus, our analysis resorted to the exponential curve fitting of the velocities in the boundary layer outside the viscous sublayer.

CONCLUDING REMARKS AND FUTURE WORK

From our experiment using a flume, flow velocity loss in the boundary layer near the swimsuit surface can be modeled with an exponentially decaying function of distance from the swimsuit surface. The decay exponent is proportional to the skin drag on the swimsuit surface. The experiment gives relative estimates of skin drag coefficients of five swimsuits. The result does not support the belief that more expensive swimsuits have lower skin drag. This result is consistent with Toussaint et al. (2002) that measured skin drag using instrumented crawl swimmers, and concluded that swimsuits with special texture designs did not show reduced skin drag outside statistical margins of error.

The scope of our conclusion is limited to skin drag. We measured skin drag because publications mentioned in the Introduction claim that expensive swimsuits have specially engineered surface texture that reduces drag, and because Mollendorf et al. (2004) demonstrate that skin friction drag is the drag most affected by swimsuits. However, skin drag is only one term that contributes to passive drag. Besides skin drag, other factors affect the relationship between swimsuit design and passive drag, such as how the swimsuit shapes the hydrodynamics of the swimmer (Marinho et al., 2012). Moreover, passive drag is only part of active drag which takes into account the movement of the swimmer. It is possible that swimsuits affect speed in other ways than lowering drag. For example, Kainuma et al. (2009) suggested that the extreme tightness of the Speedo LZR swimsuits may constrict blood flow in certain muscles and thereby boost the generation of instantaneous force which help in short-distance sprints. Placebo effects can still boost the performance of swimmers who are wearing expensive swimsuits. A thorough meta-analysis of published results concluded that "the lack of consensus due to the variety of fields of study means that improvements in competitions are still not clarified" (Morales et al., 2019).

This paper shows that our measurement method was effective in measuring skin drag with good precision as Figures 4 and 5 show, subject to the bias discussed above. For future work, a similar method for measuring skin drag is discussed in Appendix D. Additionally, Appendix

D illustrates a different method to measure passive drag beyond skin drag. There we propose the use of a water current generator, a mannequin, and a load cell. This method is similar to Vennell (2006), with the exception that we will examine the velocities in the boundary layer in addition to Venell's correlation of drag force to free-flow velocity. The boundary layer analysis would give deeper insight into how different swimsuits have different passive drags.

AUTHOR INFORMATION

Corresponding Author

*Anita X. Sumali, dolphinator7@gmail.com

ACKNOWLEDGMENT

The measurements and analysis discussed in this paper were performed at author MCS' facility when author AXS was at La Cueva High School in Albuquerque, NM. Authors AXS and MFS are grateful for valuable review and advise from Dr. Budi Gunawan, and Mrs. Lena Eddings.

REFERENCES

Benjanuvatra, N.; Dawson, G.; Blanksby, B.; Elliot, B. Comparison of buoyancy, passive and net active drag forces between Fastskin and standard swimsuits. *Journal of Science and Medicine in Sports*. **2002**, *5* (2), 115-23.

Bixler, B; Pease, D.; Fairhurst, F. The accuracy of computational fluid dynamics analysis of the passive drag of a male swimmer. *Sports Biomechanics*, **2007**, *6* (1), 81-98.

Bixler, G.; Bhushan, B. Fluid Drag Reduction with Shark-Skin Riblet Inspired Microstructured Surfaces. *Advanced Functional Materials*. **2013**, *23* (36), 4507-4528.

Chatard, J. Effect of Fastskin Suits on Performance, Drag, and Energy Cost of Swimming. *Medicine & Science in Sports & Exercise,* **2008**, *40* (6), 1149-1154.

Daroudian, B.; Bagherimiyab, F.; Lemnin, U. Improving the accuracy of four-receiver acoustic Doppler velocimeter (ADV) measurements in turbulent boundary layer flows. *Limnology and Oceanography: Methods*, **2010**, *8*, 575-591.

Dombroski, D. E.; Crimaldi, J. P. The accuracy of acoustic Doppler velocimetry measurements in turbulent boundary layer flows over a smooth bed. *Limnology and Oceanography: Methods*, **2007**, *5*, 23-33.

Kainuma, E.; Watanabe, M.; Tomiyama-Miyaji, C.; Inoue, M.; Kuwano, Y.; Ren, H. Proposal of alternative mechanism responsible for the function of high-speed swimsuits. *Biomedical Research*, **2009**, *30*, 69-70. DOI: 10.2220/biomedres.30.69

Krieger, K. Do pool sharks swim faster? *Science*, **2004**, *305* (5684), 636-637.

Kreith, F. *Fluid Mechanics*; CRC Press, 2000.

Luo, Y.; Lu, Y.; Li, J.; Wang, J. Boundary layer drag reduction research hypotheses derived from bio-inspired surface and recent advanced applications. *Micron*, **2015**, *79*, 59–73.

Marinho, D. A.; Mantha, V. R.; Vilas-Boas, J. P.; Ramos, R. J.; Machado, L.; Silva, A. J. Effect of wearing a swimsuit on hydrodynamic drag of swimmer. *Braz. Arch. Biol. Technol*, **2012**, *55*, 851–856. DOI: 10.1590/S1516-89132012000600007

Mazumder, K.; Wanchoo, S.; McLeod, P.C.; Ballard, G.S.; Mozumdar, S.; Caraballo, N. Skin friction drag measurements by LDV. *Applied Optics*, **1981**, *20* (16), 2832-2837.

Mollendorf, J.; Termin, A. C; Oppenheim, E; Pendergast D. R. Effect of swim suit design on passive drag. *Medicine & Science in Sports & Exercise*, **2004**, *36* (6), 1029-35.

Mooney, A. Swimming on Steroids: The Suits That Brought Down Records. The Harvard Sports Analysis Collective. https://harvardsportsanalysis.wordpress.com/2012/07/21/swimming-on-steroids-the-suits-that-brought-down-records/ (accessed 2020-11-07).

Morales, A. T.; Fajardo, J.A.T.; Gonzales-Garcia, E. High-Speed Swimsuits and Their Historical Development in Competitive Swimming. *Front. Psychol.*, **2019**, 11 December.

Morrison, J. How Speedo Created a Record-Breaking Swimsuit. *Scientific American*, July 27, 2012. https://www.scientificamerican.com/article/how-speedo-created-swimsuit/ (accessed 2020-11-07).

Mountjoy, M.; Gordon, I.; McKeown, J.; Constantini, N. Medical complications of an aquatic innovation. *British Journal of Sports Medicine*, **2009**, *43*, 979-980; DOI: 10.1136/bjsm.2009.067215.

Narita, K.; Nakashima, M.; Takagi, H. Developing a methodology for estimating the drag in front-crawl swimming at various velocities. *Journal of Biomechanics*, **2017**, *54*, 123-128.

Neufeld, J. A. An experimental study of shear-enhanced convection in a mushy layer. *Journal of Fluid Mechanics*, **2008**, *612*, 363-385. DOI: 10.1017/S0022112008003339

SonTek Technical Notes. *Acoustical Doppler velocimeter (ADV): Sampling Volume Size and Velocity Accuracy*. SonTek, 1998.

https://www.xylem-analytics.com.au/media/pdfs/adv-sampling-volume-size-and-velocity-accuracy.pdf (accessed 2020-11-07).

SonTek Technical Notes. *A Primer on SonTek ADV systems*. SonTek, 2016.

https://www.xylem-analytics.com.au/media/pdfs/a-primer-on-sontek-adv-systems.pdf (accessed 2020-11-07).

Toussaint, H. M; Truijens, M.; Elzinga, M. J.; Van de Ven, A; De best, H; Snabel, B; De Groot D. Effect of a fast-skin body suit on drag during front crawl swimming. *Sports Biomechanics*, **2002**, *1*, 1-10.

Toussaint, E. M.; Roos, P. E.; Kolmogorov, S. The determination of drag in front crawl swimming. *Journal of Biomechanics*, **2004**, *37*, 1655-1663. DOI:10.1016/j.jbiomech.2004.02.020.

Vennell, F.; Pease, D.; Wilson, B. Wave drag on human. *Journal of Biomechanics*, **2006**, *39*, 664-671. DOI:10.1016/j.jbiomech.2005.01.023.

Voulgaris, G.; Trowbridge, J. H. Evaluation of the Acoustic Doppler Velocimeter (ADV) for Turbulence Measurements. *Journal of Atmospheric and Oceanic Technology*, **1998**, *15* (1), 272-289.

Zhang, D. Y.; Luo, Y. H.; Li, X.; Chen, H. W. Numerical simulation and experimental study of drag-reducing surface of a real shark skin. *Journal of Hydrodynamics*, **2011**, *23* (2), 204-211. DOI: 10.1016/S1001-6058(10)60105-9.

APPENDIX A: REGRESSION ANALYSIS FOR SWIMSUITS 3, 4 AND 5

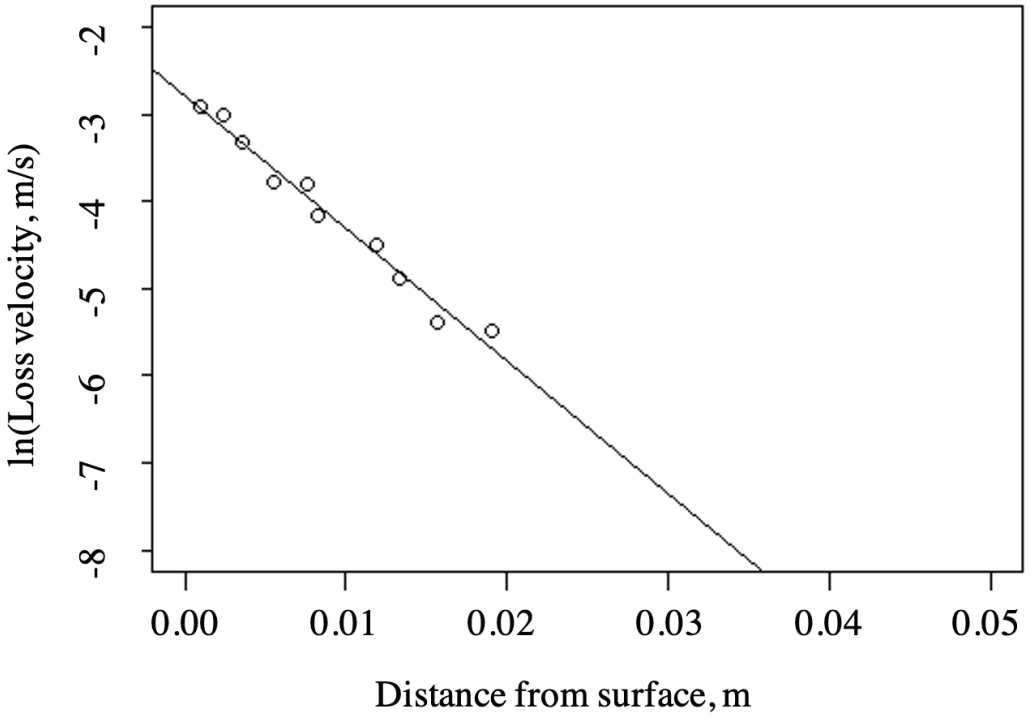

Figure A1. Regression Analysis for Swimsuit 3. Price = $150, a = 153.

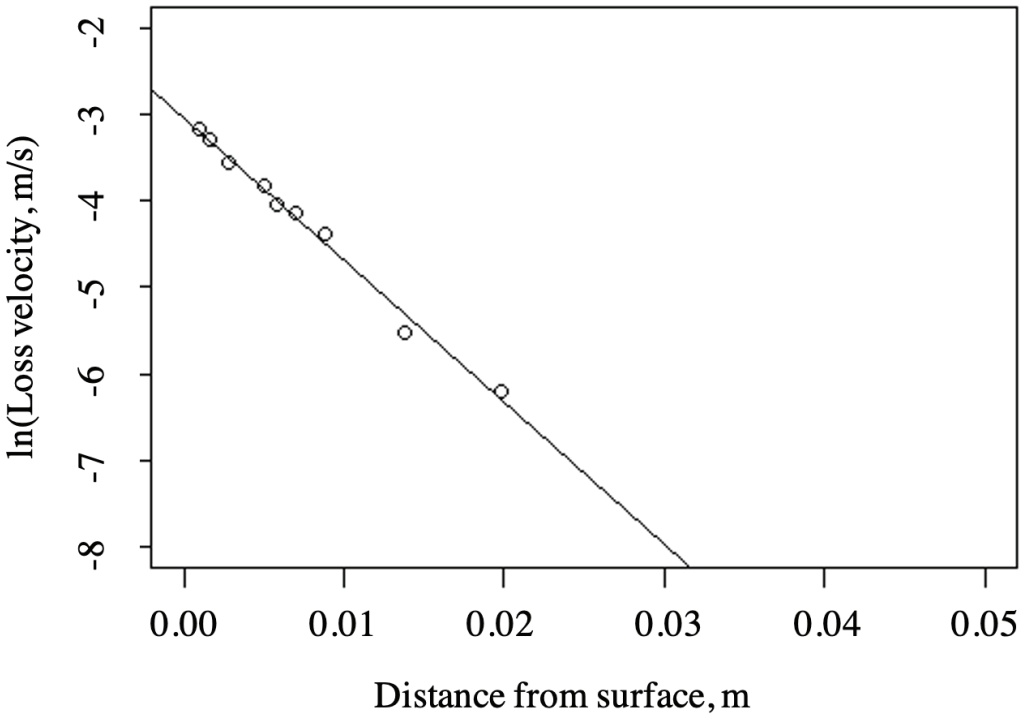

Figure A2. Regression Analysis for Swimsuit 4: Price = $250, a = 165.

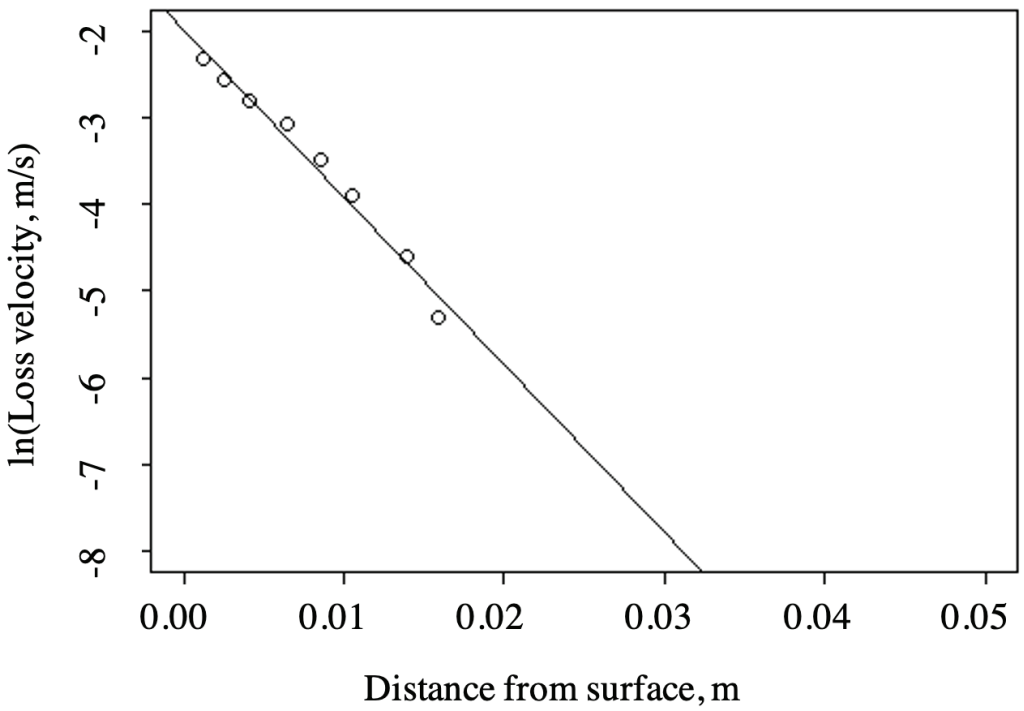

Figure A3. Regression Analysis for Swimsuit 5: Price $100, a = 194.

APPENDIX B: TURBULENCE METHOD

The Speed-Loss method above assumes that the flow is laminar and one-dimensional (that is, all water molecules move only in the downstream direction). In reality, "micro-swirl" turbulence means that each water molecule moves in three dimensions. In the turbulence method, we use the velocities u in the flow direction and w in the vertical direction. Both are measured against time t. Turbulence causes these two velocities to fluctuate. The fluctuation about the mean is calculated as

$$u'(t) = u(t) - mean(u); \tag{B1}$$

$$w'(t) = v(t) - mean(w); \tag{B2}$$

The shear stress at height y from the swimsuit surface can be obtained as

$$\tau\,(t) = \rho\, u'(t)\, w'(t) \tag{B3}$$

Where ρ = density of the water = 1000 kg/m^3.

We used the ADV to measure velocities in three directions at several heights above the swimsuit surface. In the turbulence method, we use the velocities $u(t)$ in the flow direction and $w(t)$ in the vertical direction (Fig. B1). The shear stress at height y from the suit surface can be obtained as

$$\tau = \rho\, u'\, w' \tag{B4}$$

Figures B2 show shear stress from measurement on Swimsuit 1 as a function of time, at various distances from the swimsuits. The figures also show the means of the shear stresses at the various distances. Figure B3 shows a linear regression analysis which gives the shear stress right on the swimsuit surface ($y = 0$) for Swimsuit 1.

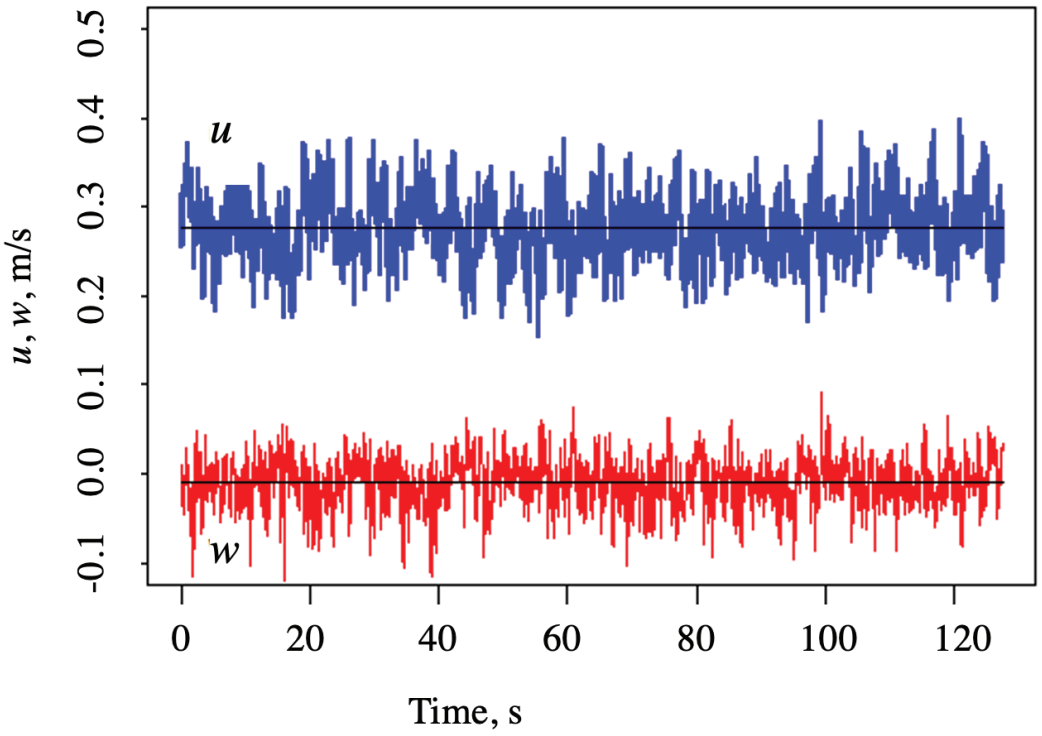

Figure B1. Downstream velocity (u) and vertical velocity (w) as functions of time.

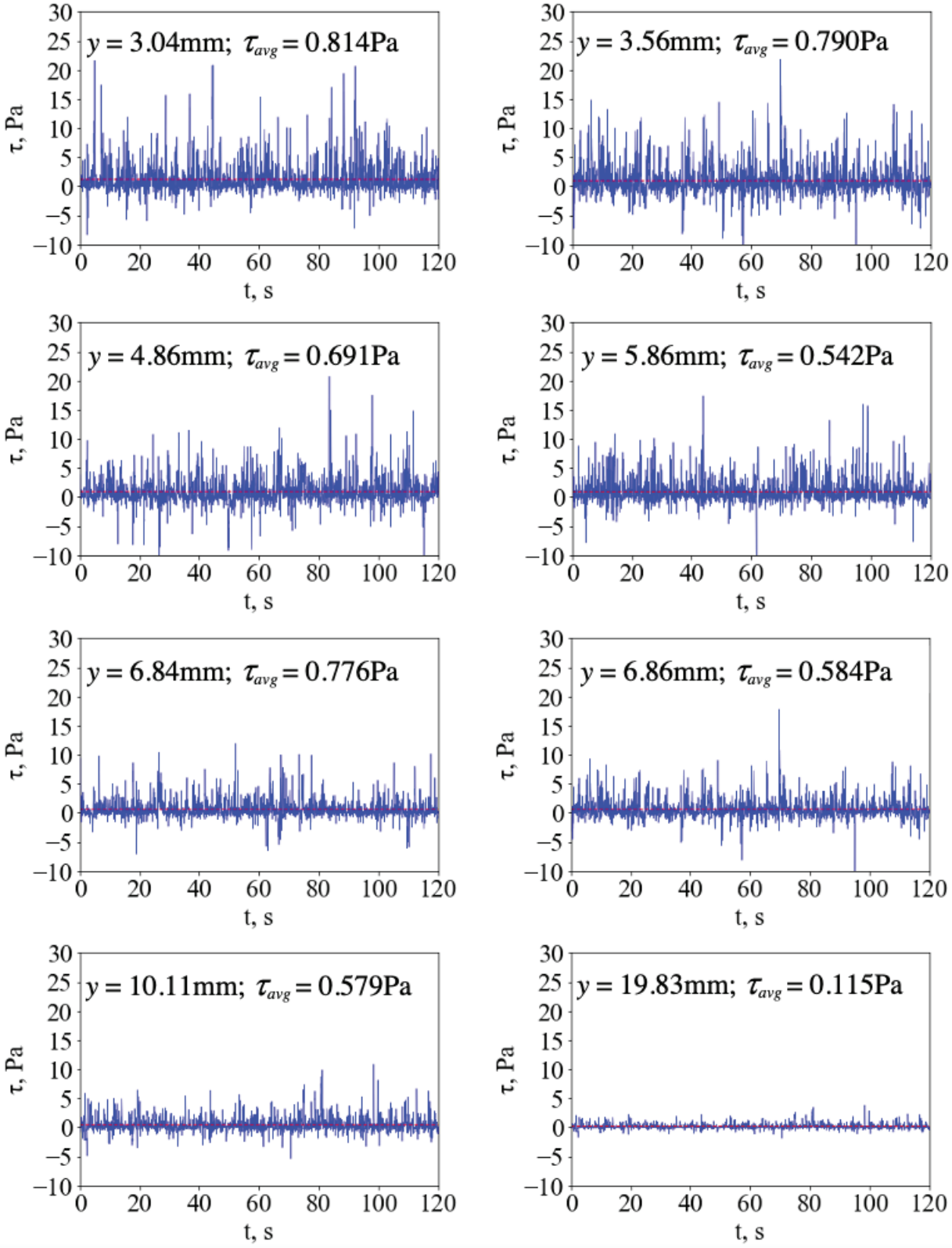

Figures B2. Shear stress as functions of time for Swimsuit 1.

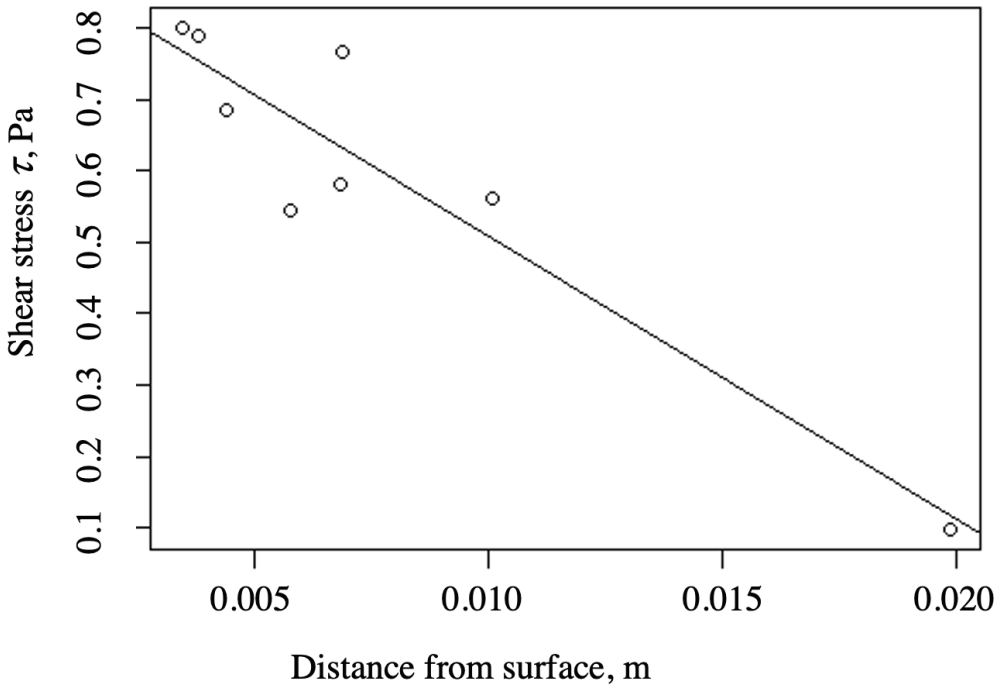

Figure B3. Linear regression of shear stress versus distance for Swimsuit 1.

APPENDIX C: CONVOLUTION BY THE ADV

From Eqs. (1) and (2), the downstream velocity of the water in the flume is

$$u(y) = u_0 \left[1 - \exp(-ay)\right] \text{ for } y > 0; \text{ zero otherwise.} \tag{C1}$$

The ADV measures the velocity not only at the exact position y that it measures and gives. Instead, it averages the velocities of particles around y, weighting the velocity by some function of y. Here, we assume a Gaussian function

$$h(y) = \frac{1}{\sigma\sqrt{2\pi}} e^{-\frac{(y-b)^2}{2\sigma^2}} \tag{C2}$$

where σ is the standard deviation and b is the distance between the measured point y and the center of the Gaussian function (Xylem Analytics, 1998). Therefore, the averaged velocity that the ADV gives is a convolution of $u(y)$ and $h(y)$ (Dombroski et al, 2007). To simplify the calculation of the convolution, define a reduced velocity from Eq. (C1)

$$u^*(y) = 1 - u(y)/u_0 = \exp(-ay) \tag{C3}$$

The convolution of the reduced velocity with the sensor's weighting function is

$$U^*(y) = \int_{-\infty}^{\infty} u^*(\varphi)\, h(y - b - \varphi) d\varphi = \int_0^{\infty} e^{-a\varphi}\, e^{-\frac{(y-b-\varphi)^2}{2\sigma^2}} d\varphi =$$

$$= \frac{1}{2} e^{-a(y-b-a\sigma^2/2)} \left[1 + erf\left(\frac{y-b-a\sigma^2}{\sigma\sqrt{2}}\right)\right] \tag{C4}$$

Transforming the above convolved reduced velocity similarly to Eq. (C3), we obtain the convolved velocity that the ADV gives:

$$\upsilon(y) = u_0 \left[1 - U^*(y)\right] \tag{C5}$$

Figure C1 shows that the convolved velocity reading from the ADV is biased high when the ADV is close to the swimsuit surface. This bias explains the apparent violation of the no-slip boundary condition in our measurements. It also indicates that the drag coefficient calculation (the slope magnitude of log velocity) is biased low. This bias is consistent among all the swimsuits that we tested.

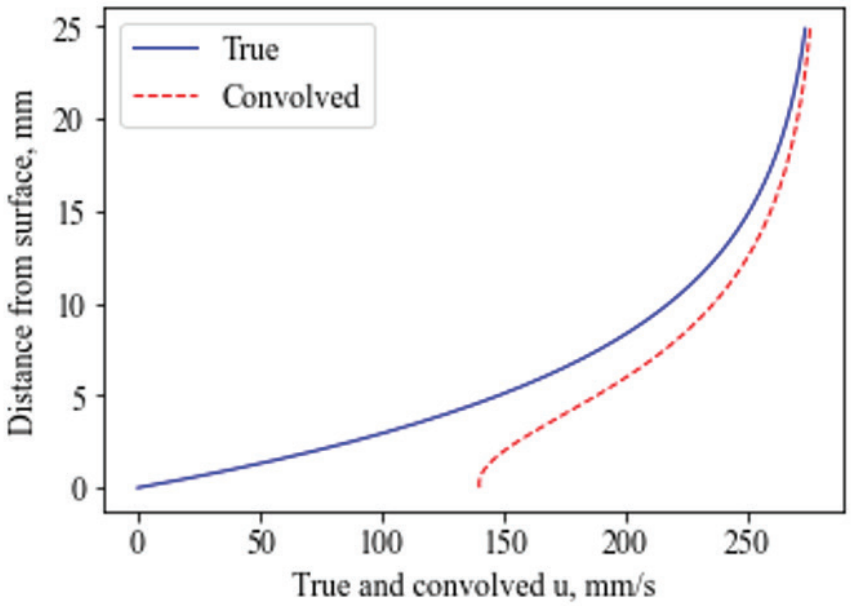

Figure C1. Velocity reading from the ADV is biased high.

APPENDIX D: TETHERED MANNEQUIN WITH A FLOW GENERATOR

In another setup for measuring drag, the swimsuit will be put on a mannequin suspended horizontally in an endless pool (Figure D1). The endless pool generates flow whose velocity will be varied. The current will impinge the mannequin from the front (head) end, thereby pushing the mannequin in the downstream direction. The mannequin will be tethered with a rope that has a load cell. Therefore, the load cell will measure the force on the mannequin caused by the impinging current. This force is the drag force. We can measure the drag force F_D as we vary the water speed V which is measured with a velocimeter. If we plot F_D as a function of V^2, then a linear regression analysis will determine the drag coefficient C_D. Each swimsuit will give a slightly different C_D than other swimsuits. Also, the mannequin without any swimsuit will give the lowest C_D because the mannequin surface is much smoother than swimsuits. The C_D of each swimsuit minus the C_D of the mannequin is the first indicator of the extra drag that each swimsuit introduces. Based on the data of drag forces versus velocity, we will develop a new metric that shows maximum distinction among all the swimsuit that we test.

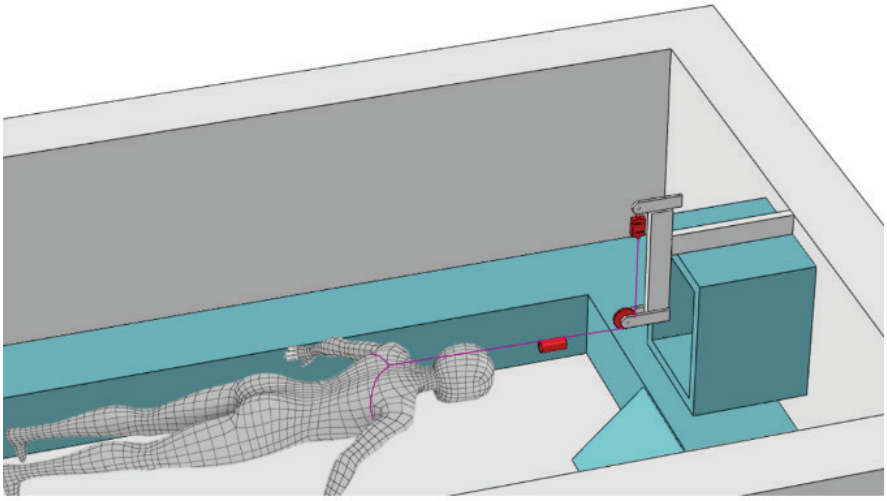

a)

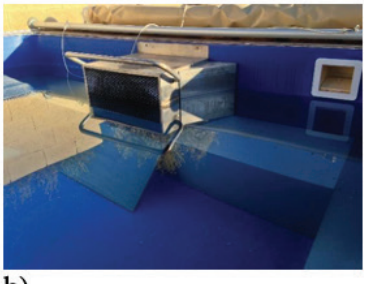

b)

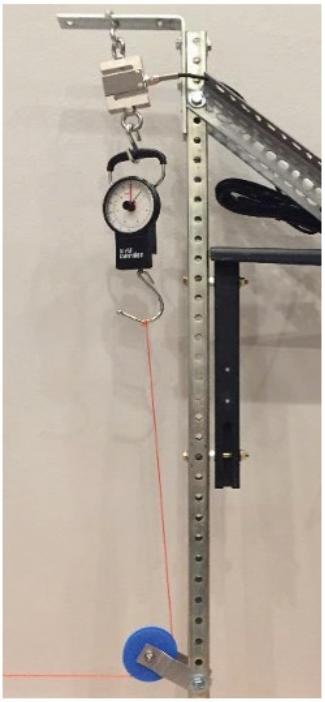

c)

Figure D1. Experiment Setup, a)3D Model; b) Photograph of Flow Generator Duct with Laminar Honeycomb; c) Load Frame Including Load Cell and Spring Scale.

A Study on Inheritance Patterns on Wing Shape, Body Color, and Eye Color in *Drosophila melanogaster*

*Yusheng Wu**

Unique Stock

Joshua Garcia-Matta

Isabel Chavez

University of the Southwest, Hobbs , NM

ABSTRACT

Due to its small size, short life cycle, abundance of genetic variability, and relative inexpensiveness, *Drosophila melanogaster*, the fruit fly, is used as the model organism. Mendelian traits studied in the project were eye color on chromosome 1 (sex-linked trait), vestigial wing (on chromosome 2), and ebony-colored body (on chromosome 3). For one-gene segregation, the flies with red eye were wild phenotype while these with white eye were mutant phenotype. For two-gene segregation, the flies being full wing and normal body color were wild phenotype while these being vestigial wing and ebony body were mutant phenotype. The traits for two-gene segregation were wing and body color. The crosses and reciprocal crosses were produced for one-gene and two-gene segregations. The expected overall phenotypic ratios for one-gene segregation were 3 red eye : 1 white eye in the cross and 1 red eye female : 1 white eye female : 1 red eye male : 1 white eye male in the reciprocal cross. The expected overall phenotypic ratios for two-gene segregation were the same, 9:3:3:1. The results of X^2 statistical test for one-gene segregation didn't fit 3:1 ratio but fit 1:1:1:1 ratio. The results of X^2 statistical test for two-gene segregation didn't fit 9:3:3:1 ratio in both crosses. The reasons that caused the distortion appear to include the purity of the commercial strains and the Meiotic Drive Elements which are the complex nuclear genetic loci found in the natural population of fruit fly and distort the fundamental laws of inheritance. Future investigations at the molecular level seems likely to provide the insightful explanations and the potential areas to study further.

KEYWORDS: *Drosophila melanogaster*, Eye Color, Body Color, X^2 Test

INTRODUCTION

Klug thoroughly described two Mendelian genetic laws and the modification of Mendelian ratios in the book titled Essentials of Genetics (Klug et al., 2010). The genes present on homologous chromosomes segregate from each other and assort independently with other segregating chromosomes during gamete formation. These two genetic laws illustrate the basic principles of gene transmission from parent to offspring. However, when gene expression does not adhere to a simple dominant/recessive mode, or when more than one pair of genes

influences the expression of a single character, or when the genes are present on the X chromosome, namely X-linkage, the classic 3:1 and 9:3:3:1 ratios are usually modified. Despite the greater complexity of these exceptions, the fundamental principles of classical Mendelian genetics still hold.

Fruit fly, *Drosophila melanogaster*, has long been useful for demonstrating the principles in the classroom and has also helped students understand biochemical and behavioral genetics. This model organism possesses many attributes which have contributed to its popularity. The fruit fly is easily cultured and its generation time is only two weeks at 21 ºC. Each individual fly is large enough for clear notation of mutant phenotypes. Carolina Biological Supply Company has a large inventory of the strains displaying the various mutant traits such as white eye, vestigial wing, etc. (Carolina Biological Supply Company, 2020). Transmission genetics plays a critical role in comprehending the many branches in modern genetics although not many such experiments are conducted nowadays. The objective of the study was to investigate gene segregation ratios in the classical, genetic patterns for eye color, wing presence and body color using the commercial strains and to verify the validation of these strains in genetic research.

METHODS

Four mutant strains were purchased from Carolina Biological Supply Company in 2019. They were wild type on chromosome 1 (X^RY, X^RX^R), white eye on chromosome 1 (X^rY, X^rX^r), vestigial-winged with red-eye, normal-colored body on chromosome 2 (vvEE), and winged with red-eye, ebony-colored body on chromosome 3 (VVee)

For the gene segregation in the dihybrid cross, vestigial-winged with red-eye, normal-colored body strain (bbAA) was mated by winged with red-eye, ebony-colored body strain. The expected segregation ratio in F_2 is 9 winged, normal (V_E_), 3 winged, ebony (V_ee), 3 vestigial, normal (vvE_), 1 vestigial, ebony (vvee). The reciprocal cross was created with the same expected segregation ratio. Male and female flies are scored separately.

For the X-link cross, wild type strain (X^RY, X^RX^R) was crossed by white eye strain (X^rY, X^rX^r). The expected female phenotypic ratio is all red eye female and the expected male phenotypic ratio is 1 red eye male : 1 white eye male. In the reciprocal X-link cross, the expected female phenotypic ratio: 1 red eye female : 1 white eye female and the expected male phenotypic ratio: 1 red eye male : 1 white eye male. Male and female flies are scored separately.

The mating maps were given as follows.

Mendelian traits: wing and body color

($P_1 \times P_2$) cross

P_1: vvEE (vestigial, normal-colored body) ♀ × P_2: VVee (winged, ebony-colored body) ♂

↓

F_1 VvEe (winged, normal) ♀ × VvEe (winged, normal) ♂

↓

F_2

Gamete genotype	VE	Ve	vE	ve
VE	VVEE	VVEe	VvEE	VvEe
Ve	VVEe	VVee	VvEe	Vvee
vE	VvEE	VvEe	vvEE	vvEe
ve	VeEe	Vvee	vvVe	vvee

($P_2 \times P_1$) reciprocal cross

P_2: VVee (winged, ebony-colored body) ♀ × P_1: vvEE (vestigial, normal-colored body) ♂

↓

F_1 VvEe (winged, normal) ♀ × VvEe (winged, normal) ♂

↓

F_2

Gamete genotype	VE	Ve	vE	ve
VE	VVEE	VVEe	VvEE	VvEe
Ve	VVEe	VVee	VvEe	Vvee
vE	VvEE	VvEe	vvEE	vvEe
ve	VeEe	Vvee	vvVe	vvee

Eye color on X chromosome

$(P_1 \times P_2)$ cross

P generation X^RX^R (Red) ♀ × X^rY (White) ♂

↓

F_1 X^RX^r (Red) ♀ × X^RY (Red) ♂

↓

F_2

Gamete genotype	X^R	Y
X^R	X^RX^R (Red) ♀	X^RY(Red) ♂
X^r	X^RX^r (Red) ♀	X^rY (White) ♂

$(P_2 \times P_1)$ reciprocal cross

P reciprocal X^rX^r (White) ♀ × X^RY (Red) ♂

↓

F_1 X^RX^r (Red) ♀ × X^rY (White) ♂

↓

F_2

Gamete genotype	X^r	Y
X^R	X^RX^r (Red) ♀	X^RY (Red) ♂
X^r	X^rX^r (White) ♀	X^rY (White) ♂

In order to cross the flies, FlyNap, an anesthesia agent available commercially through Carolina Biological Supply Company, was soaked on the end of a wand. The wand was then inserted into the vial in a manner which allowed none of the flies to escape. The flies were monitored to determine when the FlyNap should be removed from the vial once fully anesthetized. The process of anesthetizing the flies took around 2-5 minutes. Caution is taken to avoid overexposure to FlyNap which is lethal to the flies in excessive dosage.

After the flies were fully anesthetized, the cap of the vial was removed and placed under a dissecting microscope to identify sexual features. Once the sex of each fly was identified, five males and five females were placed into a vial containing culture media. A total of twenty males and twenty females were selected in four separate vials. The vials were laid on the side to ensure the flies did not get stuck to the culture medium. After the flies recuperated from the FlyNap, the vials were placed upright.

In four days, the parent flies from the previous generation was removed from the vials. The larvae were developed into mature flies within 14-20 days. In F_2 generation, mature flies were scored under a dissecting microscope according to their traits.

The flies were maintained in sponge-capped plastic vials containing roughly one inch of culture media and yeast cells. The whole culturing process took place at room temperature.

The X^2 statistical test was chosen to detect the fitness of the segregation ratios (Klug, 2010).

RESULTS

Eye color gene on X chromosome in monohybrid crosses

From a cross between red eye female and white eye male in (a) of Figure 1, the phenotypes in F_2 were present as red eye female, white eye male and white eye female, whereas from a reciprocal cross between white eye female and red eye male the phenotypes in F_2 were shown as red and white eye in both female and male.

Table 1 shows the results of the X^2 tests performed on the total number of flies in two crosses related to eye color. The results for the cross between red eye and white eye strain

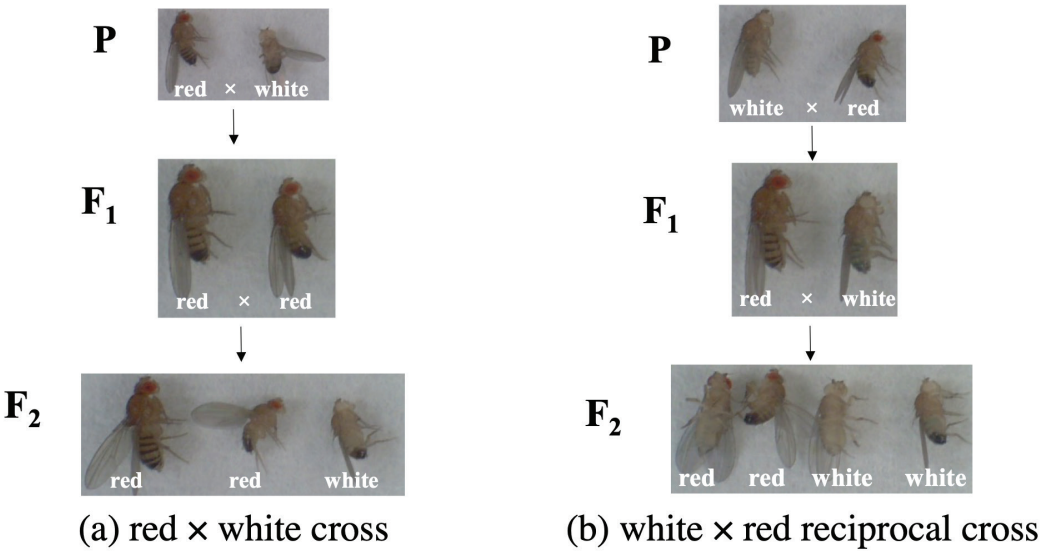

Figure 1. A display of the phenotypes of fruit flies in two crosses.

showed that X^2 value was higher than 3.84 (X^2 value at 5% significant level with degree of freedom of one). The probability was smaller than 5% indicating that the observed segregation ratio didn't fit the expected 3:1 ratio. However, the result for the reciprocal cross between white eye and red eye strain revealed that X^2 value was lower than $X^2_{0.05,3} = 7.82$. The probability was greater than 5% demonstrating that the observed segregation ratio followed the expected 1:1:1:1 ratio.

Red × White				White × Red			
Phenotype	Obs	Exp	X^2	Phenotype	Obs	Exp	X^2
Red eye (female and male)	154	185.3	5.27	Red eye (female)	186	166.3	2.35
White eye (male)	93	61.8	15.81	White eye (male)	157	166.3	0.51
Total	247	247	21.09	Red eye (male)	179	166.3	0.98
				White eye (male)	143	166.3	3.25
				Total	665	665	7.09

Table 1. The results of X^2 tests for two crosses.

Wing shape and body color in dihybrid crosses

In a dihybrid cross between the strain of vestigial wing with red-eye, normal-colored body and the strain of wing with red-eye, ebony-colored body shown in (a) of Figure 2, the phenotypes for female and male in F_2 were present as winged with normal-colored body, winged with ebony-colored body, and vestigial with normal-colored body, but the vestigial with ebony-colored body was absent in female and present in male.

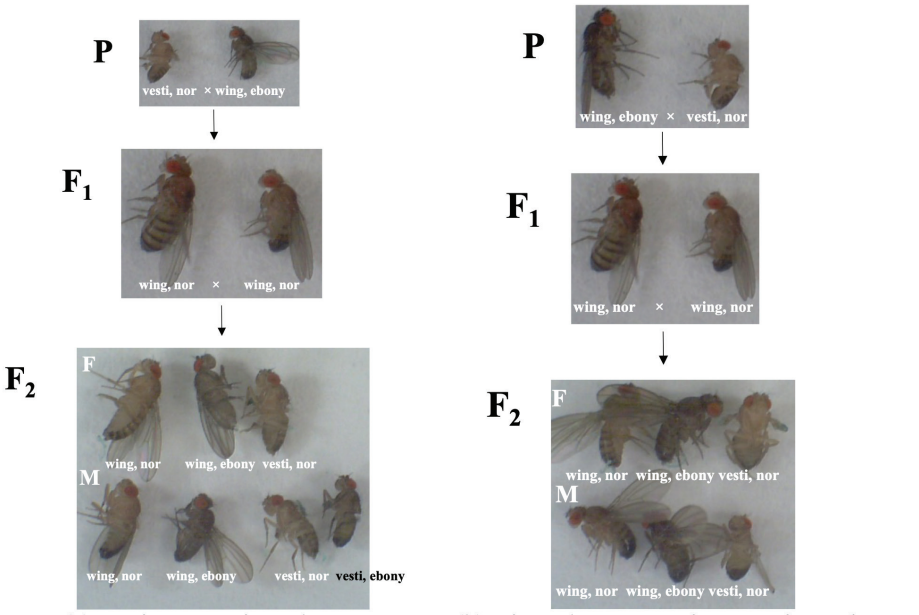

(a) vesti, nor × wing, ebony cross (b) wing, ebony × vesti, nor reciprocal cross

Figure 2. A display of the phenotypes of fruit flies in two dihybrid crosses.

In the dihybrid reciprocal cross between the strain of wing with red-eye, ebony-colored body and the strain of vestigial wing with red-eye, normal-colored body shown as (b) in Figure 2, the phenotypes for female and male in F_2 were present as winged with normal-colored body, winged with ebony-colored body, and vestigial with normal-colored body, but the vestigial with ebony-colored body was absent.

The X^2 tests were conducted for two dihybrid crosses on the female, male and the total number of flies in relation to wing presence and body shape.

	Female			Male			Female + Male		
Phenotype	Obs	Exp	X^2	Obs	Exp	X^2	Obs	Exp	X^2
Winged, normal (V_E_)	223	154.7	30.17	214	147.4	30.12	437	302.1	60.28
Winged, ebony (V_ee)	36	51.6	4.70	35	49.1	4.06	71	100.7	8.75
Vestigial, normal (eeV_)	15	51.6	25.93	12	49.1	28.06	27	100.7	53.93
Vestigial, ebony (vvee)	1	17.2	15.25	1	16.4	14.44	2	33.6	29.68
Total	275	275	76.04	262	262	76.67	537	537	152.64

Table 2. The results of X^2 tests for the dihybrid cross (vvEE × VVee).

In the dihybrid cross to observe two-gene segregation in Table 2, a total of 537 flies were counted. Of these, there were 262 female and 275 male flies. All X^2 test results indicated that probabilities were smaller than 5% because all X^2 values were greater than $X^2_{0.05,3} = 7.82$. It meant that the segregations of the genes controlling wing presence and body color didn't obey second Mendelian genetic law. The number of vestigial wing, ebony body color flies was less than expected number.

	Female			Male			Female + Male		
Phenotype	Obs	Exp	X^2	Obs	Exp	X^2	Obs	Exp	X^2
Winged, normal (V_E_)	259	202.5	15.76	194	149.1	13.55	453	351.6	29.27
Winged, ebony (V_ee)	83	67.5	3.56	67	49.7	6.03	150	117.2	9.19
Vestigial, normal (eeV_)	18	67.5	36.30	4	49.7	42.01	22	117.2	77.32
Vestigial, ebony (vvee)	0	22.5	22.50	0	16.6	16.56	0	39.1	39.06
Total	360	360	78.12	265	265	78.15	625	625	154.84

Table 3. The results of X^2 tests for the dihybrid reciprocal cross (VVee × vvEE).

As shown in Table 3, the dihybrid reciprocal cross was for the observation of two-gene segregation. A total of 625 flies were recorded. Of these, there were 360 female and 265 male flies. All X^2 test results indicated that probabilities were smaller than 5% because all X^2 values

were greater than $X^2_{0.05,3} = 7.82$. It meant that the segregations of the genes controlling wing presence and body color didn't conform to second Mendelian genetic law. The similar test results were found from the dihybrid cross above. Unfortunately, vestigial wing, ebony body color flies were not even seen in the cross.

DISCUSSION

Thomas Hunt Morgan discovered his first *Drosophila* mutant, a white-eyed male more than a century ago (Morgan, 1910). The mutant gene was named as white and resided on the X chromosome. Since then, the gene has been used to explore fundamental questions in genetics (Green, 2010). Morgan's skepticism about Mendelian genetics insired him to do research on Mendelism by searching for heritable phenotypic changes in the vinegar fly, *Drosophila melanogaster*. His research experiment related to the genes on X-chromosome was the classic example to interpret the segregating ratio. In our study, the goodness of fit test in one of the crosses for eye color gene on sex chromosome didn't conform with Morgan's early discovery indicating that the purity of parental strains from Carolina might not contain the highest quality.

The wing shape and body color didn't observe the second Mendelian genetic law, either. The possible reasons might be found in other studies. Meiotic Drive Elements (MDs) are the complex nuclear genetic loci found in various eukaryotic genomes and distorting segregation in their favor. Mendel laws of inheritance can be altered by them (Grognet et al., 2014). MDs skew the expected 1:1 ratio in their favor and are thus overrepresented in the progeny after meiosis. They have been observed in metazoans, plants, and fungi (Pennisi, 2003). They may play a critical role in population behavior, leading to sex ratio distortion and thus decreasing population size. Additionally, fitness can also be altered by MD factors if they are genetically linked to alleles that confer deleterious traits (Saupe, 2012). The results of the goodness of fit tests for the traits on X-chromosome and other autosomes in our experiment indicated that the cause of distorted ratios might come from MDs in the genes of the commercial strains used.

Investigation of "Segregation Distorter" in *Drosophila* has showed that MDs are composed of at least two linked genes, the distorter that acts as a toxin by disrupting the formation of gametes, and the responder that acts as an antitoxin that protects from the deleterious distorter effects (Larracuente and Presgraves, 2012) and (Sandler et al., 1959). Anderson et al. (2009) characterized patterns of polymorphism and divergence in the protein-coding regions of 33 genes across of *Drosophila melanogaster*. Along the *D. melanogaster* lineage several loci exhibited patterns consistent with the maintenance of protein variation (Anderson et al., 2009). Our findings in the study could provide the clue to examine whether these two linked genes in MDs and corresponding protein sequence diversity could be detected and how the genes function in the commercial strains.

It is attractive to continue investigations on the factors that cause the deviation of classical genetic ratios in these fruit fly strains, e.g., find the different interest of other gene and cross the parental strains to identify the segregation ratios, or look into the deviation at a molecular level using DNA markers.

CONCLUSION

For the eye color gene on X chromosome, the segregation in the reciprocal cross (White × Red) followed 1:1:1:1 ratio, but that in a cross didn't observe 3:1. The smaller population size in the cross (Red × White) might cause the observed ratio deviated from the expected one. The appropriate population size in the reciprocal cross resulted in the compliance with 1:1:1:1 ratio.

In two dihybrid crosses, the results the segregations in female, male, and overall didn't fit 9:3:3:1 ratio. The prospective causes can be examined through several approaches mentioned in the discussion.

AUTHOR INFORMATION

Corresponding Author

*Yusheng Wu, ywu@usw.edu
Department of Biology
College of Arts and Sciences
University of the Southwest
Hobbs, NM 88240

ACKNOWLEDGMENT

We thank College of Arts and Sciences and Department of Biology at University of the Southwest for the guidance and support in the project.

REFERENCES

Anderson, J. A., Gilliland, W. D., & Langley, C. H. Molecular population genetics and evolution of Drosophila meiosis genes. *Genetics* **2009**, *181*, 177-185.

Carolina Biological Supply Company. Drosophila Manual. https://www.carolina.com/drosophila-fruit-fly-genetics/drosophila-manual-carolina/452620.pr (accessed March 19, 2020).

Green, M. M. A century of drosophila genetics through the prism of the white gene. *Genetics* **2010**, *184*, 3-7.

Grognet, P., Lalucque, H., Malagnac, F., Silar, P. Genes that bias mendelian segregation. *PLOS Genetics* **2014**, *10(5)*, e1004387. https://doi.org/10.1371/journal.pgen.1004387

Klug, W. S., Cummings, M. R., Spencer, C. A., Palladino, M. A. *Essentials of Genetics*. 7th ed.;. Pearson Education Inc.; 2010.

Larracuente, A. M., Presgraves, D. C. The selfish segregation distorter gene complex of *Drosophila melanogaster*. *Genetics* **2012**, *192*, 33-53.

Morgan, T. H. Sex-limited inheritance in Drosophila. *Science* **1910**, *32*, 120-122.

Pennisi, E. Meiotic drive: Bickering genes shape evolution. *Science* **2003**, *301*, 1837-1839.

Sandler, L., Hiraizumi, Y., Sandler, I. Meiotic drive in natural populations of drosophila melanogaster: the cytogenetic basis of segregation/distortion. *Genetics* **1959**, *44*, 233-250.

Saupe, S. J. A fungal gene reinforces mendel's laws by counteracting genetic cheating. *Proc. Nat.l Acad. Sci. USA* **2012**, *109*, 11900-11901.

Outstanding Science Teacher Award

ABOUT THE AWARDS

Since 1968, the New Mexico Academy of Science (NMAS) has awarded the Outstanding Science Teacher Award to honor New Mexico science and math educators. This award recognizes teachers who provide opportunities for students to succeed. Nominations are open to all preK-12 teachers and informal science educators throughout New Mexico. NMAS presents a plaque and a monetary award to each teacher. The American Chemical Society also presents a monetary award to the winning teachers.

2020 Recipients

The 2020 New Mexico Outstanding Science Teacher Award winners are Eva Abeyta from Los Alamos Online Learning Academy and Lena Eddings from La Cueva High School in Albuquerque.

Eva Abeyta is in her 25th year teaching with 13 of those in Los Alamos. Mrs. Abeyta has taught 15 years of middle school, 5 years of elementary school, and 5 years of high school. She has taught various subjects including: Physical Science, Life Science, Chemistry, Physics, Anatomy & Physiology and all subjects including Spanish at the elementary level. In this COVID environment she is teaching middle school science classes totally on-line. Her first nominator, a colleague at her former school, Los Alamos Middle School, stated: "I have worked with Eva Abeyta for the last 15+ years. She has held the science department chair of our department for many of those years. I have come to appreciate being a colleague with Eva. She is always level headed and sees the big picture of where science education is going. She is willing to try new curricula and adapt what she teaches to what her students need. After 15 years of working with Eva I have nothing but praise for her professionalism and science teaching capabilities." A second nominator, from her current school, added these comments: "Ms. Abeyta teaches 6th, 7th, and 8th grade science this year totally online. Because of the new grade level, she is dealing with, and the totally online teaching, she had a steep learning curve. However, she has shown a great deal of ingenuity in teaching science effectively online. She readily takes on a new challenge and embraces it. She is responsible and dependable and is responsive to her students' parents. She ably heads up the district science fair. I know that in her previous school, as department chair, she also helped other teachers make the transition to the Next Generation Science Standards (NGSS). In short, although she is an extremely experienced science teacher, she has never stopped learning herself and is not afraid of using new techniques to address new challenges."

Lena Eddings holds a M.S. in Civil Engineering from the University South Carolina and a Secondary education License through the University of New Mexico. Prior to beginning her teaching career, Ms. Eddings worked as a Civil Engineer in Texas and South Carolina, and as a consultant for environmental clean-up at Kirtland AFB. Currently she is a Physics Instructor and Science Department Chairperson at La Cueva High School (LCHS). Ms. Eddings states her classroom objectives: "To promote a challenging and thought-provoking learning environment giving students the problem-solving skills that will inspire them to be inquisitive and push outside of their comfort zone to further their knowledge and life experiences." At LCHS, Ms. Eddings has served on the school-wide instructional Council and the district-wide team to adopt the NGSS. She has been recognized as an influential staff member and one who has made a difference in academic achievement by graduating seniors annually since 2014. In the words of her nominator: "[Ms. Eddings] has a unique teaching style: making her class not only informative but also proving that humor can help students learn better. She provides one-on-one support and meets students where they are in terms of their style of learning. She explains everything thoroughly in many different ways [and] is very genuine in the way she interacts with kids. She is very understanding; and even though she holds to a high standard of classroom etiquette, she is very supportive when a student needs support. This year's COVID-19 pandemic and concomitant restriction from in-person teaching has created extraordinary challenges for teachers. In this very challenging situation, I have observed the tremendous extra efforts that Mrs. Eddings took to ensure optimal learning experience for her students."

Outstanding Scientist Award

ABOUT THE AWARD

Beginning in 1962, NMAS has presented awards intermittently to New Mexicans for "Outstanding Contributions and Distinguished Service to Science and Scientific Education in New Mexico". Awardees in the past have included Dr. W. Randolph Lovelace II, Chief of the U.S. Army Air Corps Aero-Medical Laboratory and founder of Lovelace Clinic in Albuquerque; Clyde Tombaugh, NMSU, the discoverer of Pluto; and Norris Bradbury, Los Alamos, for whom the Bradbury Museum is named. The award was last presented in 2013. In 2020, it was presented to Dr. Angela Wandinger-Ness, UNM.

2020 Recipient

Angela Wandinger-Ness received her Ph.D. in Biochemistry at the University of California, Los Angeles and completed post-doctoral training at the European Molecular Biology Laboratory in Heidelberg, Germany. Her first faculty appointment was at Northwestern University. Since 1998, Dr. Wandinger-Ness has been on faculty in the Department of Pathology at the UNMHSC and a member of the UNM Comprehensive Cancer Center.

Currently, Dr. Wandinger-Ness is The Victor and Ruby Hansen Surface Endowed Professor in Cancer Cell Biology and Clinical Translation. She serves as Associate Director for Education, Training and Mentoring at the UNM Comprehensive Cancer Center, is the PI of multiple training programs, and is an internationally-recognized expert on Ras-related GTPases.

Passionate about science and education, Dr. Wandinger-Ness is motivated by sleuthing disease mechanisms and translating discoveries into better or new therapies. For nearly 30 years she has led a vibrant research team that includes students and fellows studying kidney disease and ovarian cancer. In the area of kidney disease she has elucidated the mechanisms underlying autosomal dominant polycystic kidney disease and relationships to oral-cranio-facial disease, and developed strategies for kidney regeneration through the use of stem cells and decellularized scaffolds. In the cancer arena, Wandinger-Ness and her team have identified new uses for known drugs and evaluated the benefits for ovarian cancer in patient trials.

Dr. Wandinger-Ness has authored over 90 peer-reviewed articles and reviews; and has eight awarded patents. Dr. Wandinger-Ness is an elected Fellow of the American Association for the Advancement of Science, served as a Visiting Professor at the Max-Planck Institute for Molecular Physiology in Dortmund, Germany, and as a Research Ambassador for the German Academic Exchange Program.

Through formal teaching and mentoring, she has launched the careers of hundreds of undergraduate, graduate and post-doctoral trainees, and junior faculty. She is the recipient of numerous awards for excellence in research, innovation and education. Most recently she was recognized as the 2019 Innovation Fellow by UNM. STC/Lobo Rainforest Innovations, the 2020 American Association for the Advancement of Science Lifetime Mentor, and the US Presidential Awardee for Excellence in Science, Mathematics and Engineering Mentoring. She attributes her success to her abilities to communicate, engage with diverse people, and secure funding, and to an entrepreneurial spirit.

Dr. Wandinger-Ness served as an active board member and leader of NMAS from 2004-2012. During her tenure she supported statewide NMAS activities for secondary school students and teachers, coordinated fundraising, the Annual meeting and banquet, and a promotional brochure.

2020 New Mexico Research Symposium

ABOUT THE RESEARCH SYMPOSIUM

The 2020 New Mexico Research Symposium was held virtually November 9 through 13 due to COVID-19. Over 250 people attended the online event and nearly 30 posters were showcased in the virtual poster session. Abstracts of these posters are included in this annual volume of the NMAS *New Mexico Journal of Science*. The Symposium closed with an awards ceremony honoring the two 2020 Outstanding New Mexico Science Teacher Award recipients, Eva Abeyta from Los Alamos Online Learning Academy and Lena Eddings from La Cueva High School in Albuquerque, the 2020 Outstanding Scientist Award, Dr. Angela Wandinger-Ness, and the student poster competition winners.

SYMPOSIUM WELCOME FROM 2020 NMAS PRESIDENT

On behalf of the New Mexico Academy of Science, I would like to welcome each of you to the 2020 Research Symposium. NMAS is pleased to partner with New Mexico EPSCoR, the UNM Center for Water and the Environment, the American Chemical Society, and New Mexico AMP to sponsor this annual conference to promote science and science education in our community. The COVID-19 pandemic this year has prevented us from gathering in person. Fortunately, EPSCoR's resources have enabled us to gather virtually. Big compliments are due to NM EPSCoR's resourceful and hard-working staff led by Dr. Selena Connealy. Our keynote speaker is Dr. Bette Korber, Laboratory Fellow at Los Alamos National Laboratory. She will be speaking about her research on the human immune system, vaccines, and vaccine strategies for AIDS and COVID-19. Join us for her outstanding presentation and answers to your questions. As we do every year, the symposium presents the awards for Outstanding Teachers in our state. We will have a few days of interesting and engaging presentations by students and professors, especially from the University of New Mexico's Smart Grid Center. Student posters will be presented and judged online, and awards will be given to the authors of the best posters. This year, NMAS will give an Outstanding Scientist award to Dr. Angela Wandinger-Ness, UNM's Victor and Ruby Hansen Surface Endowed Professor in Cancer Cell Biology and Clinical Translation. She will give a presentation entitled "GTPases to Cures: My Path to Discovery and Innovation."

Zhiming Liu, NMAS President

OPENING KEYNOTE SPEAKER: BETTE KORBER, PH.D.

Dr. Korber is a Laboratory Fellow at the Los Alamos National Laboratory in the Theoretical Biology and Biophysics Group. Her work focuses on viral evolution, the human immune response to infection, and vaccine design. She leads an interdisciplinary team that provides bioinformatics, theoretical, and statistical support in collaborative efforts with experimental researchers, working primarily on HIV, but also on Ebola, Hepatitis C, and influenza. Like so many, she has recently begun to work on coronaviruses in response to the global pandemic. Some highlights from of her work include vaccine designs to cope with viral diversity, characterizing the evolution of HIV under immune pressure during infection, and developing sequence-based signature analyses methods that include phylogenetic corrections to compensate for founder effects. Her mosaic HIV vaccine design is currently being evaluated in a Phase 2b human clinical trial called Imbokodo. Some of her awards and honors include: the E.O. Lawrence Award, the Dept. of Energy's highest scientific honor (2004); the Secretary of the Dept. of Energy Award for her work on the Ebola Task Force (2017); the Richard P. Feynman Innovation Prize (2018); R&D 100 Scientist of the Year (2018); and Battelle's Inventor of the Year (2019).

ABOUT THE SPONSORS

New Mexico Academy of Science

Founded in 1902, the New Mexico Academy of Science (NMAS) has been in continuous existence since 1915. NMAS is a member of the National Association of Academies of Science (NAAS) and an affiliate of the American Association for the Advancement of Science (AAAS). NMAS works with teachers, state agencies, and the legislature to establish appropriate standards for the teaching of the sciences. NMAS goals are to foster scientific research and scientific cooperation, increase public awareness of the role of science in human progress and human welfare, and promote science education in New Mexico. Visit www.nmas.org to learn more.

New Mexico EPSCoR

The New Mexico Established Program to Stimulate Competitive Research (NM EPSCoR) is funded by the National Science Foundation (NSF) to build the state's capacity to conduct scientific research. The infrastructure and activities of the New Mexico SMART Grid Center are designed to support shared–use equipment, engage new research and community college faculty, and support the STEM pipeline by training teachers, undergraduate and graduate students, and post–doctoral fellows. Research findings are communicated broadly through various outlets, including local museums. Visit www.nmepscor.org to learn more about NM EPSCoR, and visit www.nsf.gov/epscor to learn more about the NSF EPSCoR initiative and other jurisdictions.

American Chemical Society

The American Chemical Society (ACS) is the world's largest scientific society and one of the world's leading sources of authoritative scientific information. A nonprofit organization, chartered by Congress, ACS is at the forefront of the evolving worldwide chemical enterprise and the premier professional home for chemists, chemical engineers and related professions around the globe. The Central New Mexico Local Section of the American Chemical Society was founded in 1946 and generally serves the northern two-thirds of the state of New Mexico. The Local Section specifically includes the following New Mexico counties: Bernalillo, Los Alamos, Rio Arriba, San Miguel, Sandoval, Santa Fe, Socorro, Taos, Torrance, and Valencia.

UNM Center for Water & the Environment

The mission of the Center for Water and the Environment at the University of New Mexico is to increase the participation of underrepresented minorities (URM) in science, technology, engineering and math (STEM) professions while conducting cutting-edge research into technological and engineering-based solutions to problems with water and the environment, in a framework that considers the social, economic, policy, regulatory, and legal implications. Practical solutions to problems related to water availability in arid environments and in times of drought, and problems associated with energy generation and consumption are particularly relevant, in light of the criticality of these issues to the state of New Mexico, the southwestern United States, and their global importance. Learn more at cwe.unm.edu.

New Mexico Alliance for Minority Participation

Established in 1993 with major funding from the NSF, the New Mexico Alliance for Minority Participation (NM AMP) is a partnership of the state's two- and four-year colleges and universities, with a primary goal of increasing the number of B.S. degrees awarded to under-represented students in New Mexico. NM AMP supports students with scholarships, research assistantships, professional development, and enhanced teaching, learning, and mentoring experiences. Program activities are designed to attend to individual student retention, development, and progression; support student progression to the STEM workforce and graduate school; and promote the replication of best practices, both within New Mexico and nationally. To learn more, visit www.nmsu.edu/~nmamp/.

NM SMART GRID CENTER SEMINAR SESSION ABSTRACTS

Seminar session abstracts are listed alphabetically by last name of registered presenter.

Quality of Service Aware NDN Based Network Architecture

Anju K. James, New Mexico State University
George Torres, New Mexico State University
Satyajayant Misra, New Mexico State University
Sharad Shrestha, New Mexico State University

A reliable communication architecture is one of the main concerns of smart grid, which requires bi-directional data flow between its devices. The currently used IP architecture fall short in supporting major smart grid communication requirements such as scalability, protocol interoperability, security and Quality of Service (QoS), etc. In order to address these requirements effectively, an information centric network architecture called Named Data Networking (NDN) can be used. In our research, a QoS-aware NDN framework is used to provide Quality of Service in smart grid communication. The network traffic is classified based on its priority, using three different transmission queues and traffic is controlled using token buckets. This framework helps to address the low latency, high bandwidth, and high reliability requirements of smart grid communications.

Microgrid Installations and Consumer Acceptance: Preliminary Contingent Valuation Evidence from Arizona, Colorado, New Mexico, and Utah

Jesse Kaczmarski, The University of New Mexico

Measuring the costs and benefits of distributed feeder microgrids (DFMs) is incomplete without insight into consumer desire and acceptance. Given than grid modernization and infrastructure upgrade costs are often passed along to consumers, we present the first evidence of consumer acceptance and willingness to pay for DFM installations in the 4-corners (AZ, CO, NM, and UT). Using survey data collected from September to October of 2020 (n=5500 approx.), we present preliminary results for the median amount that consumers are willing to pay for installations dependent on the level of direct benefits the consumer would receive. In addition, we present the environmental and institutional values most closely associated with consumer acceptance of DFMs.

Resiliency Enhancement of the Smart Grid Considering Time-Varying Priority of Dynamic Loads

Shubhasmita Pati, New Mexico State University

Resiliency of the power system in the event of natural disasters or cyber-physical threats is greatly challenging. In the aftermath of disasters, damage to the electrical grid can dawdle the recovery effort and perpetuate human suffering. We present a stochastic optimization approach for resilience-oriented-design (ROD) and resilience-oriented-operation (ROO), considering the temporal variation in priority of critical loads. We focus on the management of transmission and distribution systems with objective of transferring maximum power from conventional and distributed energy resources (DERs) to the critical loads. The ROO recommends scheduling of the generators and management plan for loads to maintain and restore power after a catastrophic event due to natural disaster or a cyberattack.

UNDERGRADUATE STUDENT POSTER ABSTRACTS

Poster session abstracts are listed alphabetically by last name of registered presenter. An asterisk (*) indicates the poster received an outstanding undergraduate poster award at the 2020 New Mexico Research Symposium.

Collection of *Pinus edulis* Cones Throughout the Navajo Nation

Chase Bebo, Navajo Technical University

The impact of climate change in the Navajo Nation has threatened one of its native plant species pinyon pine (*Pinus edulis*). A pinyon pine restoration project aims to revegetate the areas lost due to the climate change. For this study pinyon pine cones were collected from five areas around the Navajo Nation. Pinyon pine cones that were green and closed were collected in order to ensure that they had viable seeds that could be used for the restoration project. Brown paper bags were used to store the cones and the tree ID number, coordinates, location, and the diameter of each tree were marked properly. The first area from where the cones were collected was Black Mesa near Kayenta, Arizona and Shonto, Arizona. At this site 40 cones were collected from 125 trees. The second area from where the cones were collected was Spider Rock near Canyon De Chelly in Arizona. Cones were collected from 28 trees at this site. The third site was Kinlechee, Arizona where the cones were collected from 15 trees. The fourth site was Defiance Plateau which is located on the outskirts of Widow Rock, Arizona and cones were collected from 3 trees at this site. The fifth and last site the cones were collected from was the restoration site at Borrego Pass, New Mexico. At this site cones were only collected from 1 tree as the pinyon pine trees at this site were not as abundant as the other collection sites. After the completion of the pinyon pine cone collection, the cones were let to sit in the brown paper bags that were used to store them in until they opened up. Once the cones were opened up, the extraction of each pinyon pine seed from the cones were done and separation of the hollow ones from the viable ones were performed. The seeds from the trees were stored inside properly labeled Ziploc bags. Finally, the seed containing bags were stored in a freezer to keep them viable for the pinyon pine restoration project. This study helped to develop collection of native variety of pinyon pine seeds that will be extremely useful for the pinyon pine restoration project in the Navajo Nation.

Structural Health Monitoring of Aerospace Structures via Acoustic Emissions

Savannah Bradley, New Mexico Tech Arvin Ebrahimkhanlou, New Mexico Tech

In general, it is more cost effective for structures to remain in operation for long periods of time. Aerospace structures undergo various stresses throughout their lifetime. By monitoring the health of these structures, improvements can be made on the overall structure. Additionally, this information can be used to make decisions regarding usage, maintenance, and retirement of the structure entirely. Acoustic emission data is ideal for use in structural health monitoring. Acoustic emissions allow the user to detect structural defects before the structure fails catastrophically. This technology will be used to find cracks induced by corrosion in panels of aerospace structures.

Structural Health Monitoring of Lunar Pipelines for Resource Extraction

Mario Escarcega, New Mexico Tech

There is a wealth of knowledge that can be acquired from the lunar surface, such as human habitation in space as well as resource acquisition. To this end, habitations could eventually exist on the Moon. The habitations must be sustainable, so water, hydrogen, and oxygen will be mined. The transportation systems for these substances will likely be pipes, which will be subjected to the harsh conditions on the Moon. On Earth, smart structural health monitoring (SHM) is an applied field of wave-based analysis that creates a virtual on a structure

that senses any damage. For example, one piezoelectric transducer can be attached to a thin-walled structure to assess the damage the material has incurred using guided-wave propagation. This type of structural analysis can accurately localize and categorize damage. Any induced damage to a pipeline via corrosion, impacts, seismic activity, etc., may cause leakage, which constitutes a loss of material. These leaks or other defects can propagate into a catastrophic event. Loss of resources and possible environmental catastrophes are the main impetus for utilizing SHM techniques on Earth. The results of this study can potentially pioneer SHM of lunar architecture. A ruptured pipeline can contaminate the lunar surface, which violates NASA's anti-contamination policies. A SHM technique would significantly complement the strategies NASA uses to prevent corrosion during operations. A SHM technique for a lunar base is necessary to gather information about extraterrestrial habitation that will aid NASA's efforts in building a base on Mars. Above all, an additional level of security is added with SHM because mission control will have access to real-time data of an unexpected event that compromises the mission and the lives of astronauts. A SHM technique that works on Earth must be adapted for lunar use. High radiation, high heat, launch, and impact stresses contribute noise to a system of sensors. Any external sensing apparatus could be catastrophically damaged. To this end, this project will research the feasibility of a novel SHM technique for lunar pipelines. A literature review was conducted in the first semester. The review focused on information pertaining to the hazards of space and designing tests and sensors that can withstand the above-mentioned conditions. The results of the literature review show that the transportation of water, hydrogen, and oxygen from mined ice can subject lunar pipelines to corrosion and damage. The active strategy NASA uses to combat corrosion in space (such as the corrosion of aluminum by atomic oxygen) is to coat structures in a thin film of a precious substance, such as gold. These films can be delaminated by space debris. Lunar dust is also an abrasive substance that can potentially weaken thin films and lunar architecture.

A Machine Learning Model to Predict Groundwater Levels in the Mesilla Transboundary Aquifer*

Jacobo Giron, New Mexico State University
Kevin Perez, New Mexico State University
Omid Jafari, New Mexico State University
Parth Nagarkar, New Mexico State University
Jonathan Montano, New Mexico State University
Khandker Mushfiqul Islam, New Mexico State University

The purpose of this research is to find the most effective way to forecast groundwater levels for wells in the Mesilla aquifer region of New Mexico. Although water level forecasting has many uses and applications, it is particularly useful in New Mexico. In 2015, New Mexico was home to 24,000 farms spanning 43.2 million acres. With more than 50% of the state's land being dedicated to agriculture, predicting groundwater levels allows municipalities to plan in terms of water conservation and allocation throughout residential and agricultural areas. In this work, we particularly focus on the Mesilla aquifer region of southern New Mexico, which is a transboundary aquifer between the US and Mexico under an intensive water use for agriculture and human consumption.

Recently, machine learning-related approaches have also shown great predictive capabilities in the field of water resources. Several works in this field have used state-of-the-art techniques based on Recurrent Neural Networks (RNNs) to predict groundwater levels by using historical data, such as groundwater levels and other weather-related attributes (e.g., precipitation, temperature, etc.). We observe that the wells in the Mesilla aquifer region are uniquely positioned, and hence propose a machine learning technique that is enhanced using spatial analysis.

In this research work, we focused on using the state-of-the-art Recurrent Neural Networks called Gated Recurrent Units (GRU). We noticed better accuracy by using GRU instead of Long Short Term Memory (LSTM). We created a baseline model (called Model1) using a groundwater well with water levels dating back 775 months. This model was built with GRU using the Adam optimizer. Further, we included additional weather-related data, such as precipitation, temperature, depth from the top of the well to the water surface, and land surface elevation in the training model (called Model2). Finally, we performed spatial analysis on each well to improve the predictions of the previous models. With over 300 wells in the data, we sorted the distance of each

well from the target well. We used the data from neighboring wells while training our model. After experimenting on different parameters (number of neighboring wells, amount of historical data to consider, number of weather-related attributes to choose from), we achieved the best results after using the data from five nearest wells, limiting the historical data to 10 years, and by using historical precipitation and temperature data along with the groundwater levels. We improved the accuracy (measured in terms of RMSE) of the baseline model by about 80% by integrating weather-related information and data from neighboring wells into the training model. For future work, we will focus on comparing our results with those using classical methods such as the modular finite-difference flow model (Modflow).

Duplication History of the Piwi Gene Family in Vertebrates

Javier Gutierrez, Eastern New Mexico University Micheal Vandewege, Eastern New Mexico University

Piwis are regulatory proteins that belong to the Argonaute gene family. Piwis are known to defend host genomes against transposable element (TE) mobilization in germline cells and use a class of small RNA, piRNA, as guides to TE transcripts and loci. The Argonaute family has members among all eukaryotes, but Piwis are only present in animals. Piwis are primarily expressed in gonadal tissues and protect inheritable genomes against the mobilization and propagation of TEs through transcript cleavage and TE methylation. Vertebrates genomes encode up to four Piwis named Piwil1, Piwil2, Piwil3 and Piwil4. Piwil1 and Piwil2 have been described in most animals, but Piwil3 and Piwil4 are specific to vertebrates and their duplication history is unresolved. Therefore, we leveraged phylogenetic, synteny, and expression analyses to address this void. We collected Piwi DNA sequences from Ensembl 101 and NCBI from species representing all major vertebrate lineages. Piwi sequences were aligned and we constructed phylogenetic trees using IQTREE and ExaBayes. Our phylogenetic analysis suggests Piwil1 and Piwil2 were retained in all vertebrate members. Piwil4 was the result of Piwil1 duplication in the ancestor of gnathostomes but was independently lost in ray-finned fishes and birds. Further, Piwil3 was also derived from a tandem Piwil1 duplicate in the common ancestor of marsupial and placental mammals. However, Piwil3 was secondarily lost in Afrotherians, Xenarthrans, and mouse-like rodents. Interestingly, the evolutionary rate of Piwil3 is considerably faster than Piwil1, consistent with gene duplication models that predict relaxation of functional constraint and subsequent neofunctionalization. Further, several amino acid sites throughout the entirety of Piwil3 were evolving in a manner consistent with positive selection. Generally, gene order Piwil1, Piwil2, and Piwil4 has been conserved through vertebrate evolution, even around the Piwil4 locus in birds and ray-finned fish that lost Piwil4. The position of Piwil3 has been less conserved during mammalian evolution and can be bordered by a diversity of genes. Lastly, our expression analyses suggest Piwi expression has mostly been constrained to gonads throughout vertebrate evolution, consistent with previous analyses. Vertebrate evolution is marked by two rounds of whole genome duplication and many multigene families can be linked to this event. However, our analyses suggest Piwi duplications were independent of these events. Further, teleost fishes lack any additional Piwi paralogs despite an independent round of whole genome duplication. The loss of Piwil4 in birds and ray-finned fishes is interesting because Piwil4 is linked to preventing TE mobilization through DNA methylation. TEs are silenced at CpG sites in mammals but CpG islands are largely un-methylated in birds. It is hypothesized methylating TEs creates a non-lethal relationship between TEs and host genomes by allowing the retention of insertions that would otherwise be purged by natural selection. Piwil4 is present in other reptiles and reptilian TEs are not methylated at CpG sites; however, there could be a possible link between the loss of Piwil4 and TE reduction in birds worthy of further investigation.

Testing Restoration Methods for Pinyon Pine on the Navajo Nation Soil Clay/Stoniness Likelihood on Successful Restoration of Pine on the Navajo Nation

Dalyna Hannah, Navajo Technical University

The Navajo Nation is the largest American Indian reservation (covering roughly 27,413 miles), including parts of New Mexico, Arizona, Utah, and Colorado, USA. A tree species within the Navajo Nation that is currently under threat is the pinyon pine (*Pinus edulis*), whose numbers have decreased over the past decade. This species is in need of conservation efforts if it's to survive climate change. In August of 2019 we began our restoration site planting at Borrego Pass, New Mexico. Borrego Pass is located approximately fifteen miles from Navajo Technical University, in Crownpoint, New Mexico. We chose this location because it is known as a pinyon-juniper woodland along with other dominant species such as mountain mahogany, sagebrush, and snakeweed. In total 232 pinyon pine seedlings were planted at Borrego Pass, New Mexico. The seedlings were separated between 51 sets of four differentiating two different areas: cliff-edge (clay), and non-cliff (sand) edge surface. A total of 56 seedlings were planted within the clay surface, and 148 seedlings were planted within the sand area. The set of four seedlings has its own substance or mycorrhizal planted, with one nurse type. After months of allowing the seedlings to grow on their own, we learned the importance of the soil moisture regarding the content playing an important role within the growth progress of the seedlings.

Geospatial Analysis of Black Mesa's Pinyon Pine Trees Growth Parameters

Randy Largo, Navajo Technical University

Navajo Nation is facing many environmental issues related to climate change. Degradation of pinyon pine (*Pinus edulis*) forests, among other native plant species, is one of such major on-going environmental challenges for the Navajo Nation. Pinyon Pines have ecological and cultural significance for the Navajo people. The objective of this study was to quantify pinyon pine trees growth parameters such cones, height, and diameter in order to assess pinyon pine forest's health and productivity. The study was conducted in Black Mesa located in the northeast region of the state of Arizona and within the Navajo Nation. Black Mesa is mostly a forest of pinyon pine, juniper, ponderosa pine, and oak. This environment has sandy shrub land of black sage and snakeweed in open fields which are scattered across Black Mesa. We mapped the area of the study and sampled approximately 175 pinyon pine trees. For each tree, we collected and counted cones. Tree height was simultaneously recorded and its diameter at breast height (dbh) measured using a slide caliper. The geographic coordinates (latitude and longitude) of each of three location were recorded using a Garmin handheld GPS. The collected data was transferred into MS-Excel then to ARCGIS ARCMAP 10.8 for mapping and geospatial analysis. Results showed that the cones, diameter, and tree height varied from 40 to 50; 5 to 61 cm and 160 to 985 cm, respectively. The coefficients of variation (CV) were 3.09% for cones, but 43% for diameter, and height, suggesting that these tree growth parameters had a high variability. Maps portraying the spatial distribution of trees showed a cluster of pinyon pines in the northern side of the study field. Further geostatistical analysis confirmed the high variability of tree diameter and height of pinyon pine trees across Black Mesa. The results of this study will be very useful for the implementation of pinyon pine management in this area.

Hierarchical Structure of Microgrid Control Systems*

Joshua May, CNM Community College Althea Denlinger, UNM Los Alamos

This poster describes the Hierarchical Structure of microgrids, the role of each control section, and a few examples of how to further one's knowledge and understanding of micro grids. This poster is the result of a two-month research project to learn the rudimentary principles of the Hierarchical Structure of microgrids and is from the

level of an undergraduate. Microgrids, according to the center for climate and energy solutions, provide less then 0.2 percent of power in the United States but can be one of the most revolutionary ways to manage, sustain, and deliver power. The efforts with this program are attempting to bring microgrids to New Mexico to help change its power systems for the better. My research partner Althea and I spent the summer being mentored by Dr. Bidram in which he gave us papers to read and research. Part of the outcome of that program was this poster! With the knowledge I have learned from this and the curiosity, it has led me to participate in the stemap plus program to delve more into microgrids and its cybersecurity aspect for the next year.

A Demonstration of Traditional Navajo Farming Technique

Phaizon Osborne, Navajo Technical University

Climate change is one of the major factors causing soil erosion and soil quality deterioration in the U.S. Overgrazing, deforestation, and unsustainable agricultural practices are equally responsible for the U.S. soil quality deterioration. Often compared in size to the state of West Virginia, the Navajo Nation has an area of over 27,000 square miles. Situated in the southwestern Colorado Plateau, the Nation's geography and topography are characterized by arid deserts, alpine forests with high plateaus, mesas, and mountains reaching up to 10,388 feet in altitude. Low desert regions have an altitude as low as 2,750 feet. Within this geography the Navajo people are dealing with serious environmental challenges, and one of them is associated with climate change-induced soil quality deterioration. Navajo culture integrates traditional ecological knowledge (TEK) that talks about maintaining a balance between Mother Earth and humankind. Traditional Navajo farming incorporates this knowledge and is an example of maintaining the harmony between humankind and nature. Absolutely no use of chemical fertilizers or pesticides is one of the environmental-friendly approaches of traditional Navajo farming technique. The way numerous First Nations including the Navajos do farming is not only beneficial to the environment, but the process can build topsoil with ancient heirloom seeds. The heirloom seeds are grown by Native Americans are known to be resilient and were bred to be nutritious. Heathy soil is especially important for many reasons; it not only increases yields dramatically but it also makes the food more nutrient-rich. The use of weeds or forbs as a mulch in the crop-field is a great way to start this process. Mulching helps water to be trapped on the ground for more effective use in a crop-field and making habitat for microorganisms that keep the plants heathy and resistant to diseases. This study applied TEK of Navajo farming while creating a garden on a 14-acre farmland owned and operated by traditional Navajo farmers in Nenahnezad, New Mexico. The garden was made up of corn, bush beans, buckwheat, sunflowers, zinnias, watermelons, and sweet potatoes. The purpose of having different species in one spot was to mimic a forest environment if planted at the right time and place. A forest is made up of four or more layers of plantation: emergent, canopy, understory, and others. In this garden, corn played the role of canopy, sunflowers played the role of forest edge, the beans, buckwheat, and watermelons played the role of understory. The seeds were planted in Spring, 2020 and irrigation was done on a periodic basis. Plants growth monitoring was conducted during this study. This study showed the traditional knowledge of seed selection and application of Navajo traditional framing practices are extremely useful in maintaining and managing highly vulnerable soil type of Navajo Nation. This rich traditional knowledge can also be applied to other parts of this country for the purpose of soil management.

Role of the bHLH Transcription Factor ASCL1 in Glial Development

Antonella Riega, The University of New Mexico Tou YiaVue, The University of New Mexico HSC

I will be analyzing the role of basic-helix-loop-helix (bHLH) transcription factor ASCL1 in glial cell development. Glial cells are a type of cells in the nervous system that surround neurons and work as support and insulation. Interest in glial cells and the abnormal development of the types of cells (such as astrocytes and

oligodendrocytes) has increased due to its potential role in neurological disorders (such as schizophrenia, autism, tumors, multiple sclerosis, and even amyotrophic lateral sclerosis). A bHLH is a protein motif that characterizes transcription factors. ASCL1 is a protein encoded by the ASCL1 gene in humans. Because of these potential diseases and the role of ASCL1 as a master regulator of neural development, studies have been conducted to understand how this protein could be potentially manipulated to help regulate certain disease developments as well as proliferation of certain types of glial cells. I will be using transgenic mice to study the role of ASCL1 in glial development in the brain. These transgenic mice allows one to directly visualize and trace the lineage of ASCL1-expressing progenitor cells using reporter proteins (GFP, tdTomato) from birth into adulthood, or to over express ASCL1 specifically in astrocyte or oligodendrocyte lineage cells in a temporally inducible manner. In order to accomplish this goal, harvesting mouse brain tissues, sectioning these tissues using a cryostat onto slides, and performing immunohistochemistry on the slides to analyze labeled or manipulated glial cells will be used. Finally, a Zeis LSM 800 would be used to perform confocal imaging of the slides to collect data.

Physico-chemical Characterization of Soil within the Navajo Nation for the Pinyon Pine Restoration Project

Devina Tayah, Navajo Technical University

Physico-chemical properties of a soil type determines its ability to support plant growth. Climate change is one of the major factors that contributes to deterioration of soil health globally. The largest Native American reservation in the United States, the Navajo Nation, is currently experiencing this problem firsthand. The Navajo Nation is comprised of approximately 16 million acres of land and is located in the Four Corners area (Arizona, New Mexico, Utah, and Colorado). Pinyon pine (*Pinus edulis*) is the state tree of New Mexico and has cultural significance for the Navajo people. Currently pinyon pine trees are threatened by climate change due to the increased temperature over the past years. This study aimed to conduct soil health monitoring in the areas within the Navajo Nation where pinyon pine trees grow in abundance. In August 2019, students from Navajo Technical University (NTU) planted 232 pinyon pine seedlings, beginning a restoration site at Borrego Pass, which is fifteen minutes from NTU Crownpoint, New Mexico campus. The seedlings of the pinyon pine were separated into four sets and planted in different areas at the restoration site. In total, 20 soil samples were tested. Physical properties of the soil samples were determined through soil textures analysis using a hydrometer and seven-layered sieves. Chemical properties of the soil samples were measured by analyzing soil pH, nitrogen concentration, potassium concentration, phosphate concentration, salinity, and cation exchange capacity. The findings of this study provided a broad data set containing physico-chemical soil properties of the area which was previously untested. With this data, soil texture determination of the areas not measured will be possible using Geographic Information System. This result will also be extremely beneficial for the pinyon pine restoration and management practices in the area.

Synthesis of Anticancer Drug-Drug Co-crystals

Raquel Trevizo, Eastern New Mexico University
Ivan Arvizo, Eastern New Mexico University
Quinton Flores, Eastern New Mexico University
Zhihan Wang, Eastern New Mexico University

Cancer has been known to be one of the leading causes of death in individuals worldwide. A variety of anticancer drugs have proven to be effective, yet present several limitations concerning bioavailability in vivo. Such limitations have been found to include poor permeability, low solubility, and high sensitivity to food intake. Several studies surrounding anticancer drug-drug co-crystals have focused on improving solubility among other deficiencies in order to facilitate drug administration in the body and improve target area impact. Through the application of intermolecular forces, several anticancer drugs have been combined with a co-former compound

to produce anticancer drug-drug co-crystals. The anticancer drugs of interest in this study include abiraterone acetate, gefitinib, imatinib, ibrutinib, and dasatinib. The various co-formers that were applied are derived from natural products and are FDA-approved drugs which include caffeic acid, cinnamic acid, ferulic acid, coumaric acid, MHD (1-methylhydantoin), aspirin, and ibuprofen. The organic solvents used included ethanol, water, DMF (dimethylformamide), acetonitrile, ethyl acetate, isopropanol, methanol, and acetone. One method used for crystallization included grinding the compounds for 10 minutes prior to dissolution in the solvent. Heating was also applied as a method to aid in dissolving the solution by speeding up the reaction. The solutions were also stirred on a magnetic stir plate to further excite the molecules for improved bonding. Another dissolution method used was the sonication of samples. Through this experimentation, several crystal structures have been sampled and prepared for characterization. The crystals will be tested using nuclear magnetic resonance spectroscopy and single crystal x-ray diffraction. Improving the solubility and bioavailability of anticancer drugs will aid the development of novel anticancer drug-drug co-crystals and will further research in cancer studies and pharmaceutics.

The Trouble with Traffic*

Clayne Williams, Eastern New Mexico University

A traffic simulation written in Python was created from scratch to model real-world traffic in a controllable environment. The simulation works and outputs reliable data to measure the effects of different circumstances on the average speed of a highway system. Insight was gained on how different distributions of car speeds effected overall average speed with a lane closure, and the effect of a lane closure length on average speed.

What Kind of Attacks are we Facing? Do we Need Swords for this Battle?

Sky Yazzie, Navajo Technical University

In a smart grid, the primary purpose is to find a cohesive interface that will work. Yet the network can be underlying problematic troubleshooting, so what happens when there's an issue? Developers are building more efficient ways to incorporate superior technology to be fully secured. The methodology was to conduct vivid research by outcomes of possible questions. The possibilities of disadvantages in utilizing bitcoin'+G19 blockchain technology were the number of thieves in money laundering. It had the management of cryptography to specialize in user privacy as well as cybersecurity. Overall when establishing a network database there will consistently be a sequence of drawbacks or benefits for the grid. The approach of this research was mainly understanding how one of the issues will fluctuate and how that can be solved.

GRADUATE STUDENT POSTER ABSTRACTS

Poster session abstracts are listed alphabetically by last name of registered presenter. An asterisk (*) indicates the poster received an outstanding graduate poster award at the 2020 New Mexico Research Symposium.

Assessment of Hantavirus Prevalence Among Rodent Communities in Eastern New Mexico

Jaecy Banther, Eastern New Mexico University
Steven B. Bradfute, The University of New Mexico
Ivana Mali, Eastern New Mexico University
Isaiah J. Moores, Eastern New Mexico University
Robert A. Nofchissey, The University of New Mexico
Samuel Goodfellow, The University of New Mexico
Thanchira Suriyamongkol, Eastern New Mexico University

Hantavirus is a zoonotic RNA virus that causes Hemorrhagic Fever with Renal Syndrome (HFRS) and Hantavirus Pulmonary Syndrome (HPS) in humans. Since the first reported case in the US in 1975, there have been approximately 118 HPS cases in New Mexico (NM). Since the majority of the cases are from northwestern NM, minimal attention has been given to the eastern portion of the state. However, the literature suggests there is a potential overlap of the Sin Nombre (SNV), El Moro Canyon, and Muleshoe virus in eastern NM, and a recent study found six species tested positive for hantavirus antibodies. Here, we aim to investigate hantavirus antibody seroprevalence, identify hosts, and genetically confirm the viral strains across eight under-surveyed counties in eastern NM. To date, we have surveyed 13 sites over 19,500 trap nights and captured 400 individuals belonging to two families: 32% Heteromyidae and 68% Cricetidae. Seven species we have captured are known hantavirus hosts. Species richness ranged from two to eight species per site, while capture per unit effort varied from 1% to 5%. Thus far we were able to test a subset of lung tissue samples of Peromyscus sp. and confirm the presence of SNV and non-SNV hantaviruses. In spring 2021, we will begin enzyme-linked immunosorbent assays (ELISA) to test blood samples for the presence of hantavirus-specific antibodies and continue to genetically test individual positive lung samples for hantavirus strains. This study significantly expands our understanding of hantavirus species distribution, hantavirus prevalence among their respective hosts, and has a potential to illuminate any spillover events and/or discovery of novel hantaviruses.

Multilevel Assessments of Contribution of Livestock Manure to Nitrogen Budget in Arid-land Ecosystems: The Case of Dairies in New Mexico

Suraj Ghimire, The University of New Mexico

The livestock industry is one of the major contributors to nitrogen pollution. Nearly one-third of the global human-induced nitrogen emissions are contributed by this sector. The intensification of dairy farms has resulted in an oversupply of nitrogen in smaller land pockets causing degradation of environmental and human health. New Mexico leads the country in terms of the average number of cows per large dairy farms and has held this position since 2002. A study by Johnson et al. (2003) indicates that nearly two-thirds of the New Mexican dairies have improper management of manure leading to groundwater pollution. This study aims to quantify the contribution of large dairy farms towards the nitrogen budget of the arid land ecosystem and recommend optimal abatement strategies. The nitrogen budget is calculated as the difference between livestock manure nitrogen loadings and crop nitrogen requirements. First, we modeled the spatial distribution of large dairy farms in New Mexico based on herd and land sizes and performed a farm-level assessment. For this, circles corresponding to the application acreage of farms were drawn and land cover data were used to calculate total nitrogen utilization by crops. For the county-level assessment, county totals were obtained by aggregating over livestock farms and croplands/grasslands in a county. Based on the geocoded locations of dairy and the number of cows in each farm, nitrogen excretion values were assigned to each county. Then, we performed a watershed level assessment by aggregating over livestock farms and croplands/grasslands in the vulnerable watersheds. Results showed that eight counties, six watersheds, and all the farms at the individual level had excess nitrogen beyond

the assimilative capacity of croplands. Then we proposed to include rangelands as possible sinks and performed a sensitivity analysis to understand the variation in nitrogen budget at 20%, 40%, 60%, and 80% willingness to accept levels. Findings indicated that at 40% and above acceptance rate, all the excreted nitrogen can be assimilated within the system. Therefore, the integration of the crop-livestock system with the rangelands can provide a viable solution to reduce the nutrient loadings in air, soil, and water and provide affordable commercial fertilizer substitutes for the farmers and ranchers.

Willingness to Pay for Distribution Feeder Microgrids in the Four Corner States

Clara Harig, The University of New Mexico

This study looks into consumer responses to the idea of Distribution Feeder Microgrids (DFMs), which is important in determining consumer demand. The current grid system is outdated and in need of repairs, but new technologies, like DFMs, are costly. Understanding consumer demand will help inform and prepare us for the transition to a more modern electricity grid.

Assessment of Freshwater Turtle Populations on the Pecos River in New Mexico and Texas*

Laramie Mahan, Eastern New Mexico University
Lawrence G. Bassett, Texas State University
Michael R. J. Forstner, Texas State University
Ivana Mali, Eastern New Mexico University
Thanchira Suriyamongkol, Eastern New Mexico University

Freshwater turtles represent vital components of aquatic and terrestrial ecosystems, providing many important ecological services (e.g., energy flow, seed dispersal, mineral cycling, etc.). Additionally, they can act as bio-indicators of environmental health by accumulating chemicals that reside in their respective water systems. The Pecos River is one of the most anthropogenically altered rivers in the United States. Agricultural practices, dam construction, channelization, and petroleum production have significantly altered the river flow and overall water quality. These factors have long threatened the connectivity and viability of wildlife populations inhabiting the Pecos River system, including freshwater turtles. Yet, the Pecos River itself has not been properly surveyed for turtles in over a decade. In this study, we report preliminary results of freshwater turtle surveys across 16 sites on the Pecos River in New Mexico and Texas. For every survey, we deployed 45 hoop net traps for two consecutive days and surveyed each site three times between May and August 2020. Upon capture, turtles were marked, measured, and returned to the water. We additionally recorded water quality parameters such as pH, conductivity (¬µ/s), temperature (¬∞C), flow (m/s), water depth (m), and water turbidity (m). Overall, we captured five species of turtles including Red-eared Slider (*Trachemys scripta*), Spiny Softshell turtle (*Apalone spinifera*), Yellow Mud turtle (*Kinosternon flavescens*), Common Snapping turtle (*Chelydra serpentina*), and New Mexico threatened Rio Grande Cooter (*Pseudemys gorzugi*). The species richness ranged from 0 to 5 species and the overall abundance ranged from 0 to 170 turtles per site. The most abundant and the most widely distributed species was *Apalone spinifera* while *Chelydra serpentina* was found at only one locality. *Pseudemys gorzugi* which is currently under review by the US Fish and Wildlife Service for potential federal protection was found at five locations: four in New Mexico and one in Texas. We captured only 11 unique *P. gorzugi* including 4 females, 6 males, and 1 juvenile. This work will continue and additional 16 sites will be surveyed in the summer of 2021. Our work will significantly contribute to our understanding of freshwater turtle distribution across this highly altered riverine system and aid in the assessment of conservation status of *Pseudemys gorzugi*.

Hypoxia Enhanced the Accumulation of Astaxanthin in *Haematococcus pluvialis*

Allison Minteer, Eastern New Mexico University Zhiming Liu, Eastern New Mexico University

Haematococcus pluvialis is a unicellular eukaryotic green alga and belongs to the Haematococcaceae family. It is known for its synthesis of a pigmented antioxidant called astaxanthin which has various commercial applications (e.g., food processing and cosmetics). In response to various environmental stresses, *H. pluvialis* transforms itself into a vegetative non-motile encysted cell and rapidly synthesizes a large amount of astaxanthin intracellularly. Astaxanthin is a keto-carotenoid and important for protecting the cell from harmful oxidization caused by other cellular compounds generated in the metabolic reactions under the stressful situation. The objective of our project was to develop a new method to induce an accelerated production of astaxanthin in the *H. pluvialis* cells by manipulating a series of environmental factors (light, temperature, pH, and hypoxic stress). *H. pluvialis* was initially cultured under a standard laboratory condition and then treated under a series of modified environmental conditions (e.g., hypoxia, high light intensity, high temperature, and low pH) to illicit stress responses inside the cells. After the treatments the cells were harvested, processed, and the quantity of the astaxanthin accumulated in the cells was quickly quantified with a spectrophotometer. Our preliminary data suggested the hypoxic treatment could accelerate the synthesis of astaxanthin in the cells of *H. pluvialis*. Other experiments are in progress according our experimental designs.

Application of High-dimensional Data Analysis in Aerospace Structural Health Monitoring and Nondestructive Testing

Hamed Momeni, New Mexico Tech Arvin Ebrahimkhanlou, New Mexico Tech

Structural health monitoring is an evaluation technology to monitor aerospace structure using sensing systems such as accelerometers, ultrasound wave response, images, and videos. In this field, there are three major steps: damage detection, localization, and quantification. The data from numerous detectors are commonly high dimensional and highly correlated. A critical challenge is manipulating noisy and lossy data to compress, transfer, and retrieve. Furthermore, to diagnose and prognosis of the existing damage, the relevant and valuable features should be extracted to have a physical meaning or reasonable interpretation. This research reviewed high dimensional data analysis methods like functional data analysis, tensor-based data analysis, compressive sensing, and matrix completion. The previous applications in structural health monitoring and nondestructive testing for aerospace structures are presented, and the potential for high dimensional analysis methods are proposed.

Optimal Power Flow for a Power System with Grid-scale Energy Storage Systems, Varying Wind Generation and a Fluctuating Load*

Owana Marzia Moushi, New Mexico Tech Kevin Wedeward, New Mexico Tech

As the amount of variable renewable energy integrated into power systems continues to increase around the world, energy storage systems (ESS) hold the promise of enabling larger amounts of renewable energy to be accommodated and provide additional flexibility in the power system's operation. This poster presents an approach based on optimal power flow to improve the performance of a power system with wind generation through the addition of ESS. The placement of the ESS is considered at the site of varying wind generation and/or location of a fluctuating load, and enables an increase in performance of the power system to be achieved over a period of time. Objectives considered for improvements in performance include reduction of a conventional (nonrenewable) generator's output power, smoothing of a conventional generator's output power to lessen ramping and reduction in transmission losses.

A single-phase, transmission-level model of a five-bus power system was selected to serve as the test system, which includes a conventional generator, a wind generator with varying power output specified by recorded data, a fluctuating load specified by recorded data, a fixed load, and ESS placed at the varying wind generator and/or fluctuating load. Values from both the varying wind generation and fluctuating load were scaled to be consistent with the five-bus test system and down sampled such that values are given at 30-minute intervals for two days. ESS are sized at 10% of the daily demand for energy, and are modeled by first-order difference equations that relate the rate (average power) of charge/discharge and amount of energy stored at every step. With selected data specified at each time, an optimal load flow problem was formulated and solved (via constrained nonlinear optimization algorithms) over all 96 time steps. The case of load flow with no ESS present served as the baseline to which three scenarios (ESS co-located with wind generation, ESS co-located with fluctuating load, and ESS at both locations) were considered for each of the three objectives such that there were nine results.

In all scenarios the performance of the power system is improved as expected with the selected objective. The improvements can be viewed qualitatively in figures of the conventional generator's power and line powers, and quantitatively through values calculated for the objective functions (metrics) in all scenarios. As is likely intuitive, the best results are achieved for ESS placed at two locations followed closely by a single installation of ESS at the bus with fluctuating load. The approach and associated results demonstrate examples of improvements that can be achieved in a power system's performance through integration of ESS along with renewable energy. An additional impact is that insight into the preferable location and size of ESS can be determined based upon the desired objective.

How the Built Environment Can Help Employees to Experience Lower Occupational Stress*

Hirbod Norouzianpour, The University of New Mexico

Stress affects every persons' health and well-being, significantly and vastly. Occupation stress negative effects are bolder in workplaces; both as a disease agent and as an obstacle to employees' productivity and satisfaction. Although occupational stress has various sources and designers have no control over many of them, there is a group of interventions that are design related. In this research, those design strategies to mitigate stress are considered as environmental interventions. The literature on occupational health, well-being, satisfaction, and productivity are huge and multi-directional; however, this research is limited to stress factors that correlated with the built environment and focus on employees who are experiencing a high rate of stress in office buildings as the target group. Due to that, the researcher finds evidence of environmental interventions that can reduce stress or enhance the stress-coping abilities of workers in offices by design and environmental health improvement. The questions that this research is answering are: what are the main environmental factors in offices that can help the employees experience lower stress or help them to mitigate the stress after facing it? How can space cause people to stress? How do stress and built environment collaborate? This research is based on the cross-disciplinarily systematic literature review of architecture, planning, public health, medical, management, and psychological sciences. The outcome of this research is the set of strategies to provide solutions for healthier and more productive working places in offices with a concentration on the reduction of the stress level of employees, which can be used as a source for workplace evidence-based designs. These strategies are discussed in three realms: urban, architecture, and conjunction area as a mediator between outside and inside.

Prospects of Jujube (*Ziziphus jujuba*) as a Future Crop in New Mexico*

Sundar Sapkota, Eastern New Mexico University Zhiming Liu, Eastern New Mexico University
Sen Wang, Central South University of Forestry and Technology
Sanjib Sapkota, Simon Fraser University

Jujube is a multipurpose fruit tree belonging to the family Rhamnaceae. The tree has wide adaptability, provides edible nutritious fruits, medicinal plant organs, and has ornamental benefits. The fruits are rich sources of vitamins, antioxidants, and minerals. Jujube tree is native to Northern China and is relatively new to the United States. More importantly, the American demand for jujube fruits has been growing due to increasing number of Asian people, increased education on nutrition, and health concerns, however, the supply is short. New Mexico has a great potential to produce jujubes at a volume high enough to meet domestic demand, but the lack of proper extension services has caused many New Mexican farmers to be unfamiliar with this important crop. Other constraints for commercial cultivation include the unavailability of planting materials and limited study of plant species. There is an immediate need of improved propagation techniques to ensure adequate supply of planting materials. Farmer field-based research projects might be helpful in identifying and tackling the challenges that arise in crop establishment and cultivation. Better promotion strategies and crop information could encourage people to start planting jujubes. To sum, jujube farming could be a profitable enterprise in New Mexico.

Effects of Water and Fertilizer Application on Jujube Growth in New Mexico

Sundar Sapkota, Eastern New Mexico University Zhiming Liu, Eastern New Mexico University
Sen Wang, Central South University of Forestry and Technology
Sanjib Sapkota, Simon Fraser University

Jujube is a perennial tree primarily planted for edible fruits. The crop is famous in Asia but relatively unknown in the United States. Prospects of jujubes as an alternative future crop in New Mexico are increasing but the lack of proper extension and promotion caused many farmers to be unfamiliar with the crop. Also, the lack of saplings and field-based research information have restricted its cultivation in New Mexico. Thus, we performed field experiments (2019 and 2020) to investigate water and fertilizer influence on jujube growth performance. For this study, we applied three levels of water (2 L: low, 8 L: medium, and 16 L: high), and fertilizers (35 g: low, 70 g: medium, and 140 g: high) to jujube plants. Control treatments did not receive any amount of water and fertilizer. Variables such as increment in plant height, stem diameter, number of leaves, leaf sizes, and chlorophyll contents were recorded. The 16 L water and 70 g fertilizer increased plant height and diameter by 60.1 cm and 5.23 mm in 2019, and 67.81 cm and 6.18 mm in 2020, respectively. Leaf length and width under W3F2 were 5.68 cm and 2.80 mm in 2019, and 5.85 cm and 2.98 mm in 2020, respectively. A similar trend was found in terms of leaf number. Leaf chlorophyll concentration was also positively influenced by water-fertilizer application. Based on the findings of our research project, we recommend 16 L water and 70 g fertilizer per plant in young jujube orchards in order to maximize growth. This information guides farmers to adopt better water fertilizer management strategies in the orchards to enhance crop performance. These findings might encourage farmers to consider jujubes as an alternative crop in New Mexico.

About the New Mexico Academy of Science

The New Mexico Academy of Science (NMAS) was founded in 1902 to foster scientific research and scientific cooperation, to increase public awareness of the role of science in human progress and welfare, and to promote science education in New Mexico.

Membership in NMAS is open to anyone interested in science, formal and informal science education, or the other goals and programs of NMAS. Individuals engaged in scientific research or teaching at all levels are particularly encouraged to become members. Applications for membership as well as more information about NMAS and its programs can be found at www.nmas.org.

CONTACT INFORMATION

The New Mexico Academy of Science
c/o The New Mexico Museum of Natural History and Science
1801 Mountain Road NW
Albuquerque, New Mexico 87104
nmas@nmas.org www.nmas.org

OFFICERS AND EXECUTIVE BOARD 2020

Officers

President: Dr. Zhiming Liu
President-Elect: Dr. Gretchen Gürtler
Vice-President: Dr. Anton Sumali
Treasurer: Dr. Deb Thrall
Secretary: Malva Knoll
Past President: Dr. Steven Jett

Directors

Jayne C. Aubele, NMAS Education Awards
Lynn Brandvold, New Mexico Junior Academy of Science
Gretchen Gürtler, Museums
Dr. Shanalyn Kemme, Director at Large
Jane Liu, Liaison for Eastern New Mexico University
Dr. Richard Nygren, National Youth Science Camp
Amalia Parra, Director at Large
Dr. Rod Rock, Liaison for NM Highlands University
Dr. Anton Sumali, Journal of Science, Community Relations

Directors Emeritus

David Duggan
Dr. David Hsi
Harry Pomeroy (NMAS Fellow)
Mona Pomeroy
Dr. Maureen Romine

This is a publication of the New Mexico Academy of Science. NMAS does not discriminate on the basis of race, creed, color, national or ethnic origin, gender, physical disability, or sexual orientation.


NMAS
NEW MEXICO
ACADEMY OF SCIENCE